2010-05-11

Role of Internal Calcium Stores in Exocytosis and Neurotransmission: A Dissertation

Jason J. Lefkowitz
University of Massachusetts Medical School

Role of Internal Calcium Stores in Exocytosis and Neurotransmission

A Dissertation Presented

By

Jason J. Lefkowitz

Submitted to the faculty of the University of Massachusetts Graduate School of Biomedical Sciences, Worcester

In Partial Fulfillment of the Requirements for the Degree of

Doctor of Philosophy

May 11th 2010

PROGRAM IN NEUROSCIENCE

Role of Internal Calcium Stores in Exocytosis and Neurotransmission

A Dissertation Presented
By

Jason J. Lefkowitz

The Signatures of the Dissertation Defense Committee Signifies Completion and Approval as to Style and Content of the Dissertation

John V. Walsh, Jr., M.D. Thesis Advisor

Scott Waddell, Ph.D. Committee Member

Vivian Budnik, Ph.D. Committee Member

Hong-Sheng Li, Ph.D. Committee Member

Corey Smith, Ph.D. Committee Member

The signature of the chair of the committee signifies that the written dissertation meets the requirements of the Dissertation Committee

Harvey Florman, Ph.D. Chair of Committee

The signature of the Dean of the Graduate School of Biomedical Sciences signifies that the student has met all graduation requirements of the school

Anthony Carruthers, Ph.D.
Dean of the Graduate School of Biomedical Sciences

PROGRAM IN NEUROSCIENCE

To my family,

who know not what I do but,

are proud nonetheless.

And, to Kate

Acknowledgements

I wish to extend my sincerest thanks to all who have contributed to my research and training at the University of Massachusetts Medical School. I particularly need to thank the department of Physiology for their continued support in numerous ways over the years. I would also like to thank the students, staff and faculty of the Program in Neuroscience, including its director Dave Weaver, for providing a top notch program.

Special thanks must go to my many mentors for their outstanding scientific guidance, stimulating discussions (scientific or otherwise) and perhaps not least, for their tolerance of my nocturnal disposition and inability to do mornings.

My official advisor, John Walsh, could not have provided me with a better mentorship. His criticisms were always constructive, his experimental advice logically sound, and he pushed me to become a better communicator and presenter of my data. Importantly, he never said no to an experiment, even if it seemed anti-dogmatic or risky at the time. Also, I will add that his colorful personality and ever willingness to crack a joke, with no expense spared, have not gone unappreciated over the years.

Valerie DeCrescenzo and Kevin Fogarty have been my informal, but invaluable, co-mentors. Valerie taught me everything I know about imaging and analyzing calcium syntillas and Kevin, who served as the chair of my thesis advisory committee, helped with the quantitative and modeling end of things. Both have a particular eye for detail and not a single experiment was executed without my first seeking the opinion of Valerie or Kevin, which often led to lengthy and productive discussions. To this end, I also need to specially thank Ronghua

ZhuGe, from whose research this thesis work was born, and who has constantly provided me with valuable insight since.

I also want to thank I the members all of the Biomedical Imaging Group, Kevin Fogarty, Richard Tuft, Karl Bellve, Larry Liftshitz, Clive Standley and Paul Furcinitti, whom I have had the honor of working amongst on a day to day basis. From the simplest technical assistance to reading through manuscripts, listening to and critiquing my presentations, they have helped me immensely.

I must acknowledge former Walsh lab post docs Matthew Turvey, for teaching me capacitance and amperometry and Kailai Duan for his advice on the elicited release experiments and his help with syntilla imaging.

These individuals from the Walsh lab and the Biomedical Imaging Group have collectively provided me with a unique training experience second to none, and I cannot express enough how grateful I am for it.

Furthermore, for their helpful suggestions and general guidance over the past few years, I want to thank the members of my thesis advisory committee, Kevin Fogarty, José Lemos, Harvey Florman, Ronghua ZhuGe and Scott Waddell. I would especially like to thank Scott for allowing me rotate in his lab and for chairing my qualifying exam committee. I would also like to thank my dissertation examination committee for taking the time to read this thesis and in particular, Corey Smith for travelling from Case Western University on this occasion.

I would also like to acknowledge some of my other mentors along the way. Bill Brunken, formerly of Tufts University School of Medicine, helped me with my decision to pursue a Ph.D. and it was during the two years I spent working in his lab that I gained most of my skill in molecular and protein techniques. I also want

to thank Rona Delay of the University of Vermont for teaching me the fundamentals of electrophysiology over a decade ago and in whose lab I spent many long nights perfecting those techniques.

Finally, I would like to thank my wife, Kate for her unconditional love and unwavering support. It was her astute insight that ultimately brought me to the University of Massachusetts Medical School. And, I would be remiss if I did not mention my little beagle, Princess (who came with that name from a research lab), whose company can turn the bluest day upside down.

Abstract

A central concept in the physiology of neurosecretion is that a rise in cytosolic [Ca^{2+}] in the vicinity of plasmalemmal Ca^{2+} channels due to Ca^{2+} influx, elicits exocytosis. This dissertation examines the effect on both spontaneous and elicited exocytosis of a rise in focal cytosolic [Ca^{2+}] in the vicinity of ryanodine receptors (RYRs) due to release from internal stores in the form of Ca^{2+} syntillas. Ca^{2+} syntillas are focal cytosolic transients mediated by RYRs, which we first found in hypothalamic magnocellular neuronal terminals. (*Scintilla*, Latin for spark, found in nerve terminals, normally synaptic structures.) We have also observed Ca^{2+} syntillas in mouse adrenal chromaffin cells (ACCs). Here the effect of Ca^{2+} syntillas on exocytosis is examined in ACCs, which are widely used as model cells for the study of neurosecretion.

Elicited exocytosis employs two sources of Ca^{2+}, one due to influx from the cell exterior through voltage-gated Ca^{2+} channels (VGCCs) and another due to release from intracellular stores. To eliminate complications arising from Ca^{2+} influx, the first part of this dissertation examines spontaneous exocytosis where influx is not activated. We report that decreasing syntillas leads to an increase in spontaneous exocytosis measured amperometrically. Two independent lines of experimentation each lead to this conclusion. In one case release from stores was blocked by ryanodine; in another, stores were partially emptied using thapsigargin

plus caffeine after which syntillas were decreased. We conclude that Ca^{2+} syntillas act to inhibit spontaneous exocytosis, and we propose a simple model to account quantitatively for this action of syntillas.

The second part of this dissertation examines the role of syntillas in elicited exocytosis whereby Ca^{2+} influx is activated by physiologically relevant levels of stimulation. Catecholamine and neuropeptide release from ACCs into the circulation is controlled by the sympathetic division of the Autonomic Nervous System. To ensure proper homeostasis tightly controlled exocytic mechanisms must exist both in resting conditions, where minimal output is desirable and under stress, where maximal, but not total release is necessary. It is thought that sympathetic discharge accomplishes this task by regulating the frequency of Ca^{2+} influx through VGCCs, which serves as a direct trigger for exocytosis. But our studies on spontaneous release in ACCs revealed the presence of Ca^{2+} syntillas, which had the opposite effect of inhibiting release. Therefore, assuming Ca^{2+}-induced Ca^{2+} release (CICR) via RYRs due to Ca^{2+} influx through VGCCs, we are confronted with a contradiction. Sympathetic discharge should increase syntilla frequency and that in turn should *decrease* exocytosis, a paradox. A simple "explanation" might be that the increase in syntillas would act as a brake to prevent an overly great exocytic release. But upon investigation of this question a different finding emerged.

We examined the role of syntillas under varying levels of physiologic stimulation in ACCs using simulated action potentials (sAPs) designed to mimic

native input at frequencies associated with stress, 15 Hz, and the basal sympathetic tone, 0.5 Hz. Surprisingly, we found that sAPs delivered at 15 Hz or 0.5 Hz were able to completely *abolish* Ca^{2+} syntillas within a time frame of two minutes. This was not expected. Further, a single sAP is all that was necessary to initiate suppression of syntillas. Syntillas remained inhibited after 0.5 Hz stimulation but were only temporarily suppressed (for 2 minutes) by 15 Hz stimulation, where global $[Ca^{2+}]_i$ was raised to 1 – 2 μM. Thus we propose that CICR, if present in these cells, is overridden by other processes. Hence it appears that inhibition of syntillas by action potentials in ACCs is due to a new process which is the opposite of CICR. This process needs to be investigated, and that will be one of the very next steps in the future. Finally we conclude that syntilla suppression by action potentials is part of the mechanism for elicited exocytosis, resolving the paradox.

In the last chapter speculation is discussed into the mechanisms by which physiologic input in the form of an action potential can inhibit Ca^{2+} syntillas and furthermore, how the Ca^{2+} syntilla can inhibit exocytic output.

Table of Contents

List of Figures and Tables

List of Abbreviations

Abbreviation	Term
ACC	adrenal chromaffin cell
ACh	acetylcholine
ANS	autonomic nervous system
AP	action potential
ARVD	arrythmogenic right ventricular dysplasia
ATP	adenosine triphosphate
Ba^{2+}	barium
BMP	bone morphogenetic protein
Ca^{2+}	calcium
$[Ca^{2+}]$	calcium concentration
$[Ca^{2+}]_{cyto}$	cytosolic calcium concentration
$[Ca^{2+}]_i$	intracellular calcium concentration
CAPS	Ca^{2+}-dependent activator protein for secretion
CASK	calcium/calmodulin-dependent serine protein kinase
CICR	Ca^{2+}-induced-Ca^{2+}-release
DHP	1,4-dihydropyridine
ER	endoplasmic reticulum
F-actin	filamentous actin

FGF	fibroblast growth factor
GDNF	glial cell line-derived neurotrophic factor
GTP	guanidine triphosphate
IP3	inositol triphosphate
K^+	potassium
LDCG	large dense core granule
L/HVA	low/high voltage activated
mEPSC	miniature excitatory post synaptic potential
Munc13	mammalian uncoordinated-13 protein
Munc18-1	mammalian uncoordinated-18 protein
Na^+	sodium
NF	neurofilament
NGF	nerve growth factor
NSF	N-ethylmaleimide-sensitive factor
PIP	phosphatidylinositol 4-phosphate
PIP2	phosphatidylinositol 4,5-bisphosphate
PIP5KI	type I phosphatidylinositol 4-phosphate-5-kinase
PITP	phosphatidylinositol transfer protein
PNMT	phenylethanolamine N-methyltransferase
RalA/B	v-ral simian leukemia viral oncogene homolog A/B (ras related)
RP	reserve pool

RRP	readily releasable pool
RYR	ryanodine receptor
RYR1	Type 1 “skeletal muscle” ryanodine receptor
RYR2	Type 2 “cardiac muscle” ryanodine receptor
RYR3	Type 3 ryanodine receptor
SAF	stand alone foot event
sAP	simulated action potential
SCG10	superior cervical ganglion-10 protein
SNAP-25	Synaptosomal-associated protein 25
SNARE	Soluble *N*-ethylmaleimide-sensitive factor Attachment protein REceptor
SR	sarcoplasmic reticulum
SRP	slowly releasable pool
Syt	synaptotagmin
Tg	thapsigargin
TH	tyrosine hydroxylase
t-SNARE	target-SNARE
UPP	unprimed pool
VGCC	voltage-gated calcium channel
VICaR	Voltage induced calcium release
VMA	vanillylmandelic acid
v-SNARE	vesicle-SNARE

Co-Author Contributions

My advisor John V. Walsh, Jr. and unofficial advisors Valerie DeCrescenzo and Kevin E. Fogarty participated in, supervised and approved all aspects of the planning of this research. This work also benefited from frequent strategy, technical, and statistical consults from the various members of the Biomedical Imaging Group.

Valerie DeCrescenzo helped to acquire some of the earlier syntilla data and global Ca^{2+} controls in the work presented on spontaneous release in Chapter 5. Kailai Duan gathered some of the syntilla data acquired during the single action potential experiment in Chapter 6, dealing with elicited release.

Valerie DeCrescenzo provided expertise to help analyze syntilla data and Kevin Fogarty provided expertise to help interpret the data in Figure 5.6 relating to syntilla index and microdomains.

Copyright Information

Material presented in chapter 5 has appeared in the following places:

Manuscripts

Lefkowitz JJ, Fogarty KE, Lifshitz LM, Bellve KD, Tuft RA, ZhuGe R, Walsh JV, Jr., De Crescenzo V (2009) Suppression of Ca^{2+} syntillas increases spontaneous exocytosis in mouse adrenal chromaffin cells. **J Gen Physiol** 134:267-280.

Abstracts

Jason J. Lefkowitz, Kevin E. Fogarty, John V. Walsh Jr., Valerie De Crescenzo, Ca^{2+} Syntillas Inhibit Spontaneous Exocytosis In Mouse Adrenal Chromaffin Cells, **Biophysical Journal**, Volume 96, Issue 3, Supplement 1, February 2009, Page 99a, ISSN 0006-3495, DOI: 10.1016/j.bpj.2008.12.420.

(http://www.sciencedirect.com/science/article/B94RW-4VK7BB2-M5/2/c62e8c6f8be18d41c31f1b0cd1ca1fd8)

Jason J. Lefkowitz, Kevin E. Fogarty, Lawrence M. Lifshitz, Karl D. Bellve, Ronghua ZhuGe, Richard A. Tuft, John V. Walsh, Valerie De Crescenzo, Ca^{2+} Syntillas Decrease Spontaneous Exocytosis In Mouse Chromaffin Cells Exocytosis & Endocytosis - I, **Biophysical Journal**, Volume 94, Issue 2, Supplement 1, 2008 Annual Meeting Abstracts - a supplement of Biophysical Journal, February 2008, Pages 425-435, ISSN 0006-3495, DOI: 10.1016/S0006-3495(08)79072-6.

(http://www.sciencedirect.com/science/article/B94RW-4VP6T50-3K/2/070cb21f68393135a786f0d0fda73342)

Chapter 1

A short introduction

We already know a lot about the roles of calcium ions (Ca^{2+}) in the regulation of exocytosis. But that information focuses on Ca^{2+} influx from outside of the cell through Ca^{2+} channels into a distinct microdomain wherein lie docked, primed vesicles. There, Ca^{2+} executes its most notorious role, serving as a final signal to trigger release. But Ca^{2+} is also stored inside cells and neurons at high concentrations within organelles such as the endoplasmic reticulum. Interestingly, this Ca^{2+} can be released into separate microdomains distinct from those generated by influx (ZhuGe et al., 2006). Nonetheless, there is little information to date about how this type of Ca^{2+} release affects the process of exocytosis and neurotransmission (Figure 1.1).

This dissertation examines possible roles of internal Ca^{2+} stores in the process of exocytosis. Some very surprising discoveries are uncovered when the focus is shifted away from Ca^{2+} in the extracellular saline to that stored within the cell. Three background chapters follow, describing in relevant detail the model system employed in this work to study neurotransmission – the chromaffin cell, the process of exocytosis in these cells and Ca^{2+} signaling specifically as it

relates to this system. In chapter five, a new and quite unexpected role for Ca^{2+} in exocytosis is presented in detail. That is, Ca^{2+} syntillas, which are brief, focal cytosolic Ca^{2+} transients arising from internal stores, are shown to cause an *inhibition* of spontaneous exocytosis in mouse chromaffin cells!

Following this discovery, work presented in chapter six shows that this inhibition of exocytosis is relieved by physiologically relevant levels of stimulation. Unexpectedly, when the cell receives input and fires an action potential, Ca^{2+} syntillas become inhibited within the time course of a few minutes. These findings suggest that internal Ca^{2+} stores serve as an important mediator of the exocytotic output based on physiologic input. Accordingly, this chapter presents evidence to support another entirely new idea that spontaneous release and *not* elicited release may account for basal levels of catecholamine output into the circulation during resting conditions in an organism.

In the final chapter seven, these findings are summarized and discussed in terms of their place in physiology and neurotransmission. Speculation is also presented into the mechanisms by which Ca^{2+} syntillas could inhibit exocytosis and furthermore, how physiologic stimulation in the form of action potentials could inhibit syntillas. After reading this dissertation you will find that internal Ca^{2+} stores are anything but insignificant in the process of exocytosis and, that

Ca^{2+} released from these stores, actually lies at the center of cell to cell communication in excitable cells and neurotransmission.

Importance in physiology and neuroscience

An inhibitory function of syntillas on spontaneous exocytosis has profound implications in neuroscience and general physiology. Spontaneous exocytosis has specific functions in a range of neurons, including synapse stabilization and maintenance, regulation of post synaptic protein synthesis, and regulation of excitability in postsynaptic neurons. Therefore syntillas could serve as an upstream regulator of these important functions. Moreover, since this study was done in the chromaffin cell it directly implies that syntillas can serve as a potent regulator of catecholamine release into the circulation.

Another significant implication of this work is that at basal levels of physiologic stimulation set by the sympathetic tone, known as the "rest and digest" state, the major driving force behind long term, low level output into the circulation may in fact be due to the suppression of syntillas. Therefore it may be that spontaneous release, and *not* the direct triggering of exocytosis by Ca^{2+} influx (i.e., elicited release), is the predominate form of exocytosis in adrenal chromaffin cells.

Disease relevance

As a homeostatic regulatory mechanism that prevents mass output of catecholamines into the circulation, aberrations in the syntilla process could lead to severe pathologies. For example, high catecholamine levels in the circulation due to elevated sympathetic tone is thought to be an aetiological factor in a broad range of diseases, including various types of cancer, diabetes mellitus, open-angle glaucoma, osteo- and rheumatoid arthritis and asthma (Fitzgerald, 2009).

Ca^{2+} spontaneously released from internal stores in the form of syntillas is mediated through ryanodine receptors (RYRs), which have three isoforms (RYR1, 2, and 3). RYR1 mutations are associated with malignant hyperthermia and central core disease (Benkusky et al., 2004). RYR2 mutations in cardiac tissue play a role in stress-induced polymorphic ventricular tachycardia (a form of cardiac arrhythmia) and arrhythmogenic right ventricular dysplasia ARVD (Zucchi and Ronca-Testoni, 1997). It has also been shown that levels of type RYR3 are greatly increased in PC12 cells over expressing mutant human Presenilin 1, and in brain tissue in knockin mice that express mutant Presenilin 1 at normal levels, and thus may play a role in the pathogenesis of neurodegenerative diseases, like Alzheimer's disease (Thibault et al., 2007; Zhang et al., 2009). The presence of antibodies against ryanodine receptors in blood serum has also been associated with myasthenia gravis (Skeie et al., 2003).

References

Benkusky NA, Farrell EF, Valdivia HH (2004) Ryanodine receptor channelopathies. Biochem Biophys Res Commun 322:1280-1285.

Fitzgerald PJ (2009) Is elevated noradrenaline an aetiological factor in a number of diseases? Auton Autacoid Pharmacol 29:143-156.

Skeie GO, Romi F, Aarli JA, Bentsen PT, Gilhus NE (2003) Pathogenesis of myositis and myasthenia associated with titin and ryanodine receptor antibodies. Ann N Y Acad Sci 998:343-350.

Thibault O, Gant JC, Landfield PW (2007) Expansion of the calcium hypothesis of brain aging and Alzheimer's disease: minding the store. Aging Cell 6:307-317.

Zhang C, Wu B, Beglopoulos V, Wines-Samuelson M, Zhang D, Dragatsis I, Sudhof TC, Shen J (2009) Presenilins are essential for regulating neurotransmitter release. Nature 460:632-636.

ZhuGe R, DeCrescenzo V, Sorrentino V, Lai FA, Tuft RA, Lifshitz LM, Lemos JR, Smith C, Fogarty KE, Walsh JV, Jr. (2006) Syntillas release Ca2+ at a site different from the microdomain where exocytosis occurs in mouse chromaffin cells. Biophys J 90:2027-2037.

Zucchi R, Ronca-Testoni S (1997) The sarcoplasmic reticulum Ca2+ channel/ryanodine receptor: modulation by endogenous effectors, drugs and disease states. Pharmacol Rev 49:1-51.

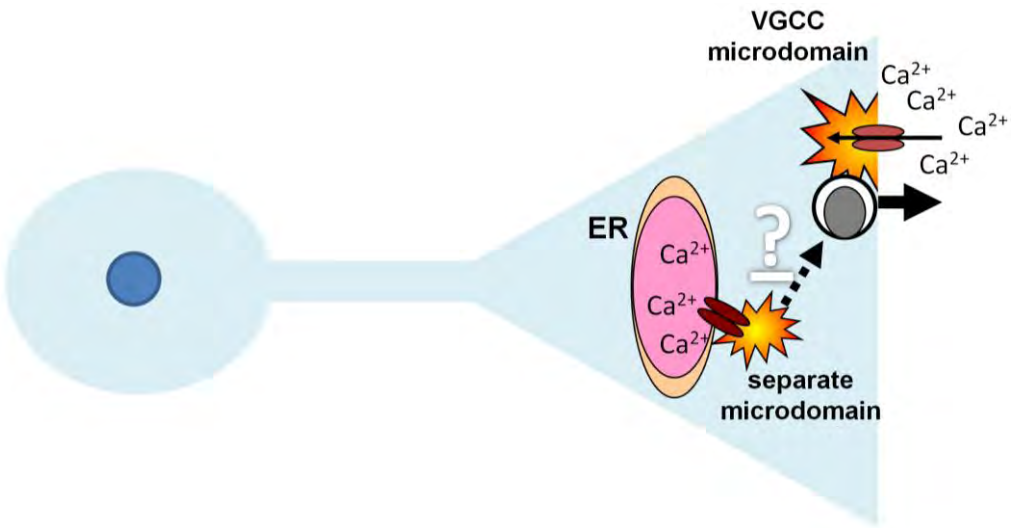

Figure 1.1 **What is the role of internal Ca^{2+} stores in exocytosis?** It is well known that Ca^{2+} influx through voltage-gated calcium channels (VGCC) into the microdomain where vesicles, in neurons and dense core granules, in adrenal chromaffin cells are docked and primed serves as a trigger for their exocytosis. On the other hand, Ca^{2+} is also stored at high concentrations within cellular organelles. Ca^{2+} can be released from these stores into a separate microdomain. But much less is known about the role that this Ca^{2+} plays in the process of exocytosis.

Chapter 2

The chromaffin cell: an ideal system for the study of neurotransmission

The work presented in this dissertation is carried out in the mouse adrenal chromaffin cell (ACC). ACCs are often used as models of neurons since they are quite unique in that they share the same properties of neurons and secretory cells (Winkler and Fischer-Colbrie, 1998; Garcia et al., 2006).

At the time of this dissertation there is a sizeable knowledge base for the ACC. Here I outline the most interesting features of these cells as they necessarily provide a foundation for the biological interpretations within this work. The interested reader can find a more in depth account of the developmental, morphologic and functional properties of ACCs cross-species in the very comprehensive review series on chromaffin cells published in Acta Physiologica 2008, 192 (143-335).

Brief background

ACCs were first described in useful detail at the turn of the 19th century, when Alfred Kohn discovered these cells were closely related to neurons in the sympathetic ganglia and showed that they have secretory properties (Kohn, 1898, 1902, 1903). The name "chromaffin" cell actually comes from Kohn's observation that the cells reacted with chromium salts, imbuing them with a yellowish-brown staining pattern (the brown color is a product of the reaction whereby chromium salts oxidize and polymerize catecholamines stored inside granules within the cell) (Hingerty and O'Boyle, 1972). In the 1960's advances in microscopy technology and access provided morphologists a means to begin describing the developmental, structural, ultra-structural and functional characteristics of these cells (Coupland, 1965a, b; Coupland and Hopwood, 1966; Coupland, 1989). By the end of the 1960's William Douglas had first postulated his theory of stimulus-secretion coupling based on data from perfused cat adrenals, which underscored the important role of Ca^{2+} ions as signals linking cellular excitation with the initiation of exocytic secretion (Douglas, 1968). As tissue culture techniques were developed during the 1970's, the earlier studies on the adrenal that were previously performed *in situ* or *in vitro* were extended as ACCs became amenable to molecular biology, fluorescence microscopy, biochemical and electrophysiological techniques. In the early 1980's through the

turn of the next century, powerful electrophysiological and electrochemical recording techniques for single cell recording of exocytosis emerged. From the first reports on patch clamp capacitance (Neher and Marty, 1982), amperometry (Leszczyszyn et al., 1990) and patch amperometry (Albillos et al., 1997), the ACC has consistently proven to be the model of choice for the study of exocytosis. To date, we have a detailed picture of the morphologic, molecular and functional features of these cells which is evermore evolving.

Basic anatomy and physiology

Chromaffin cells are largely found within the adrenal medulla where they comprise the majority of that tissue (Figure 2.1). Ganglion and supporting sustentacular cells are also present in the medulla, but to a lesser extent. While ACCs tend to be arranged in clusters and trabeculae, ganglion cells can be singly interspersed or clustered among the ACCs and are often found in association with nerve fibers. The support cells surround the clusters of ACCs (O'Connor, 2003).

Some chromaffin cells are also located at what is called the organ of Zuckerkandl, at the inferior mesenteric artery where they form paraganglia about both sides of the aorta. The majority of precursor chromaffin cells, however,

differentiate at the center of the adrenal gland in response to the glucocorticoid cortisol, and do not migrate to the organ of Zuckerkandl.

Within the ACCs are catecholamine-storing secretory vesicles called large dense core granules (LDCGs). Catecholamines inside the LDCGs are released from ACCs and sympathetic nerve terminals through exocytosis. In this process, other contents of these granules, including chromogranins, various peptides and enzymes can also be co-released into the circulation.

Neuronal reuptake provides the primary method by which catecholamines are removed from the synaptic cleft. To a lesser extent, non-neuronal reuptake mediated by the family of organic cation transporters can also play a role in catecholamine clearance. After reuptake, cytosolic catecholamines can be repackaged into granules via active transport or become deaminated and metabolized through O-methylation or oxidation. The liver enzyme, alcohol dehydrogenase is necessary to undergo complete catecholamine degradation to vanillylmandelic acid (VMA). Once released into the bloodstream, catecholamines have a brief half-life of about 1-2 minutes. They are removed from the circulation primarily by neuronal reuptake, but they are also subject to renal excretion (O'Connor, 2003; Fung et al., 2008).

Neurogenesis of ACCs

Chromaffin cells are born from the same multipotent embryonic stem cells in the trunk of the neural crest that give rise to sympathetic neurons (Figure 2.2). During development these stem cells migrate from the dorsal surface of the neural tube along specified pathways determined by specific guidance factors within their microenvironment (Le Douarin et al., 1994).

In the developing adrenal gland, before the capsule is complete, neuroblasts and nerve fibers migrate from the neural crest and penetrate between the cortical cells (Crowder, 1957). The invading neuroblasts originate cords of pheochromoblasts, in various stages of differentiation (Hervonen, 1971; Coupland, 1989), containing cortical cell islets. The pheochromoblasts initially display a high proportion of nucleus to cytoplasm, marked polyribosomes and some LDCGs. Pheochromoblasts and cortical cells, including those that are functionally active with catecholamines and neuropeptides, remain interrelated up to the fetal period (Wilburn and Jaffe, 1988).

After postnatal degeneration of cells of the fetal cortex and during formation of the final cortex, the islands of neuroblasts settle against the central vein, and reach a compact, highly vascularized structure in the medulla of the adrenal gland. At that time the reticular zone begins to develop, and cortical cells

begin to appear among chromaffin cell groups (Figure 2.3 A) (Diaz-Flores et al., 2008).

Structural and functional characteristics

In humans, ACCs in the medulla are located in a 2 mm thick region proximal to the adrenal cortical reticularis (Quinan and 1933, 1933), where they are in direct contact and surround small groups of cortical cells (Figure 2.3 A). Since the two endocrine components are interwoven, with cortical cells located within the medulla and vice versa, the suggestion of paracrine interaction has been proposed (Bornstein et al., 1997).

Interestingly, ACCs conserve plasticity and can be induced to express neuronal characteristics including neurite growth (Unsicker et al., 1978; Aloe and Levi-Montalcini, 1979; Doupe et al., 1985). For example, it has been reported that striated astroglia can induce morphologic and neurochemical changes in adrenergic-enriched ACCs (Uceda et al., 1995).

Within the medullary tissue, ACCs are constrained within clusters and short trabeculae between sustentacular cells. The ACCs are directly apposed to each other, separated by a gap of 150–250 Å in width, where they present interdigitating processes with their neighboring cells in the tissue clusters. The

medulla is highly innervated by preganglionic sympathetic fibers and small numbers of sympathetic ganglion cells are also interspersed within the tissue (Figure 2.3 B). Microvillae are observed on the cell surface and extend into the extracellular space where several cells converge. The surface area proximal to the capillary endothelium is separated from the capillary by a fibrillary, granular material and a basement membrane (Figure 2.3 B) (Diaz-Flores et al., 2008).

In the medullary tissue ACCs are moderately large and exhibit a polygonal or columnar shape. On the other hand, cultured or dissociated ACCs are spherical (see Figures 2.3 B and 2.2).

The nucleus of the ACC can display marked variability. For example, ACCs generally have a single nucleus, but the appearance of two or more is not so uncommon. The nuclei can be round or ellipsoidal, large or small and, may contain up to three nucleoli. While the nucleus is most frequently centrally located, eccentric location is also possible. In a clear nuclear background, the chromatin tends to be arranged about the periphery and its pattern can be finely or coarsely clumped (Diaz-Flores et al., 2008).

The cytoplasm, which tends to be finely granular, most notably contains the chromaffin granules which define the cell as well as the common cellular organelles. These include a large Golgi apparatus, rough endoplasmic reticulum,

free ribosomes, round and oval mitochondria with parallel and narrow cristae, lysosomes, vacuoles, multivesicular bodies, microtubules, microfilaments, centrioles and occasionally cilia. The Golgi is located proximal to the nucleus and sometimes forms an arch about it. The other organelles are generally distributed about the chromaffin granules (Diaz-Flores et al., 2008).

ACCs are generally thought to form two separate populations of adrenergic and noradrenergic cells, based on their capacity to synthesize, store and release either epinephrine or norepinephrine. In the adrenal medulla of the adult rat, 15–20% of adrenal chromaffin cells exhibit the noradrenergic phenotype, while 80–85% are adrenergic (Coupland, 1989; Hodel, 2001). The noradrenergic cells are often found in the center of the medulla, while adrenergic cells tend to reside in areas adjacent to the adrenal cortex (Coupland, 1989). It is important to note that these observations whereby each chromaffin cell appears to contain a single type of granule come mostly from studies in rat and cow. In mouse ACCs, two populations of differently sized LDCGs have been described within the same cell (Figure 2.4 A). Whether these separate populations represent two distinct synthetic pathways or simply different stages of biosynthesis is unknown (Grabner et al., 2005). However, in our own amperometric recordings from mouse chromaffin cells bathed in 100 μM ryanodine, an intense form of stimulation that promotes more complete release

from granules, we indeed observe heterogeneity in the quantal size (Q) distributed as $Q^{1/3}$, where two or even three distributions best fit the data (Lefkowitz et al., 2008).

Chromaffin granules and secretory products

In ACCs secretory products are stored in large dense core granules (LDCGs) of the classical regulated secretory pathway (Burgess and Kelly, 1987) and are analogous to the LDCGs found in neurons. Chromaffin cell LDCGs are known to contain a majority of the established neuropeptides, although often at low concentrations (Toth and Hinson, 1995). In addition, LDCGs contain the catecholamines, epinephrine or norepinephrine, as well as serotonin and ATP (Winkler and Fischer-Colbrie, 1998; Chen et al., 2005). Consequently, the catecholamines are oxidizable molecules and thus are amenable to electrochemical measurements, such as amperometry and voltammetry (Teschemacher, 2005). Not only do the LDCGs of chromaffin cells contain similar molecules to the LDCGs of neurons, but they also share a similar morphology, biogenesis, life cycle and membrane composition (De Camilli and Jahn, 1990; Thomas-Reetz and De Camilli, 1994).

Depending on the type of secretory content (i.e., epinephrine or norepinephrine), LDCGs display variations in their size, shape and electron density. These variations are strikingly marked in certain species, while in others the differences are subtle. For example, in mice, rats, hamsters and dogs the differences are clearly distinct (Coupland, 1965a, b; Carmichael et al., 1987; Grabner et al., 2005), while in primates the differences are few (al-Lami, 1969; al-Lami and Carmichael, 1991). Epinephrine LDGCs vary by species and range between 50 and 350 nm in diameter (in mouse ACCs 170–350 nm). They have a round morphology, present a moderate electron density with a fine granular content appearance, and tend to exhibit a narrow and uniform light halo (Figure 2.4 B). Alternatively norepinephrine LDGCs have a larger diameter (185–495 nm in mouse ACCs) and an irregular, oval or elliptical shape with higher electron density. The core of norepinephrine LDGCs tends to be eccentrically located about its surrounding membrane (Figure 2.4 B) (Coupland, 1965a, b; Grabner et al., 2005).

In addition to the catecholamines, LDCGs contain abundant amounts of granule matrix protein chromogranins, which are precursors to the neuropeptides catestatin and pancreastatin. Amongst these are chromogranins A and B or secretogranin I, C or secretogranin II (Winkler and Fischer-Colbrie, 1992; Montero-Hadjadje et al., 2008). LDCGs also contain neuropeptides and

enkephalins (Kataoka et al., 1985), adenine nucleotides, high concentrations of Ca^{2+} (Winkler and Westhead, 1980; Winkler and Carmichael, 1982; Winkler, 1993), syntaxin 1A, synaptotagmin I (Yoo et al., 2005) and plasminogen activator (Parmer et al., 1997).

ACCs also express adrenomedullin, a peptide of the proadrenomedullin N-terminal 20 peptide (Kobayashi et al., 2003) and enzymes, such as dopamine β-hydroxylase and tyrosine hydroxylase. Epinephrine cells, but not norepinephrine cells, express phenylethanolamine-*N* methyltransferase, which catalyses the methylation reaction that converts norepinephrine into epinephrine. This reaction takes place in the cytosol and therefore the epinephrine molecules are necessarily transported back into the LDCGs via a vesicular monoamine transporter (VMAT) pump. This process is stimulated by glucocorticoids (Hodel, 2001). Additionally, ACCs secrete trophic factors that promote survival of various types of neurons (Schumm et al., 2004).

ACCs also contain a population of microvesicles that is distinct from the population of LDCGs and are closely related to neuronal synaptic vesicles. That is, these microvesicles are similar to synaptic vesicles in morphology, membrane composition, and like synaptic vesicles, they undergo exo/endocytotic recycling. In chromaffin cells these microvesicles take up and store acetylcholine but not catecholamines. Conversely, it has been shown that catecholamines, but not

acetylcholine, is taken up and stored in two populations of mature LDCGs, that differ in their relative size (Bauerfeind et al., 1993).

Physiologic effects of secretory products

From a physiological viewpoint, one of the most important jobs carried out by ACCs is to synthesize and secrete epinephrine and norepinephrine. Following release into the blood, these monoamines bind to alpha or beta adrenergic receptors on target cells of various organs, where they induce essentially the same effects as direct sympathetic nervous stimulation, though their release from ACCs leads to longer lasting and more widespread effects since they can cause effects in cells and tissues that are not directly innervated (Figure 2.5). The adrenergic target receptors belong to the family of seven-pass transmembrane proteins known as G-protein coupled receptors (GPCRs) which stimulate or inhibit intracellular signaling pathways via second messengers such as cyclic adenosine monophosphate (cAMP) and Ca^{2+}. Thus, complex physiologic responses result from stimulation of the adrenal medulla based on the differential expression of multiple receptor types in different tissues and cells. Some of the major effects mediated by catecholamine release include increased rate and force of contraction of heart muscle, constriction of blood vessels and therefore

increased arterial blood pressure, dilation of bronchioles, stimulation of lipolysis in fat cells, increased metabolic rate and glycolysis in skeletal muscle, dilation of the pupils and the inhibition of specific parasympathetic activities such as gastrointestinal secretion and motor activity (Guyton and Hall, 2000, 2006).

In addition to the catecholamines, ACCs release the neurologically active neuropeptides, which also help mediate widespread physiologic responses. For example, the chromogranins, the major peptide cargo of the LDCGs, can be cleaved after exocytosis into the neuroactive catestatins to negatively modulate the neuroendocrine activity of the releasing ACC or nearby ACCs. Furthermore, neuropeptide Y (NPY) can modulate vasoconstriction and the release of enkephalins from ACCs can serve as an endogenous opioid, acting as an analgesic to allow an organism to focus on escape or defense during the sympathetic stress response, “fight or flight” (O'Connor and Frigon, 1984; O'Connor, 2003).

Regulation by the sympathetic nervous system and “tone”

Secretion from ACCs is under control of the sympathetic autonomic nervous system. Like the neurons of the sympathetic system, ACCs are also controlled by preganglionic acetylcholine-secreting nerves originating in the spinal cord.

While the sympathetic neurons, which have fine axons that extend into their target organs, exert localized control at their axon terminals, the secretion of hormones from ACCs elicits a widespread response (Figure 2.5). Common stimuli for secretion include exercise, hypoglycemia, hemorrhage and emotional distress.

A critical feature of the autonomic nervous system is that only a very low frequency of stimulation is necessary to maintain full activation of is targeted effectors. For example, only one nerve impulse every other second is enough to maintain a normal, basal parasympathetic or sympathetic effect. Moreover maximal activation is achieved by an impulse rate near 15 times per second. By comparison, the skeletal nervous system requires a rate of 50 – 500 impulses per second to achieve maximal activation (Guyton and Hall, 2000).

Under resting conditions, colloquially known as “rest and digest”, the parasympathetic and sympathetic nervous systems are continually active at basal rates. These basal rates of activity are known as the tone. The importance of tone is that it allows the nervous system to both increase and decrease the activity of an effector organ. For example, the sympathetic tone normally keeps systemic arterioles constricted to half their maximal diameter. By increasing the degree of sympathetic stimulation above normal (supertonic),

these vessels can be further constricted. On the other hand, subtonic stimulation allows the arterioles to dilate (Guyton and Hall, 2000, 2006).

While supertonic sympathetic stimulation through direct innervation of target organs can only increase organ activity by increasing norepinephrine output, supertonic stimulation through ACCs has a more complex effect. That is, during higher rates of stimulation, ACCs also secrete neuropeptides in addition to increasing catecholamine output into the blood (Fulop et al., 2005).

References

al-Lami F (1969) Light and electron microscopy of the adrenal medulla of Macaca mulata monkey. Anat Rec 164:317-332.

al-Lami F, Carmichael SW (1991) Microscopic anatomy of the baboon (Papio hamadryas) adrenal medulla. J Anat 178:213-221.

Albillos A, Dernick G, Horstmann H, Almers W, Alvarez de Toledo G, Lindau M (1997) The exocytotic event in chromaffin cells revealed by patch amperometry. Nature 389:509-512.

Aloe L, Levi-Montalcini R (1979) Nerve growth factor-induced transformation of immature chromaffin cells in vivo into sympathetic neurons: effect of antiserum to nerve growth factor. Proc Natl Acad Sci U S A 76:1246-1250.

Bauerfeind R, Regnier-Vigouroux A, Flatmark T, Huttner WB (1993) Selective storage of acetylcholine, but not catecholamines, in neuroendocrine synaptic-like microvesicles of early endosomal origin. Neuron 11:105-121.

Bornstein SR, Ehrhart-Bornstein M, Scherbaum WA (1997) Morphological and functional studies of the paracrine interaction between cortex and medulla in the adrenal gland. Microsc Res Tech 36:520-533.

Burgess TL, Kelly RB (1987) Constitutive and regulated secretion of proteins. Annu Rev Cell Biol 3:243-293.

Carmichael SW, Spagnoli DB, Frederickson RG, Krause WJ, Culberson JL (1987) Opossum adrenal medulla: I. Postnatal development and normal anatomy. Am J Anat 179:211-219.

Chen XK, Wang LC, Zhou Y, Cai Q, Prakriya M, Duan KL, Sheng ZH, Lingle C, Zhou Z (2005) Activation of GPCRs modulates quantal size in chromaffin cells through G(betagamma) and PKC. Nat Neurosci 8:1160-1168.

Coupland RE (1965a) (Electron Microscopic Observations on the Structure of the Rat Adrenal Medulla. I. the Ultrastructure and Organization of Chromaffin Cells in the Normal Adrenal Medulla.). J Anat 99:231-254.

Coupland RE (1965b) Electron microscopic observations on the structure of the rat adrenal medulla: II. Normal innervation. J Anat 99:255-272.

Coupland RE (1989) The natural history of the chromaffin cell--twenty-five years on the beginning. Arch Histol Cytol 52 Suppl:331-341.

Coupland RE, Hopwood D (1966) The mechanism of the differential staining reaction for adrenaline-and noreadrenaline-storing granules in tissues fixed in glutaraldehyde. J Anat 100:227-243.

Crowder RE (1957) The development of the adrenal gland in man, with special reference to the origin and ultimate location of cell types and evidence in favor of the cell migration theory. Contrib Embryol 36:195-210.

De Camilli P, Jahn R (1990) Pathways to regulated exocytosis in neurons. Annu Rev Physiol 52:625-645.

Diaz-Flores L, Gutierrez R, Varela H, Valladares F, Alvarez-Arguelles H, Borges R (2008) Histogenesis and morphofunctional characteristics of chromaffin cells. Acta Physiol (Oxf) 192:145-163.

Douglas WW (1968) Stimulus-secretion coupling: the concept and clues from chromaffin and other cells. Br J Pharmacol 34:451-474.

Doupe AJ, Landis SC, Patterson PH (1985) Environmental influences in the development of neural crest derivatives: glucocorticoids, growth factors, and chromaffin cell plasticity. J Neurosci 5:2119-2142.

Fulop T, Radabaugh S, Smith C (2005) Activity-dependent differential transmitter release in mouse adrenal chromaffin cells. J Neurosci 25:7324-7332.

Fung MM, Viveros OH, O'Connor DT (2008) Diseases of the adrenal medulla. Acta Physiol (Oxf) 192:325-335.

Garcia AG, Garcia-De-Diego AM, Gandia L, Borges R, Garcia-Sancho J (2006) Calcium signaling and exocytosis in adrenal chromaffin cells. Physiol Rev 86:1093-1131.

Grabner CP, Price SD, Lysakowski A, Fox AP (2005) Mouse chromaffin cells have two populations of dense core vesicles. J Neurophysiol 94:2093-2104.

Guyton AC, Hall JE (2000) Textbook of medical physiology, 10th Edition. Philadelphia: Saunders.

Guyton AC, Hall JE (2006) Textbook of medical physiology, 11th Edition. Philadelphia: Elsevier Saunders.

Hervonen A (1971) Development of catecholamine--storing cells in human fetal paraganglia and adrenal medulla. A histochemical and electron microscopical study. Acta Physiol Scand Suppl 368:1-94.

Hingerty D, O'Boyle A (1972) Clinical chemistry of the adrenal medulla. Springfield, Ill.,: Thomas.

Hodel A (2001) Effects of glucocorticoids on adrenal chromaffin cells. J Neuroendocrinol 13:216-220.

Kataoka Y, Majane EA, Yang HY (1985) Release of NPY-like immunoreactive material from primary cultures of chromaffin cells prepared from bovine adrenal medulla. Neuropharmacology 24:693-695.

Kobayashi H, Yanagita T, Yokoo H, Wada A (2003) Pathophysiological function of adrenomedullin and proadrenomedullin N-terminal peptides in adrenal chromaffin cells. Hypertens Res 26 Suppl:S71-78.

Kohn A (1898) Uber die Nebenniere. Prag Med Wochenschr 23:193-195.

Kohn A (1902) Das chromaffine Gewebe. Ergeb Anat Entwicklungsgesch 12:253-348.

Kohn A (1903) Die Paraganglien. Arch Mikr Anat 62:263-365.

Le Douarin NM, Dupin E, Ziller C (1994) Genetic and epigenetic control in neural crest development. Curr Opin Genet Dev 4:685-695.

Lefkowitz JJ, Fogarty KE, Lifshitz LM, Bellve KD, ZhuGe R, Tuft RA, Walsh JV, Crescenzo VD (2008) Ca2+ Syntillas Decrease Spontaneous Exocytosis In Mouse Chromaffin Cells. In: Biophysical Journal, Exocytosis & Endocytosis - I, pp 425-435.

Leszczyszyn DJ, Jankowski JA, Viveros OH, Diliberto EJ, Jr., Near JA, Wightman RM (1990) Nicotinic receptor-mediated catecholamine secretion from individual chromaffin cells. Chemical evidence for exocytosis. J Biol Chem 265:14736-14737.

Montero-Hadjadje M, Vaingankar S, Elias S, Tostivint H, Mahata SK, Anouar Y (2008) Chromogranins A and B and secretogranin II: evolutionary and functional aspects. Acta Physiol (Oxf) 192:309-324.

Neher E, Marty A (1982) Discrete changes of cell membrane capacitance observed under conditions of enhanced secretion in bovine adrenal chromaffin cells. Proc Natl Acad Sci U S A 79:6712-6716.

O'Connor DT (2003) The adrenal medulla,catecholamines, and phaeochromocytoma. In: Cecil Textbook of Medicine, 22 Edition (Goldman L, Ausiello D, eds), pp 1419-1424. Philadelphia, PA: Saunders.

O'Connor DT, Frigon RP (1984) Chromogranin A, the major catecholamine storage vesicle soluble protein. Multiple size forms, subcellular storage, and regional distribution in chromaffin and nervous tissue elucidated by radioimmunoassay. J Biol Chem 259:3237-3247.

Parmer RJ, Mahata M, Mahata S, Sebald MT, O'Connor DT, Miles LA (1997) Tissue plasminogen activator (t-PA) is targeted to the regulated secretory pathway. Catecholamine storage vesicles as a reservoir for the rapid release of t-PA. J Biol Chem 272:1976-1982.

Quinan C, 1933 AAB (1933) Observations on human adrenals with special reference to the relative weight of the normal medulla. Ann Intern Med 6:1180–1192.

Schumm MA, Castellanos DA, Frydel BR, Sagen J (2004) Improved neural progenitor cell survival when cografted with chromaffin cells in the rat striatum. Exp Neurol 185:133-142.

Teschemacher AG (2005) Real-time measurements of noradrenaline release in periphery and central nervous system. Auton Neurosci 117:1-8.

Thomas-Reetz AC, De Camilli P (1994) A role for synaptic vesicles in non-neuronal cells: clues from pancreatic beta cells and from chromaffin cells. Faseb J 8:209-216.

Toth IE, Hinson JP (1995) Neuropeptides in the adrenal gland: distribution, localization of receptors, and effects on steroid hormone synthesis. Endocr Res 21:39-51.

Uceda G, Colombo JA, Michelena P, López MA (1995) Rat striatal astroglia induce morphological and neurochemical changes in adult bovine, adrenergic-enriched adrenal chromaffin cells in vitro. Rest Neurol Neurosci 8:129–136.

Unsicker K, Krisch B, Otten U, Thoenen H (1978) Nerve growth factor-induced fiber outgrowth from isolated rat adrenal chromaffin cells: impairment by glucocorticoids. Proc Natl Acad Sci U S A 75:3498-3502.

Wilburn LA, Jaffe RB (1988) Quantitative assessment of the ontogeny of met-enkephalin, norepinephrine and epinephrine in the human fetal adrenal medulla. Acta Endocrinol (Copenh) 118:453-459.

Winkler H (1993) The adrenal chromaffin granule: a model for large dense core vesicles of endocrine and nervous tissue. J Anat 183 (Pt 2):237-252.

Winkler H, Westhead E (1980) The molecular organization of adrenal chromaffin granules. Neuroscience 5:1803-1823.

Winkler H, Carmichael SW (1982) The chromaffin granule. In: A.M. Poisner & J.M. Trifaró (eds) The Secretory Granule, pp 3–79. Amsterdam: Elsevier.

Winkler H, Fischer-Colbrie R (1992) The chromogranins A and B: the first 25 years and future perspectives. Neuroscience 49:497-528.

Winkler H, Fischer-Colbrie R (1998) Regulation of the biosynthesis of large dense-core vesicles in chromaffin cells and neurons. Cell Mol Neurobiol 18:193-209.

Yoo SH, You SH, Huh YH (2005) Presence of syntaxin 1A in secretory granules of chromaffin cells and interaction with chromogranins A and B. FEBS Lett 579:222-228.

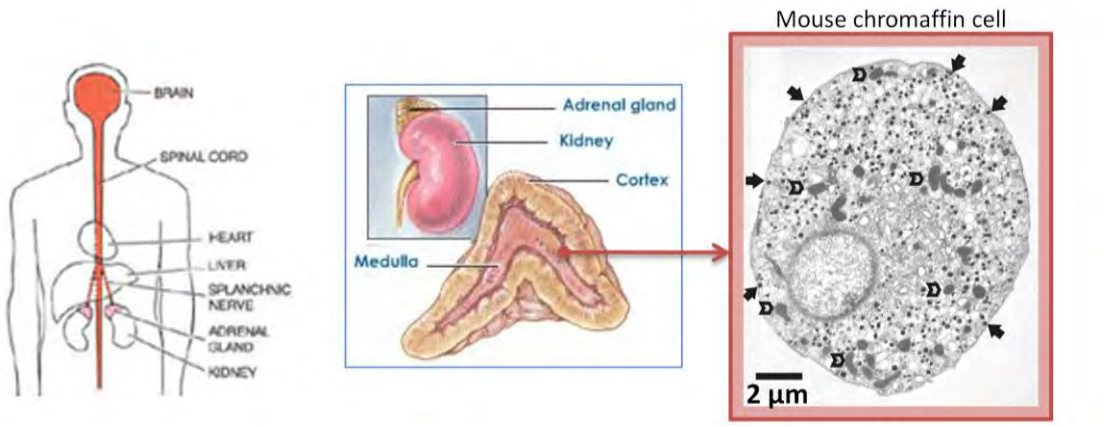

Figure 2.1 Adrenal chromaffin cells (ACCs) reside within the adrenal medulla. The adrenal glands are located just above the kidneys (Left) and are comprised of the inner medulla, where the ACCs reside, and an outer cortex surrounded by the capsule (Center). An electron micrograph of a section from an isolated mouse ACC is shown at right, where the filled arrows depict Large Dense Core Granules (LDCGs) at the cell membrane and open arrowheads point to mitochondria.

(Figure adapted from Carmichael, S.W. 1979-84. The Adrenal medulla. In Eden Press ; Agent, Montréal, Québec, Canada; Buffalo, N.Y. v. and Grabner et al., 2005)

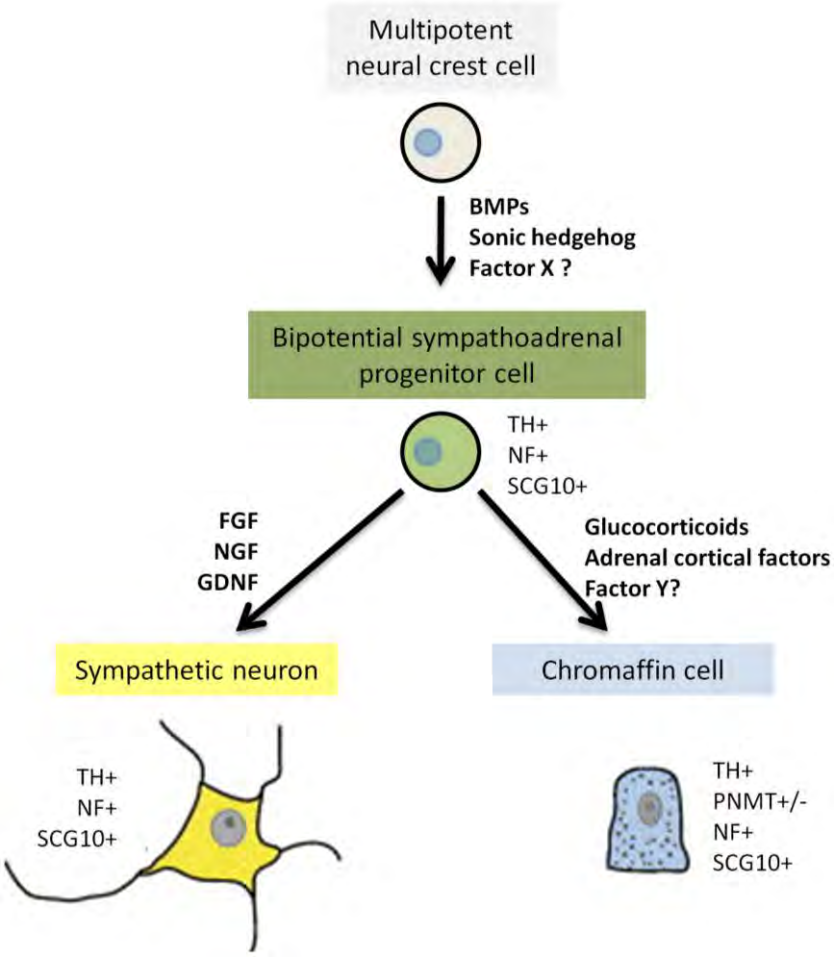
Multipotent
neural crest cell
BMPs
Sonic hedgehog
Factor X ?
Bipotential sympathoadrenal
progenitor cell
TH+
NF+
SCG10+
FGF
NGF
GDNF
Glucocorticoids
Adrenal cortical factors
Factor Y?
Sympathetic neuron
Chromaffin cell
TH+
NF+
SCG10+
TH+
PNMT+/-
NF+
SCG10+

Figure 2.2 Adrenal chromaffin cells and sympathetic neurons both derive from multipotent neural crest cells. Sympathetic neurons and chromaffin cells originate from a pool of bipotential TH+ positive sympathoadrenal progenitors that are initially located in the primary sympathetic ganglia. These cells re-migrate to the secondary sympathetic ganglia or the adrenal anlage, where they undergo final differentiation in response to the local environment. BMPs, bone morphogenetic proteins; FGF, fibroblast growth factor; GDNF, Glial cell line-derived neurotrophic factor; NGF, nerve growth factor.

(Figure modified after Ghzili, H.L. GrumolatoE. ThouennonY. TanguyV. TurquierH. VaudryY. Anouar. 2008. Role of PACAP in the physiology and pathology of the sympathoadrenal system. *Front Neuroendocrinol*. 29:128-141. and Huber, K. 2006. The sympathoadrenal cell lineage: specification, diversification, and new perspectives. *Dev Biol*. 298:335-343.)

A

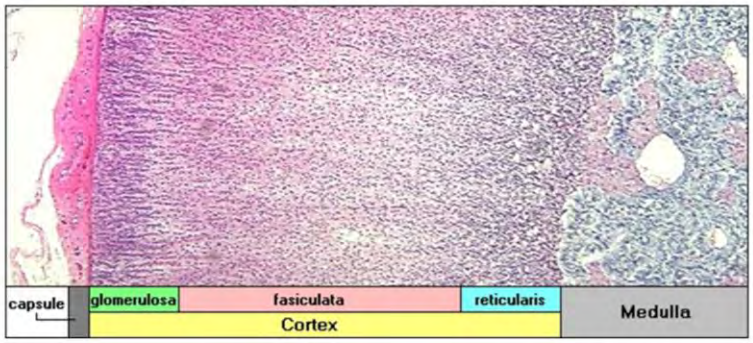
capsule
glomerulosa
fasiculata
reticularis
Cortex
Medulla

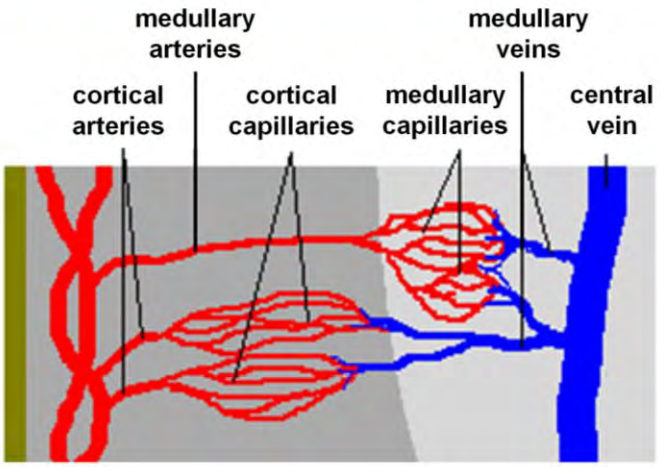
medullary arteries
medullary veins
cortical arteries
cortical capillaries
medullary capillaries
central vein

B

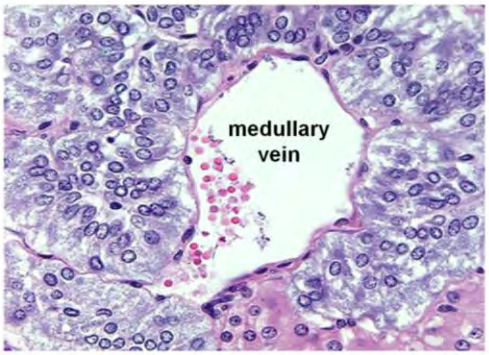
medullary vein

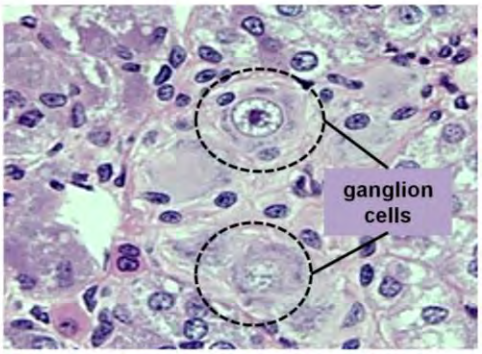
ganglion cells

Figure 2.3 **Structural and functional characteristics of the adrenal gland and medulla.** **A. (Top)** Three cortical zones and part of the medulla are depicted in a section of rabbit adrenal gland. **(Bottom)** The adrenal is a highly vascularized structure. Blood empties from the cortical and medullary veins through a single large central vein, which leaves the adrenal either by the vena cava or renal vein. **B. (Left)** In the intact medulla, ACCs are columnar or ellipsoidal in shape and rather basophilic. They present with a granular cytoplasm due to hormone-containing granules. They are typically arranged in clusters around medullary veins, as seen in this image of a rabbit adrenal (H&E stain). **(Right)** The adrenal medulla is abundantly innervated by preganglionic sympathetic fibers. Small numbers of sympathetic ganglion cells are also commonly observed in the medulla. Two ganglion cells are circled.

(Courtesy of Richard A. Bowen, DVM, PhD, Colorado State University.)

A

Mouse adrenal chromaffin cell

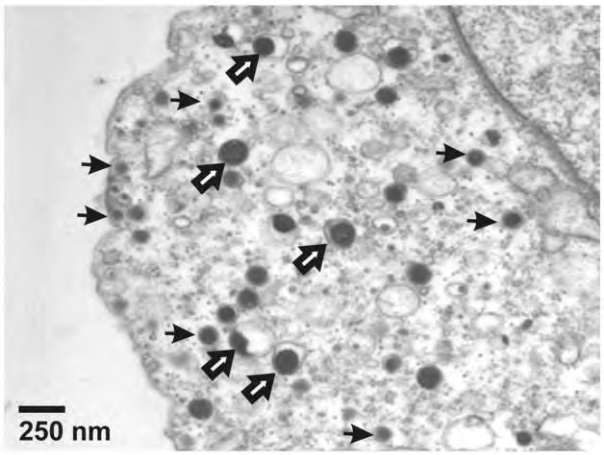

B

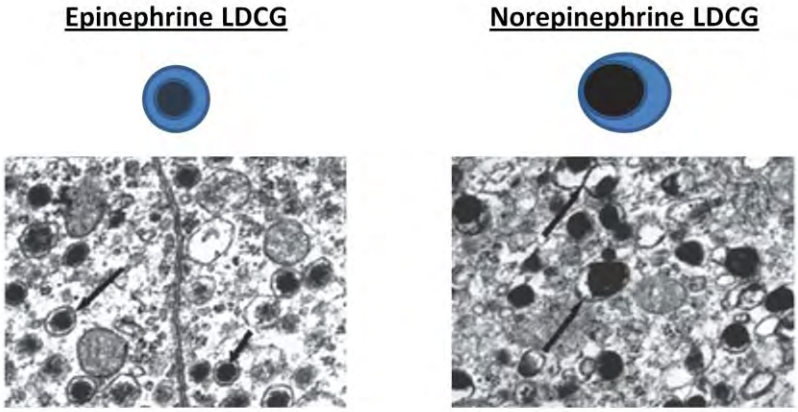

Rat adrenal chromaffin cells

Figure 2.4 Electron micrographs of large dense core granules (LDCGs) in mouse and rat adrenal chromaffin cells (ACCs). A. There appear to be two populations of different sized LDCGs centered at 187 and 330 nm in mouse ACCs. Typically the larger LDCGs (open arrows) possess excess membrane giving a halo appearance around the granule's dense core, while the cores of smaller granules (filled arrow) appear to have a tightly associated membrane. **B.** Epinephrine granules are round, present moderate density, and the light halo is narrow and uniform (Left, arrows), while norepinephrine granules can exhibit variable shape and generally have a larger diameter, higher electron density and their dense cores are eccentrically situated with regard to their surrounding membranes (Right, arrows). (EM at 14,000X).

(Adapted from Grabner et al., 2005 (Top) and Diaz-Flores et al., 2008)

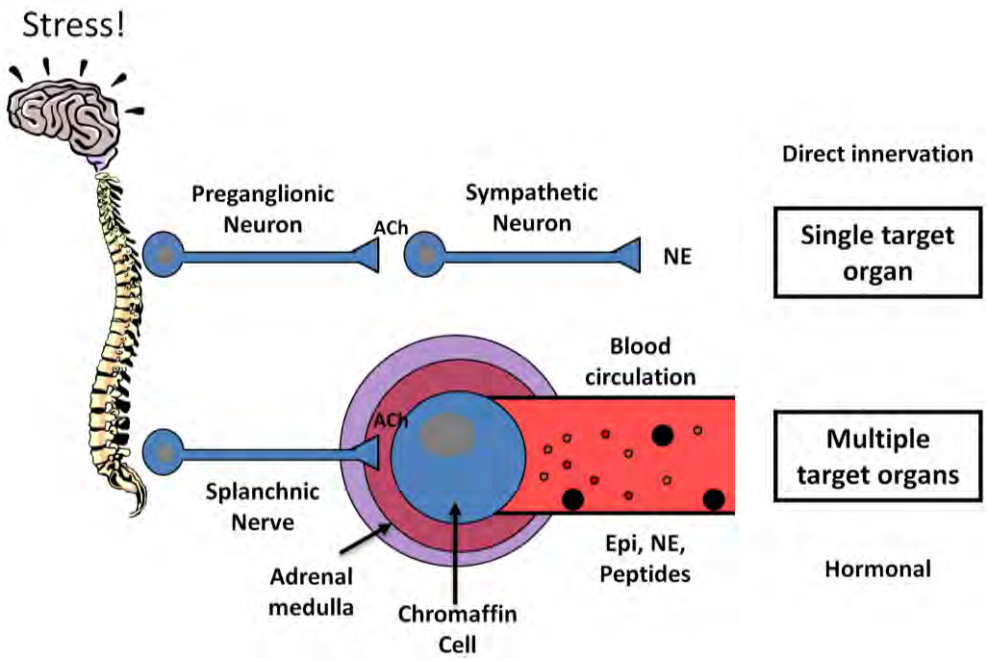

Figure 2.5 Regulation of ACC secretion by the sympathetic nervous system. Catecholamine or peptide secretion from ACCs of the adrenal medulla is regulated by neural stimuli. During moderate stimulation, associated with the basal sympathetic tone, only low levels of catecholamines are released into the blood. During higher levels of stimulation associated with the stress response known as "fight or flight" more catecholamines and also peptides are released. Stress leads to secretion both in ACCs and sympathetic neurons. Impulses arrive at both kinds of cells through preganglionic cholinergic neurons originating in the spinal cord. Sympathetic neurons discharge norepinephrine (NE) locally, while ACCs secrete epinephrine (Epi), NE and peptides into the bloodstream, affecting multiple organs.

Chapter 3

Exocytosis in the chromaffin cell: machinery and mechanisms

Compared to neurons

Not surprisingly, the release process in ACCs also shares basic principles with the release process in neurons. Yet, important differences exist. The most salient difference lies in the spatial organization of LDCGs and voltage-gated Ca^{2+} channels. That is, chromaffin cells are characterized by a large distance between LDCGs and Ca^{2+} channels. Accordingly, isolated ACCs lack active zones and experience only a limited degree of regionalized LDCG release, which may in part be related to the overall spherical shape of isolated chromaffin cells. Another difference is that the coupling of Ca^{2+} channels to the release process is less tight than in synapses. The same high threshold Ca^{2+} channel subtypes described in neurons (Olivera et al., 1994) have also been identified and characterized in mouse ACCs, although the extent to which each type contributes to release varies (Cuchillo-Ibanez et al., 2002). In addition, the coupling between individual action potentials (APs) and release events is usually loose. In spite of this loose coupling, however, the presence of multiple channel types and vesicle pools that are released with different delays, in concert with

adaptations in firing properties of these cells, give rise to a system that can be finely modulated, and seem to ensure a reliable coupling between AP, Ca^{2+} influx and release (Moser and Neher, 1997b, a; Winkler and Fischer-Colbrie, 1998).

Granule pools and mobilization

The average bovine ACC contains between 17,000 - 22,000 LDCGs (Vitale et al., 1995; Plattner et al., 1997). Different LDCG pools have been defined by the readiness of granules within that pool to be released depending on kinetic, morphologic, and regulatory properties (Garcia et al., 2006) (Figure 3.1). The majority of granules are found in a distinct cellular compartment called the reserve pool, where they may remain for an extended period of time after their formation. From the reserve pool, LDCGs are mobilized into another distinct compartment called the readily releasable pool, whereby granules can be mobilized for release within a time frame of seconds. As Figure 3.1 depicts, an intermediate pool, the slowly releasable pool, has also been described where granules reside in a docked but unprimed state (Steyer et al., 1997; Trifaro et al., 1997; Voets et al., 1999). It has been estimated that about 1–3% of LDCGs comprise the readily releasable pool (Plattner et al., 1997).

LDCG density is decreased as the granules approach the cell membrane (Plattner et al., 1997) and this traffic is highly regulated by the remodeling of the subplasmalemmal filamentous actin (F-actin) cytoskeleton (Aunis and Bader, 1988; Vitale et al., 1995; Gasman et al., 2003). Upon stimulation, the subplasmalemmal F-actin network undergoes rapid disassembly in a reversible manner (Cheek and Burgoyne, 1986; Burgoyne et al., 1993).

LDCGs situated within the releasable pool are docked at the plasma membrane and may be in a primed (readily releasable pool) or unprimed stage (unprimed pool). That is, the granules are either fully fusion competent or may require more priming steps to enter that stage. The final priming steps have been shown to require ATP. Of the 22,000 LDCGs in a bovine ACC, the number of docked LDCGs is estimated between 364 and 629 (Plattner et al., 1997). Furthermore, the reserve pool and the readily releasable pool can be selectively mobilized depending upon differential levels of secretion and the required secretagogue (Duncan et al., 2003; Fulop et al., 2005; Haynes et al., 2007; Doreian et al., 2009).

Stages in the exocytosis of LDCGs

After LDCGs are recruited to the plasma membrane, they go through several stages before their exocytic release (Figure 3.2). In the first stage, LDCGs undergo docking, where they are linked and tethered to the plasma membrane. This is followed by a priming step, where attachment to the final release site is advanced and the granule becomes competent for exocytosis. The contents of the LDCGs are ultimately released into the extracellular space when a sufficient rise in Ca^{2+} within the vicinity of the granules serves as the final trigger for exocytosis, whereby the LDCG and the plasma membrane fuse with each other. After exocytosis, fused LDCGs can be retrieved through endocytosis and thereby undergo another round of secretion (Sudhof, 1995).

Machinery and mechanisms by exocytotic stage

Docking: Electron micrographs of mouse embryonic ACCs reveal that about 30% of LDCGs localize to within 50 nm of the plasma membrane. LDCGs located within this distance of the membrane are anatomically regarded as being in a docked state.

Of the major molecules identified to be involved in exocytosis, Munc18-1 and the syntaxins play a crucial role in docking. In ACCs from Munc18-1

knockout mice, the fact that less than 5% of LDCGs are able to dock at the plasma membrane strongly suggests that Munc18-1 is the critical molecule in this process (Voets et al., 2001b; Gulyas-Kovacs et al., 2007). Since Munc18-1 is a soluble protein, it is thought that it regulates docking of LDCGs by binding to the membrane proteins on the granules or the plasma membrane or both.

The syntaxins, which are able to interact with munc18-1 (Hata et al., 1993; Pevsner et al., 1994), are also critical for docking. There are many isoforms of syntaxin and at least five isoforms (syntaxin1A, 1B, 2, 3 and 4) are localized at the plasma membrane. Due to possible functional redundancy among the isoforms, examination of the precise role for syntaxin in docking has been difficult. Nonetheless recent evidence has emerged that support a critical role for plasma membrane syntaxins in docking. First, the expression level of syntaxin1 is reduced by about half in Munc18-1-deficient neurons and ACCs (Voets et al., 2001b; Gulyas-Kovacs et al., 2007). And second, viral infection of ACCs with botulinum neurotoxin C1, which cleaves syntaxin1A, 1B, 2 and 3, is shown to significantly reduce docking of LDCGs (deWit et al., 2006).

Other members of the soluble *N*-ethylmaleimide-sensitive factor attachment protein receptor (SNARE) proteins, including SNAP-25 and synaptobrevin, do not seem to be involved in the docking of LDCGs. Although secretion is strongly suppressed in SNAP-25 deficient ACCs, the docking of the

LDCGs is not affected (Sorensen et al., 2003b). A study involving the double knockout of synaptobrevin2 and cellubrevin, a ubiquitous isoform of synaptobrevin, yields similar results (Borisovska et al., 2005). Therefore, it is the interaction of Munc18-1 and syntaxin and, not the SNARE protein complex that is crucial in docking (Gulyas-Kovacs et al., 2007).

Priming: Once the LDCGs are docked, they must be primed to undergo fast Ca^{2+}-triggered fusion with the plasma membrane. The priming process involves both ATP-dependent and -independent steps. In ACCs it has been shown that ATP is a necessary component prior to the final exocytic Ca^{2+} trigger (Holz et al., 1989; Xu et al., 1998). Three cytosolic proteins have been identified to assume a prominent role in the ATP-dependent priming steps of Ca^{2+}-triggered exocytosis. These proteins include phosphatidylinositol transfer protein (PITP) (Hay and Martin, 1993), type I phosphatidylinositol 4-phosphate-5-kinase (PIP5KI) (Hay et al., 1995) and NSF (Malhotra et al., 1988).

The recruitment of phosphoinositide by PITP followed by the phosphorylation of phosphoinositide by PIP5KI is thought to constitute a major component of ATP-dependent priming. This is based on the fact that PITP and PIP5KI are found to be essential for priming to occur in PC12 cells, derivatives of ACCs (Hay and Martin, 1993; Hay et al., 1995). Essentially, PIP5KI requires ATP

to phosphorylate phosphatidylinositol 4-phosphate (PIP) and generate phosphatidylinositol 4,5-bisphosphate (PIP2). PIP2 then binds to synaptotagmin (Syt) and the Ca^{2+}-dependent activator protein for secretion 1 (CAPS1), two major proteins implicated in the final steps of Ca^{2+}-triggered exocytosis. In support of this view, the level of PIP2 has been shown to control the size of the releasable granule pool in ACCs (Milosevic et al., 2005). The α- and γ- isoforms of PIP5KI can prime LDCG secretion (Wang et al., 2005), while LDCG secretion is partially reduced in PIP5KIγ knockout mice (Gong et al., 2005). Therefore, the generation and regulation of PIP2 by the PITP and PIP5KI proteins seem to be crucial events in ATP-dependent priming.

The ATPase protein, N-ethylmaleimide-sensitive factor (NSF), is also known to serve a crucial role in ATP-dependent priming (Malhotra et al., 1988). This is supported by studies in PC12 cells where NSF increases granule priming leading to secretion (Banerjee et al., 1996a) and where the endogenous t-SNARE proteins, syntaxin 1 and SNAP-25 are found to be highly reactive, readily forming SNARE complexes with exogenously added v-SNAREs, due to high levels of NSF activity (Lang et al., 2002). Basically, once SNARE proteins have participated in a round of exocytosis they are left in a residual stable complex within the plasma membrane. In this conformation known as the *cis*-complex, SNARE proteins are tethered together on the same membrane and are

considered inactive for exocytosis. NSF importantly disassembles this complex into the *trans*-complex whereby the SNARE proteins are no longer on the same membrane so that another round of exocytosis can proceed. That is, NSF binds to SNAP proteins in the cis-SNARE complex in an ATP-dependent manner. Once bound, NSF then hydrolyzes ATP to pry the SNARE complex apart. Since the *trans*-complex is resistant to NSF-mediated disruption (Weber et al., 2000), NSF is thought to promote the active form of the SNARE complex.

At least two protein groups, the Munc13 proteins and CAPS1, are thought to serve a crucial role in ATP-independent priming. In neurons, Munc13-1, -2 and -3 are considered to be the major players in this type of priming (Augustin et al., 1999; Varoqueaux et al., 2002). The priming function of Munc13-1 is thought to proceed through a syntaxin1 binding interaction that displaces Munc18-1 and renders the t-SNARE protein into an open conformation whereby it can form a SNARE complex (Dulubova et al., 1999; Sassa et al., 1999). The C-terminal residues of Munc13-1 and Munc18-1 are thought to compete for binding to an overlapping domain on syntaxin1 (Betz et al., 1997). In ACCs, though, the expression level of Munc13-1 is low, and Munc13-1 knockout mice show no signs of secretion defects (Stevens et al., 2005). Even so, over expressing Munc13-1 in ACCs leads to an increase in LDCG secretion (Ashery et al., 2000;

Stevens et al., 2005). Furthermore, Munc13-1 point mutants that do not bind syntaxin1 also do not prime LDCG exocytosis (Stevens et al., 2005).

While it is established that Munc13-1 is critical for priming, the current view of its specific function, to displace Munc18-1 from syntaxin1 by competitively binding to syntaxin1, has recently become questionable. In neurons, for example, a smaller domain (residues 1045–1531) within the domain (residues 1100–1735) for LDCG priming in ACCs (Stevens et al., 2005) has been uncovered that does not contain a syntaxin1 binding site (Basu et al., 2005). So the binding of Munc13-1 to syntaxin1 may exclusively contribute to priming in ACCs. Furthermore, Munc18-1 not only can bind to syntaxin1, but it can also bind to the entire SNARE complex (Dulubova et al., 1999; Zilly et al., 2006). Munc18-1 also facilitates SNARE-mediated lipid fusion reactions *in vitro* (Shen et al., 2007). For LDCG exocytosis in ACCs Munc 18-1 also serves an additional role in priming beyond that of docking (Gulyas-Kovacs et al., 2007). These studies suggest that Munc13-1 and Munc18-1 may not compete for binding to syntaxin1, but could instead act together on the SNARE complex to promote priming.

Ca^{2+}-dependent activator protein for secretion 1 (CAPS1), a cytosolic protein which contains a Munc13 homology domain, is also involved in priming (Fujita et al., 2007; Sugita, 2008). At least in PC12 cells, the protein acts at a

rate-limiting, Ca^{2+}-dependent priming step. Specifically, CAPS1 contains a Pleckstrin homology (PH) domain that binds to PIP2 in a Ca^{2+}-based manner. This interaction with PIP2 seems to regulate the number of LDCGs that undergo exocytosis (Grishanin et al., 2002; Grishanin et al., 2004).

In mouse ACCs, however, the priming function of CAPS1 is not so clear. This is because CAPS1-deficient embryonic ACCs suggest that CAPS1 may play a different role in loading catecholamines into LDCGs without necessarily having a role in the actual exocytosis (Speidel et al., 2005), since that study found no defects in LDCG exocytosis. But embryonic ACCs also express CAPS2, a close isoform of CAPS1, which raises the possibility of a functional redundancy. Since CAPS1 knockout mice die immediately after birth it is difficult to analyze the function of this protein in the Adult ACC, where CAPS2 is no longer expressed (Speidel et al., 2003). A CAPS1 knockdown line of PC12 cells, which also do not express CAPS2, has recently been employed to circumvent this issue (Fujita et al., 2007). That study finds CAPS1 to be critical in the priming and refilling of the releasable pool of LDCGs, but *not* for granule loading. These conclusions are based on capacitance recordings that showed reductions in the fast and the slow burst components as well as in the sustained release component when CAPS1 is knocked down. Therefore CAPS1 not only plays a critical role in Ca^{2+}-

dependent, regulated exocytosis but also in constitutive exocytosis downstream of granule docking (Fujita et al., 2007).

Triggering: After LDCGs are docked and primed, they are triggered to fuse with the plasma membrane. The trigger is well known to be Ca^{2+} influx into the same microdomain of the LDCGs through Ca^{2+} channels during membrane depolarization. This implies the presence of a Ca^{2+} sensor at the exocytic site. That sensor has been thought for some time to be synaptotagmin (Syt), a membrane protein associated with LDCGs and synaptic vesicles (Perin et al., 1990).

There is compelling evidence for this idea. In neurons, Syt1-knockout mice show a marked decrease in Ca^{2+}-dependent neurotransmitter release from synaptic vesicles (Geppert et al., 1994; Fernandez-Chacon et al., 2001) and in ACCs from these mice, LDCG secretion is also partially reduced (Voets et al., 2001a). Exocytosis in ACCs can be broken down into three components: a fast burst component, a slow burst component and a refilling or sustained component which are representative of the RRP, SRP and the UPP, respectively (Figure 3.1) (Neher and Sakaba, 2008). Since Syt1-deficient ACCs show a selective reduction in the fast bursting component of Ca^{2+}-dependent exocytosis it is most

likely that Syt1 serves as the Ca^{2+}-sensor (Voets et al., 2001a; Sorensen et al., 2003a).

The mechanism Syt1 employs to trigger exocytosis is still unknown. The fact that there are at least 14 isoforms of Syt1 makes this particularly hard to investigate (Sudhof, 2002). For example, at least in PC12 cells, Syt1 and Syt9 may function as redundant Ca^{2+} sensors (Lynch and Martin, 2007). On the other hand, a clue comes from the fact that Syt1 and its targets must interact within a range of Ca^{2+} concentrations optimal for triggering exocytosis. In ACCs, this range is 1-10 μM (Neher and Sakaba, 2008). Furthermore, Syt contains two Ca^{2+}-binding C2 domains that bind to phospholipids, including PIP2, in a Ca^{2+}-dependent manner (Brose et al., 1992; Sutton et al., 1995; Arac et al., 2006). Accordingly, the major targets of Syt appear to be phospholipids. This is supported by the fact that C2 domains inhibit Ca^{2+}-triggered exocytosis when introduced into permeabilized PC12 cells. Moreover, the ability of the C2 domains to inhibit secretion correlates with their ability to bind phospholipids (Sugita et al., 2002; Sugita, 2008).

Syt can also interact with syntaxin1 (Bennett et al., 1992; Shao et al., 1997) and SNAP-25 (Zhang et al., 2002) in a Ca^{2+}-dependent manner. In PC12 cells Syt1 specifically binds to the C-terminal residues of SNAP-25 and LDCG secretion is decreased if those residues are mutated.

GTP can also serve as a trigger for exocytosis in a Ca^{2+}-independent manner in ACCs (Bittner et al., 1986; Ahnert-Hilger et al., 1992; Burgoyne and Handel, 1994). In fact, GTP triggers exocytosis without increasing intracellular Ca^{2+} in a range of other secretory cells including PC12 cells (Klenchin et al., 1998), pancreatic beta cells (Regazzi et al., 1989) and mast cells (Gomperts, 1983; Fernandez et al., 1984). In PC12 cells, this GTP-triggered form of exocytosis does not require cytosolic proteins, ATP or Ca^{2+} (Klenchin et al., 1998). Furthermore, since the clostridial neurotoxins can block both GTP-triggered (Banerjee et al., 1996b; Glenn and Burgoyne, 1996; Wang et al., 2004) and Ca^{2+}-triggered exocytosis, the only difference between the two forms may be the signal sensor that triggers exocytosis in each case.

The major GTP sensors in this type of secretion are currently thought to be the RalA and RalB GTPases (Wang et al., 2004; Li et al., 2007). These proteins interact with an octameric protein complex termed the exocyst complex, which contains Sec5 (Hsu et al., 1996). Ral physically binds to Sec5 in a GTP-based manner (Moskalenko et al., 2002; Sugihara et al., 2002). Unfortunately, just as the Ca^{2+}-dependent mechanism by which Syt1 triggers exocytosis is unknown, the mechanism by which the GTP-dependent interaction between Ral and the exocyst complex are employed to trigger exocytosis also remain a mystery.

Fusion: The fusion step in exocytosis requires that the LDCG come into contact with the plasma membrane, allowing lipids to flow from one bilayer to the other. To accomplish this, the energetically highly unfavorable process of displacing water from between the two hydrophilic bilayers must be overcome. The SNARE proteins are thought to catalyze this final fusion step (Jahn and Scheller, 2006).

The SNARE complex essentially consists of four SNARE motifs; one from syntaxin1, two from SNAP-25 and one from synaptobrevin2. These motifs are aligned in parallel with their transmembrane domains next to each other (Sutton et al., 1995). The current view is that the zippering of the SNARE motifs from their N-terminus to their C-terminal membrane domains act like a winch using energy freed when the interacting helices wrap around each other to pull the two bilayers together (See Figure 3.2, Fusion).

Many studies have tested this idea in the ACC. Basically, any mutations designed to impair the zippering of SNAREs lead to a decrease in exocytosis in these cells (Sugita 2008). Furthermore, studies where the C-terminus of SNAP-25 is mutated reveal a decrease in the fast burst phase of exocytosis. This suggests that the C-terminal region of the SNARE complex is strongly coupled to exocytosis triggering. On the other hand, the N-terminal region probably is not,

since mutations in the N-terminus do not significantly affect exocytosis (Borisovska et al., 2005; Sorensen et al., 2006).

Fusion pores & mode

ACCs secrete their transmitter molecules when LDCGs fuse with the cell membrane, and form what is termed a fusion pore, which connects the granule lumen with the cell exterior. Once formed, the fusion pore either closes, allowing the granule to be reused (kiss-and-run or transient exocytosis) (Ceccarelli et al., 1973), or it fully expands whereby the granule membrane merges with the plasma membrane (full fusion exocytosis) (Heuser and Reese, 1973). The fusion pore can also fluctuate between an open and a closed state within the millisecond timeframe (flickering) before fully fusing (Fernandez et al., 1984). Thus, fusion pore behavior can lead to two separate modes of exocytosis based on whether the dense-core of the granule is completely or incompletely released.

The exocytic mode is thought to be heavily influenced by sympathetic activity (Takiyyuddin et al., 1990; Watkinson et al., 1990). This means that the various constituents within the granule can be retained in a selective manner. For example, intense stimuli results in full fusion and complete release of granule contents (Viveros et al., 1971), where catecholamines and neuropeptides within

the same LDCG (Winkler and Westhead, 1980) are released at the same time. Conversely, more modest levels of stimulation lead to the kiss-and-run mode. This mode is characterized by a more rapid and transient release of catecholamines through a restricted fusion pore (~4 nm in diameter) (Klyachko and Jackson, 2002). In this case the granules remain intact after exocytosis, and the larger neuropeptide cargos within the granule are retained (Fulop et al., 2005). Thus, LDCG exocytosis seems to employ a size exclusion mechanism to differentially release catecholamines and neuropeptides that are co-packaged in the same granule (Takiyyuddin et al., 1990; Watkinson et al., 1990; Takiyyuddin et al., 1994). In addition to fusion pore size, pore duration can also importantly affect the amount of transmitter released during the exocytic response. In sum, the ACC can selectively release its secretory molecules by complete or incomplete exocytosis by dilating with full fusion, or by closing with transient fusion. In transient fusion, the amount of transmitter released can be further modulated by controlling the open time of the pore (An and Zenisek, 2004) (Zhou et al., 1996; Albillos et al., 1997; Ales et al., 1999).

Analyzing exocytosis with amperometry

Much of what we know about exocytic modes of fusion in ACCs derives from studies using carbon fiber amperometry (Figure 3.3). This technique produces a current trace at high temporal resolution (< 1 ms) and sensitivity (< 1,000 molecules), whereby spikes in the current represent the molecules released from single granules. While the area under the spike is proportional to the amount of transmitter, the spike shape provides kinetic information about each step of release, from formation of the fusion pore, to pore expansion, through diffusion of the vesicular contents. In contrast to the quantal responses in postsynaptic cells, which typically vary only in frequency, amperometric presynaptic recordings have revealed that individual events can vary in size and shape (Evanko, 2005; Mosharov and Sulzer, 2005).

These variations are thought to depend on the opening and closing of the fusion pore (Fisher et al., 2001). Upon the initial formation of the fusion pore, a small amount of transmitter diffuses out as the pore slowly expands and produces what is known as a prespike foot signal on the current trace (Figure 3.3). Dependent upon fusion pore modulation, the initial pore can either rapidly expand or become unstable and close. Rapid pore expansion produces a quick spike in the trace immediately following the prespike foot. This type of amperometric signal is difficult to interpret in terms of exocytic mode, since an

expanding fusion pore that collapses into the cell membrane (full fusion) could produce the same spike signal as a fusion pore that first dilates, and then rapidly closes (kiss-and-run) (Figure 3.3). Furthermore, sometimes the fusion pore forms and expands so quickly that just a spike shows up in the record with no prespike foot, another situation where it is difficult to discern the mode. On the other hand, when the fusion pore closes without dilating, only the prespike foot is left on the current trace. These stand-alone-foot (SAF) events are much easier to interpret, as they are taken to exclusively represent the kiss-and-run mode. In one other type of event, the fusion pore fluctuates between an open and a closed state (flickering) before closing or dilating, which can show up on the amperometric record as a longer duration bumpy SAF or a bumpy prespike foot (Chow et al., 1992; Wang et al., 2001; Wang et al., 2003).

Endocytosis of LDCGs

After exocytosis, the LDCG membrane and its components can be recovered from the cell membrane by a process called endocytosis. In ACCs there are two basic mechanisms of endocytosis which largely depend on the mode of exocytosis. That is, incomplete or kiss-and-run exocytosis results in an endocytic process distinct from that by which granule membrane retrieval is accomplished after complete or full fusion exocytosis.

In kiss-and-run style exocytosis, where the dense core is retained by the granule, the endocytic mechanism is a clathrin-independent reversal of the fusion process that depends on the activation of protein kinase C (PKC) (Chan and Smith, 2003). In this case, the fusion pore opens only enough to allow small transmitter release and then rapidly closes, maintaining an intact granule (Barg et al., 2002). This form of rapid endocytosis, compensatory endocytosis, is energetically efficient since it allows granule components to remain in position together on the same granule, therefore making the granule instantly available for catecholamine reloading (Henkel and Almers, 1996; Engisch and Nowycky, 1998; Holroyd et al., 2002; Taraska et al., 2003; Taraska and Almers, 2004). In ACCs there is a significant fraction of LDCGs, corresponding to those proteins whose elimination is slower, which undergo rapid compensatory endocytosis (Perrais et al., 2004). This rapid endocytosis (msec – sec), is triggered by Ca^{2+} (Neher and Zucker, 1993; Artalejo et al., 1995), and the recapture of fusing secretory granules involves the protein dynamin-1. Another form of rapid endocytosis, excess endocytosis, can occur in ACCs whereby membrane retrieval exceeds the amount of exocytosis. This process is mediated by GTP and calmodulin (Artalejo et al., 1995; Artalejo et al., 1996).

Full fusion exocytosis, on the other hand, results in a slower form of endocytosis. Once the LDCG has fused with the cell membrane and all its

contents are completely released, the retrieval of granule membrane and its components are accomplished by a Ca^{2+}-independent, clathrin-mediated mechanism (Geisow et al., 1985). In this process granule membrane is selectively retrieved from the cell surface according to its membrane components. Specific granule proteins, such as synaptotagmin, are marked by accessory proteins which recruit a clathrin coat to that membrane area to reform a granule. The clathrin-coated granule is then severed by the protein dynamin-2, which is thought to form a ring around the neck of the endocytosing granule. The granule is next internalized by the endosome and transported by to the trans-Golgi network for repacking. In the ACC this process occurs in a timeframe of about 30 minutes. By 6 hours LDCG membrane components reappear in new granules (Lingg et al., 1983; Patzak and Winkler, 1986; Fulop et al., 2005).

References

Ahnert-Hilger G, Wegenhorst U, Stecher B, Spicher K, Rosenthal W, Gratz M (1992) Exocytosis from permeabilized bovine adrenal chromaffin cells is differently modulated by guanosine 5'-[gamma-thio]triphosphate and guanosine 5'-[beta gamma-imido]triphosphate. Evidence for the involvement of various guanine nucleotide-binding proteins. Biochem J 284 (Pt 2):321-326.

Albillos A, Dernick G, Horstmann H, Almers W, Alvarez de Toledo G, Lindau M (1997) The exocytotic event in chromaffin cells revealed by patch amperometry. Nature 389:509-512.

Ales E, Tabares L, Poyato JM, Valero V, Lindau M, Alvarez de Toledo G (1999) High calcium concentrations shift the mode of exocytosis to the kiss-and-run mechanism. Nat Cell Biol 1:40-44.

An S, Zenisek D (2004) Regulation of exocytosis in neurons and neuroendocrine cells. Curr Opin Neurobiol 14:522-530.

Arac D, Chen X, Khant HA, Ubach J, Ludtke SJ, Kikkawa M, Johnson AE, Chiu W, Sudhof TC, Rizo J (2006) Close membrane-membrane proximity induced by Ca(2+)-dependent multivalent binding of synaptotagmin-1 to phospholipids. Nat Struct Mol Biol 13:209-217.

Artalejo CR, Elhamdani A, Palfrey HC (1996) Calmodulin is the divalent cation receptor for rapid endocytosis, but not exocytosis, in adrenal chromaffin cells. Neuron 16:195-205.

Artalejo CR, Henley JR, McNiven MA, Palfrey HC (1995) Rapid endocytosis coupled to exocytosis in adrenal chromaffin cells involves Ca2+, GTP, and dynamin but not clathrin. Proc Natl Acad Sci U S A 92:8328-8332.

Ashery U, Varoqueaux F, Voets T, Betz A, Thakur P, Koch H, Neher E, Brose N, Rettig J (2000) Munc13-1 acts as a priming factor for large dense-core vesicles in bovine chromaffin cells. Embo J 19:3586-3596.

Augustin I, Rosenmund C, Sudhof TC, Brose N (1999) Munc13-1 is essential for fusion competence of glutamatergic synaptic vesicles. Nature 400:457-461.

Aunis D, Bader MF (1988) The cytoskeleton as a barrier to exocytosis in secretory cells. J Exp Biol 139:253-266.

Banerjee A, Barry VA, DasGupta BR, Martin TF (1996a) N-Ethylmaleimide-sensitive factor acts at a prefusion ATP-dependent step in Ca2+-activated exocytosis. J Biol Chem 271:20223-20226.

Banerjee A, Kowalchyk JA, DasGupta BR, Martin TF (1996b) SNAP-25 is required for a late postdocking step in Ca2+-dependent exocytosis. J Biol Chem 271:20227-20230.

Barg S, Olofsson CS, Schriever-Abeln J, Wendt A, Gebre-Medhin S, Renstrom E, Rorsman P (2002) Delay between fusion pore opening and peptide release from large dense-core vesicles in neuroendocrine cells. Neuron 33:287-299.

Basu J, Shen N, Dulubova I, Lu J, Guan R, Guryev O, Grishin NV, Rosenmund C, Rizo J (2005) A minimal domain responsible for Munc13 activity. Nat Struct Mol Biol 12:1017-1018.

Bennett MK, Calakos N, Scheller RH (1992) Syntaxin: a synaptic protein implicated in docking of synaptic vesicles at presynaptic active zones. Science 257:255-259.

Betz A, Okamoto M, Benseler F, Brose N (1997) Direct interaction of the rat unc-13 homologue Munc13-1 with the N terminus of syntaxin. J Biol Chem 272:2520-2526.

Bittner MA, Holz RW, Neubig RR (1986) Guanine nucleotide effects on catecholamine secretion from digitonin-permeabilized adrenal chromaffin cells. J Biol Chem 261:10182-10188.

Borisovska M, Zhao Y, Tsytsyura Y, Glyvuk N, Takamori S, Matti U, Rettig J, Sudhof T, Bruns D (2005) v-SNAREs control exocytosis of vesicles from priming to fusion. Embo J 24:2114-2126.

Brose N, Petrenko AG, Sudhof TC, Jahn R (1992) Synaptotagmin: a calcium sensor on the synaptic vesicle surface. Science 256:1021-1025.

Burgoyne RD, Handel SE (1994) Activation of exocytosis by GTP analogues in adrenal chromaffin cells revealed by patch-clamp capacitance measurement. FEBS Lett 344:139-142.

Burgoyne RD, Morgan A, Robinson I, Pender N, Cheek TR (1993) Exocytosis in adrenal chromaffin cells. J Anat 183 (Pt 2):309-314.

Ceccarelli B, Hurlbut WP, Mauro A (1973) Turnover of transmitter and synaptic vesicles at the frog neuromuscular junction. J Cell Biol 57:499-524.

Chan SA, Smith C (2003) Low frequency stimulation of mouse adrenal slices reveals a clathrin-independent, protein kinase C-mediated endocytic mechanism. J Physiol 553:707-717.

Cheek TR, Burgoyne RD (1986) Nicotine-evoked disassembly of cortical actin filaments in adrenal chromaffin cells. FEBS Lett 207:110-114.

Chow RH, von Ruden L, Neher E (1992) Delay in vesicle fusion revealed by electrochemical monitoring of single secretory events in adrenal chromaffin cells. Nature 356:60-63.

Cuchillo-Ibanez I, Albillos A, Aldea M, Arroyo G, Fuentealba J, Garcia AG (2002) Calcium entry, calcium redistribution, and exocytosis. Ann N Y Acad Sci 971:108-116.

deWit H, Cornelisse LN, Toonen RF, Verhage M (2006) Docking of secretory vesicles is syntaxin dependent. PLoS ONE 1:e126.

Doreian BW, Fulop TG, Meklemburg RL, Smith CB (2009) Cortical F-actin, the exocytic mode, and neuropeptide release in mouse chromaffin cells is regulated by myristoylated alanine-rich C-kinase substrate and myosin II. Mol Biol Cell 20:3142-3154.

Dulubova I, Sugita S, Hill S, Hosaka M, Fernandez I, Sudhof TC, Rizo J (1999) A conformational switch in syntaxin during exocytosis: role of munc18. Embo J 18:4372-4382.

Duncan RR, Greaves J, Wiegand UK, Matskevich I, Bodammer G, Apps DK, Shipston MJ, Chow RH (2003) Functional and spatial segregation of secretory vesicle pools according to vesicle age. Nature 422:176-180.

Engisch KL, Nowycky MC (1998) Compensatory and excess retrieval: two types of endocytosis following single step depolarizations in bovine adrenal chromaffin cells. J Physiol 506 (Pt 3):591-608.

Evanko D (2005) Primer: spying on exocytosis with amperometry. Nat Methods 2:650.

Fernandez-Chacon R, Konigstorfer A, Gerber SH, Garcia J, Matos MF, Stevens CF, Brose N, Rizo J, Rosenmund C, Sudhof TC (2001) Synaptotagmin I functions as a calcium regulator of release probability. Nature 410:41-49.

Fernandez JM, Neher E, Gomperts BD (1984) Capacitance measurements reveal stepwise fusion events in degranulating mast cells. Nature 312:453-455.

Fisher RJ, Pevsner J, Burgoyne RD (2001) Control of fusion pore dynamics during exocytosis by Munc18. Science 291:875-878.

Fujita Y, Xu A, Xie L, Arunachalam L, Chou TC, Jiang T, Chiew SK, Kourtesis J, Wang L, Gaisano HY, Sugita S (2007) Ca2+-dependent activator protein for secretion 1 is critical for constitutive and regulated exocytosis but not for loading of transmitters into dense core vesicles. J Biol Chem 282:21392-21403.

Fulop T, Radabaugh S, Smith C (2005) Activity-dependent differential transmitter release in mouse adrenal chromaffin cells. J Neurosci 25:7324-7332.

Garcia AG, Garcia-De-Diego AM, Gandia L, Borges R, Garcia-Sancho J (2006) Calcium signaling and exocytosis in adrenal chromaffin cells. Physiol Rev 86:1093-1131.

Gasman S, Chasserot-Golaz S, Bader MF, Vitale N (2003) Regulation of exocytosis in adrenal chromaffin cells: focus on ARF and Rho GTPases. Cell Signal 15:893-899.

Geisow MJ, Childs J, Burgoyne RD (1985) Cholinergic stimulation of chromaffin cells induces rapid coating of the plasma membrane. Eur J Cell Biol 38:51-56.

Geppert M, Goda Y, Hammer RE, Li C, Rosahl TW, Stevens CF, Sudhof TC (1994) Synaptotagmin I: a major Ca2+ sensor for transmitter release at a central synapse. Cell 79:717-727.

Glenn DE, Burgoyne RD (1996) Botulinum neurotoxin light chains inhibit both Ca(2+)-induced and GTP analogue-induced catecholamine release from permeabilised adrenal chromaffin cells. FEBS Lett 386:137-140.

Gomperts BD (1983) Involvement of guanine nucleotide-binding protein in the gating of Ca2+ by receptors. Nature 306:64-66.

Gong LW, Di Paolo G, Diaz E, Cestra G, Diaz ME, Lindau M, De Camilli P, Toomre D (2005) Phosphatidylinositol phosphate kinase type I gamma regulates dynamics of large dense-core vesicle fusion. Proc Natl Acad Sci U S A 102:5204-5209.

Grishanin RN, Klenchin VA, Loyet KM, Kowalchyk JA, Ann K, Martin TF (2002) Membrane association domains in Ca2+-dependent activator protein for secretion mediate plasma membrane and dense-core vesicle binding required for Ca2+-dependent exocytosis. J Biol Chem 277:22025-22034.

Grishanin RN, Kowalchyk JA, Klenchin VA, Ann K, Earles CA, Chapman ER, Gerona RR, Martin TF (2004) CAPS acts at a prefusion step in dense-core vesicle exocytosis as a PIP2 binding protein. Neuron 43:551-562.

Gulyas-Kovacs A, de Wit H, Milosevic I, Kochubey O, Toonen R, Klingauf J, Verhage M, Sorensen JB (2007) Munc18-1: sequential interactions with the fusion machinery stimulate vesicle docking and priming. J Neurosci 27:8676-8686.

Hata Y, Slaughter CA, Sudhof TC (1993) Synaptic vesicle fusion complex contains unc-18 homologue bound to syntaxin. Nature 366:347-351.

Hay JC, Martin TF (1993) Phosphatidylinositol transfer protein required for ATP-dependent priming of Ca(2+)-activated secretion. Nature 366:572-575.

Hay JC, Fisette PL, Jenkins GH, Fukami K, Takenawa T, Anderson RA, Martin TF (1995) ATP-dependent inositide phosphorylation required for Ca(2+)-activated secretion. Nature 374:173-177.

Haynes CL, Siff LN, Wightman RM (2007) Temperature-dependent differences between readily releasable and reserve pool vesicles in chromaffin cells. Biochim Biophys Acta 1773:728-735.

Henkel AW, Almers W (1996) Fast steps in exocytosis and endocytosis studied by capacitance measurements in endocrine cells. Curr Opin Neurobiol 6:350-357.

Heuser JE, Reese TS (1973) Evidence for recycling of synaptic vesicle membrane during transmitter release at the frog neuromuscular junction. J Cell Biol 57:315-344.

Holroyd P, Lang T, Wenzel D, De Camilli P, Jahn R (2002) Imaging direct, dynamin-dependent recapture of fusing secretory granules on plasma membrane lawns from PC12 cells. Proc Natl Acad Sci U S A 99:16806-16811.

Holz RW, Bittner MA, Peppers SC, Senter RA, Eberhard DA (1989) MgATP-independent and MgATP-dependent exocytosis. Evidence that MgATP primes adrenal chromaffin cells to undergo exocytosis. J Biol Chem 264:5412-5419.

Hsu SC, Ting AE, Hazuka CD, Davanger S, Kenny JW, Kee Y, Scheller RH (1996) The mammalian brain rsec6/8 complex. Neuron 17:1209-1219.

Jahn R, Scheller RH (2006) SNAREs--engines for membrane fusion. Nat Rev Mol Cell Biol 7:631-643.

Klenchin VA, Kowalchyk JA, Martin TF (1998) Large dense-core vesicle exocytosis in PC12 cells. Methods 16:204-208.

Klyachko VA, Jackson MB (2002) Capacitance steps and fusion pores of small and large-dense-core vesicles in nerve terminals. Nature 418:89-92.

Lang T, Margittai M, Holzler H, Jahn R (2002) SNAREs in native plasma membranes are active and readily form core complexes with endogenous and exogenous SNAREs. J Cell Biol 158:751-760.

Li G, Han L, Chou TC, Fujita Y, Arunachalam L, Xu A, Wong A, Chiew SK, Wan Q, Wang L, Sugita S (2007) RalA and RalB function as the critical GTP sensors for GTP-dependent exocytosis. J Neurosci 27:190-202.

Lingg G, Fischer-Colbrie R, Schmidt W, Winkler H (1983) Exposure of an antigen of chromaffin granules on cell surface during exocytosis. Nature 301:610-611.

Lynch KL, Martin TF (2007) Synaptotagmins I and IX function redundantly in regulated exocytosis but not endocytosis in PC12 cells. J Cell Sci 120:617-627.

Malhotra V, Orci L, Glick BS, Block MR, Rothman JE (1988) Role of an N-ethylmaleimide-sensitive transport component in promoting fusion of transport vesicles with cisternae of the Golgi stack. Cell 54:221-227.

Milosevic I, Sorensen JB, Lang T, Krauss M, Nagy G, Haucke V, Jahn R, Neher E (2005) Plasmalemmal phosphatidylinositol-4,5-bisphosphate level regulates the releasable vesicle pool size in chromaffin cells. J Neurosci 25:2557-2565.

Moser T, Neher E (1997a) Estimation of mean exocytic vesicle capacitance in mouse adrenal chromaffin cells. Proc Natl Acad Sci U S A 94:6735-6740.

Moser T, Neher E (1997b) Rapid exocytosis in single chromaffin cells recorded from mouse adrenal slices. J Neurosci 17:2314-2323.

Mosharov EV, Sulzer D (2005) Analysis of exocytotic events recorded by amperometry. Nat Methods 2:651-658.

Moskalenko S, Henry DO, Rosse C, Mirey G, Camonis JH, White MA (2002) The exocyst is a Ral effector complex. Nat Cell Biol 4:66-72.

Neher E, Zucker RS (1993) Multiple calcium-dependent processes related to secretion in bovine chromaffin cells. Neuron 10:21-30.

Neher E, Sakaba T (2008) Multiple roles of calcium ions in the regulation of neurotransmitter release. Neuron 59:861-872.

Olivera BM, Miljanich GP, Ramachandran J, Adams ME (1994) Calcium channel diversity and neurotransmitter release: the omega-conotoxins and omega-agatoxins. Annu Rev Biochem 63:823-867.

Patzak A, Winkler H (1986) Exocytotic exposure and recycling of membrane antigens of chromaffin granules: ultrastructural evaluation after immunolabeling. J Cell Biol 102:510-515.

Perin MS, Fried VA, Mignery GA, Jahn R, Sudhof TC (1990) Phospholipid binding by a synaptic vesicle protein homologous to the regulatory region of protein kinase C. Nature 345:260-263.

Perrais D, Kleppe IC, Taraska JW, Almers W (2004) Recapture after exocytosis causes differential retention of protein in granules of bovine chromaffin cells. J Physiol 560:413-428.

Pevsner J, Hsu SC, Scheller RH (1994) n-Sec1: a neural-specific syntaxin-binding protein. Proc Natl Acad Sci U S A 91:1445-1449.

Plattner H, Artalejo AR, Neher E (1997) Ultrastructural organization of bovine chromaffin cell cortex-analysis by cryofixation and morphometry of aspects pertinent to exocytosis. J Cell Biol 139:1709-1717.

Regazzi R, Li G, Ullrich S, Jaggi C, Wollheim CB (1989) Different requirements for protein kinase C activation and Ca2+-independent insulin secretion in response to guanine nucleotides. Endogenously generated diacylglycerol requires elevated Ca2+ for kinase C insertion into membranes. J Biol Chem 264:9939-9944.

Sassa T, Harada S, Ogawa H, Rand JB, Maruyama IN, Hosono R (1999) Regulation of the UNC-18-Caenorhabditis elegans syntaxin complex by UNC-13. J Neurosci 19:4772-4777.

Shao X, Li C, Fernandez I, Zhang X, Sudhof TC, Rizo J (1997) Synaptotagmin-syntaxin interaction: the C2 domain as a Ca2+-dependent electrostatic switch. Neuron 18:133-142.

Shen J, Tareste DC, Paumet F, Rothman JE, Melia TJ (2007) Selective activation of cognate SNAREpins by Sec1/Munc18 proteins. Cell 128:183-195.

Sorensen JB, Fernandez-Chacon R, Sudhof TC, Neher E (2003a) Examining synaptotagmin 1 function in dense core vesicle exocytosis under direct control of Ca2+. J Gen Physiol 122:265-276.

Sorensen JB, Nagy G, Varoqueaux F, Nehring RB, Brose N, Wilson MC, Neher E (2003b) Differential control of the releasable vesicle pools by SNAP-25 splice variants and SNAP-23. Cell 114:75-86.

Sorensen JB, Wiederhold K, Muller EM, Milosevic I, Nagy G, de Groot BL, Grubmuller H, Fasshauer D (2006) Sequential N- to C-terminal SNARE complex assembly drives priming and fusion of secretory vesicles. Embo J 25:955-966.

Speidel D, Varoqueaux F, Enk C, Nojiri M, Grishanin RN, Martin TF, Hofmann K, Brose N, Reim K (2003) A family of Ca2+-dependent activator proteins for secretion: comparative analysis of structure, expression, localization, and function. J Biol Chem 278:52802-52809.

Speidel D, Bruederle CE, Enk C, Voets T, Varoqueaux F, Reim K, Becherer U, Fornai F, Ruggieri S, Holighaus Y, Weihe E, Bruns D, Brose N, Rettig J (2005) CAPS1 regulates catecholamine loading of large dense-core vesicles. Neuron 46:75-88.

Stevens DR, Wu ZX, Matti U, Junge HJ, Schirra C, Becherer U, Wojcik SM, Brose N, Rettig J (2005) Identification of the minimal protein domain required for priming activity of Munc13-1. Curr Biol 15:2243-2248.

Steyer JA, Horstmann H, Almers W (1997) Transport, docking and exocytosis of single secretory granules in live chromaffin cells. Nature 388:474-478.

Sudhof TC (1995) The synaptic vesicle cycle: a cascade of protein-protein interactions. Nature 375:645-653.

Sudhof TC (2002) Synaptotagmins: why so many? J Biol Chem 277:7629-7632.

Sugihara K, Asano S, Tanaka K, Iwamatsu A, Okawa K, Ohta Y (2002) The exocyst complex binds the small GTPase RalA to mediate filopodia formation. Nat Cell Biol 4:73-78.

Sugita S (2008) Mechanisms of exocytosis. Acta Physiol (Oxf) 192:185-193.

Sugita S, Shin OH, Han W, Lao Y, Sudhof TC (2002) Synaptotagmins form a hierarchy of exocytotic Ca(2+) sensors with distinct Ca(2+) affinities. Embo J 21:270-280.

Sutton RB, Davletov BA, Berghuis AM, Sudhof TC, Sprang SR (1995) Structure of the first C2 domain of synaptotagmin I: a novel Ca2+/phospholipid-binding fold. Cell 80:929-938.

Takiyyuddin MA, Cervenka JH, Sullivan PA, Pandian MR, Parmer RJ, Barbosa JA, O'Connor DT (1990) Is physiologic sympathoadrenal catecholamine release exocytotic in humans? Circulation 81:185-195.

Takiyyuddin MA, Brown MR, Dinh TQ, Cervenka JH, Braun SD, Parmer RJ, Kennedy B, O'Connor DT (1994) Sympatho-adrenal secretion in humans: factors governing catecholamine and storage vesicle peptide co-release. J Auton Pharmacol 14:187-200.

Taraska JW, Almers W (2004) Bilayers merge even when exocytosis is transient. Proc Natl Acad Sci U S A 101:8780-8785.

Taraska JW, Perrais D, Ohara-Imaizumi M, Nagamatsu S, Almers W (2003) Secretory granules are recaptured largely intact after stimulated exocytosis in cultured endocrine cells. Proc Natl Acad Sci U S A 100:2070-2075.

Trifaro JM, Glavinovic M, Rose SD (1997) Secretory vesicle pools and rate and kinetics of single vesicle exocytosis in neurosecretory cells. Neurochem Res 22:831-841.

Varoqueaux F, Sigler A, Rhee JS, Brose N, Enk C, Reim K, Rosenmund C (2002) Total arrest of spontaneous and evoked synaptic transmission but normal synaptogenesis in the absence of Munc13-mediated vesicle priming. Proc Natl Acad Sci U S A 99:9037-9042.

Vitale ML, Seward EP, Trifaro JM (1995) Chromaffin cell cortical actin network dynamics control the size of the release-ready vesicle pool and the initial rate of exocytosis. Neuron 14:353-363.

Viveros OH, Arqueros L, Kirshner N (1971) Mechanism of secretion from the adrenal medulla. VII. Effect of insulin administration on the buoyant density, dopamine -hydroxylase, and catecholamine content of adrenal storage vesicles. Mol Pharmacol 7:444-454.

Voets T, Neher E, Moser T (1999) Mechanisms underlying phasic and sustained secretion in chromaffin cells from mouse adrenal slices. Neuron 23:607-615.

Voets T, Moser T, Lund PE, Chow RH, Geppert M, Sudhof TC, Neher E (2001a) Intracellular calcium dependence of large dense-core vesicle exocytosis in the absence of synaptotagmin I. Proc Natl Acad Sci U S A 98:11680-11685.

Voets T, Toonen RF, Brian EC, de Wit H, Moser T, Rettig J, Sudhof TC, Neher E, Verhage M (2001b) Munc18-1 promotes large dense-core vesicle docking. Neuron 31:581-591.

Wang CT, Grishanin R, Earles CA, Chang PY, Martin TF, Chapman ER, Jackson MB (2001) Synaptotagmin modulation of fusion pore kinetics in regulated exocytosis of dense-core vesicles. Science 294:1111-1115.

Wang CT, Lu JC, Bai J, Chang PY, Martin TF, Chapman ER, Jackson MB (2003) Different domains of synaptotagmin control the choice between kiss-and-run and full fusion. Nature 424:943-947.

Wang L, Li G, Sugita S (2004) RalA-exocyst interaction mediates GTP-dependent exocytosis. J Biol Chem 279:19875-19881.

Wang L, Li G, Sugita S (2005) A central kinase domain of type I phosphatidylinositol phosphate kinases is sufficient to prime exocytosis: isoform specificity and its underlying mechanism. J Biol Chem 280:16522-16527.

Watkinson A, O'Sullivan AJ, Burgoyne RD, Dockray GJ (1990) Differential accumulation of catecholamines, proenkephalin- and chromogranin A-derived peptides in the medium after chronic nicotine stimulation of cultured bovine adrenal chromaffin cells. Peptides 11:435-441.

Weber T, Parlati F, McNew JA, Johnston RJ, Westermann B, Sollner TH, Rothman JE (2000) SNAREpins are functionally resistant to disruption by NSF and alphaSNAP. J Cell Biol 149:1063-1072.

Winkler H, Westhead E (1980) The molecular organization of adrenal chromaffin granules. Neuroscience 5:1803-1823.

Winkler H, Fischer-Colbrie R (1998) Regulation of the biosynthesis of large dense-core vesicles in chromaffin cells and neurons. Cell Mol Neurobiol 18:193-209.

Xu T, Binz T, Niemann H, Neher E (1998) Multiple kinetic components of exocytosis distinguished by neurotoxin sensitivity. Nat Neurosci 1:192-200.

Zhang X, Kim-Miller MJ, Fukuda M, Kowalchyk JA, Martin TF (2002) Ca2+-dependent synaptotagmin binding to SNAP-25 is essential for Ca2+-triggered exocytosis. Neuron 34:599-611.

Zhou Z, Misler S, Chow RH (1996) Rapid fluctuations in transmitter release from single vesicles in bovine adrenal chromaffin cells. Biophys J 70:1543-1552.

Zilly FE, Sorensen JB, Jahn R, Lang T (2006) Munc18-bound syntaxin readily forms SNARE complexes with synaptobrevin in native plasma membranes. PLoS Biol 4:e330.

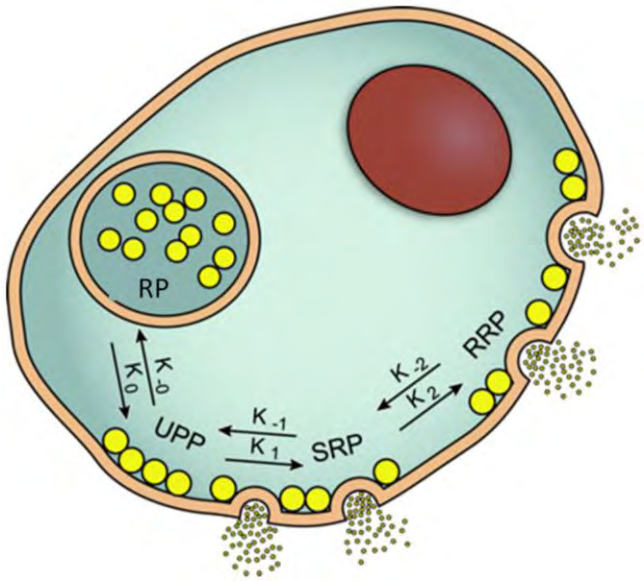

Figure 3.1 Different LDCG pools in chromaffin cells exist according to their readiness to participate in exocytosis. The readily releasable pool (RRP), contains granules that are in the final stage of maturation, just before fusion is triggered by the last Ca^{2+}-dependent step. The RRP is depleted with relatively short delay (100 ms). The slowly releasable pool (SRP), contains granules that are associated with the cell membrane as a result of the formation of the SNARE complex and is depleted within a few seconds. Its delay may be explained by additional priming steps required by granules to become release competent and enter the RRP. Another pool, the unprimed pool (UPP) has also been described wherein granules are docked but unprimed. The reserve pool (RP) contains granules that are recruited from the cytoskeleton to become docked.

(Adapted from Garcia et al., 2006)

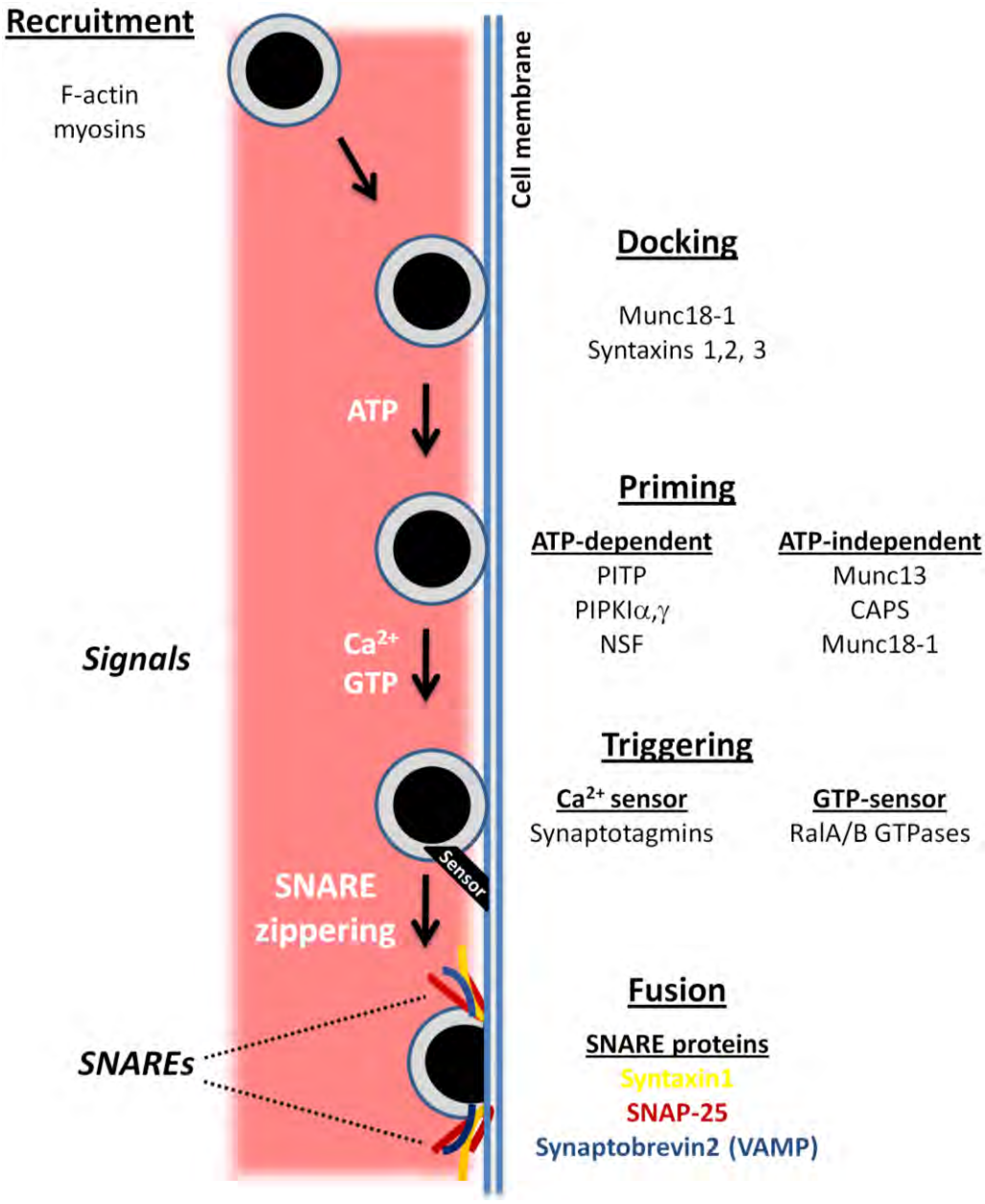
Recruitment
F-actin
myosins
Cell membrane
Docking
Munc18-1
Syntaxins 1,2, 3
ATP
Priming
ATP-dependent
PITP
PIPKIα,γ
NSF
ATP-independent
Munc13
CAPS
Munc18-1
Signals
Ca2+
GTP
Triggering
Ca2+ sensor
Synaptotagmins
GTP-sensor
RalA/B GTPases
Sensor
SNARE
zippering
Fusion
SNARE proteins
Syntaxin1
SNAP-25
Synaptobrevin2 (VAMP)
SNAREs

Figure 3.2 Exocytosis of large dense core granules (LDCGs) in chromaffin cells. Once LDCGs are recruited to the cell membrane, they must proceed through docking and priming steps before they receive the trigger signal to fuse with the plasma membrane. The proteins involved at each step are shown for each stage of exocytosis. See text for details.

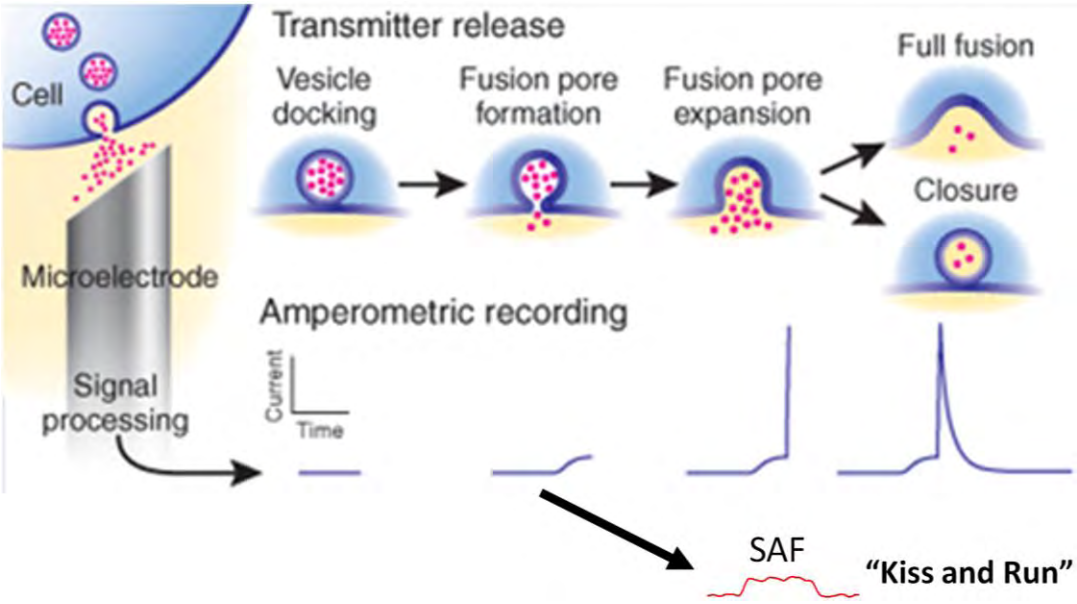

Figure 3.3 Amperometry reveals kinetic details of individual exocytotic events. See text for details.

(Figure adapted from Evanko, 2005)

Chapter 4

Calcium and the chromaffin cell: sources, signals and syntillas

The Ca^{2+} ion serves a crucial role in cell to cell communication within neural networks and excitable cells. In the chromaffin cell, Ca^{2+} is most prominently responsible for connecting the electrical input into a cell, the action potential, to the chemical output from the cell, exocytosis. But Ca^{2+} is a potent second messenger with a large array of targets attributed to this divalent cation and its ability to activate numerous cell functions could become problematic if not tightly controlled. Thus, intricate regulatory mechanisms abound to ensure that the Ca^{2+} ion is able to provide a reliable coupling signal within this electrochemical input-output system and therefore high fidelity communication. Accordingly, these regulatory mechanisms tend to center around controlling the amount of Ca^{2+} within a specific space, or microdomain, within the cell at the precise time.

Cytosolic [Ca^{2+}] *in ACCs*

Fluctuations of intracellular free [Ca^{2+}] must be highly coordinated in space and time within the ACC to regulate exocytosis and other processes. Therefore under basal conditions, the ACC importantly maintains a free $[Ca^{2+}]_{cyto}$ around 130 nM, about 10,000-fold lower than the extracellular [Ca^{2+}] (Xu et al., 1997). To do this, the ACC employs specific membrane proteins, such as Na^+/Ca^{2+} exchangers and Ca^{2+} ATPase pumps located on the cell membrane or the membranes of internal compartments within the cell such as the ER, mitochondria, or LDCGs (Zhou and Neher, 1993; Xu et al., 1997). Pumps alone, however, are not sufficient to maintain the low resting levels of free $[Ca^{2+}]_{cyto}$. The ACC additionally contains a multitude of Ca^{2+} buffering proteins. In fact, the total cytosolic [Ca^{2+}] is in the super-micromolar range, but the majority of this Ca^{2+} is bound to high-affinity Ca^{2+} binding proteins such as calmodulin (Zhou and Neher, 1993).

These endogenous Ca^{2+} buffers result in very fine control over $[Ca^{2+}]_{cyto}$, creating micro- or even nano-domains whereby Ca^{2+} rises only in a distinct space within the cell proximal to a Ca^{2+} source, before it is quickly buffered (Neher, 1998a) (Figure 4.1). For example, Ca^{2+} influx through voltage-gated Ca^{2+} channels (VGCCs) has been shown to result in discrete rises in [Ca^{2+}] within a micrometer of these channels (Simon and Llinas, 1985). In bovine ACCs, it has

been calculated that during stimulation the majority of LDGCs are exposed to a [Ca^{2+}] which rises monotonically to a peak of < 10 μM and decays over tens of milliseconds, due to their non co-localization with Ca^{2+} channels on a molecular scale (Chow et al., 1994). That is, 90% of LDCGs have been estimated to reside approximately 200 – 300 nm from the nearest Ca^{2+} channel (Klingauf and Neher, 1997). Rises in [Ca^{2+}] within a smaller domain (in the range of nanometers) is also possible, say in the case of influx through a single channel (Augustine et al., 2003). For example, in bovine ACCs it is estimated that about 10 % of LDCGs reside within 30 nm from the nearest Ca^{2+} channel and can experience peak [Ca^{2+}] of ~ 100 μM (Klingauf and Neher, 1997).

Cytosolic Ca^{2+} Sources in ACCs

Ca^{2+} can enter the cytosol from two sources, the extracellular fluid and the various intracellular storage compartments. While Ca^{2+} influx is mostly mediated by voltage-dependent Ca^{2+} channels embedded in the cell membrane, release of Ca^{2+} from internal stores into the cytosol is largely mediated through IP3 and RYR channels.

Ca^{2+} channels: ACCs fire action potentials which in turn open plasmalemmal Ca^{2+} channels. The resultant Ca^{2+} influx leads to the rapid triggering of exocytosis (Penner and Neher, 1988; Cheek and Barry, 1993; Livett, 1993; Aunis, 1998). These voltage-gated Ca^{2+} channels are formed by a multi-subunit protein complex which consists of a pore-forming α1-subunit with several auxiliary proteins, including the intracellular β-subunit and a disulfide-linked α-δ-subunit (Garcia et al., 2006) (Figure 4.2 A). Genetic variation, differential expression as well as alternative splicing mechanisms are thought to contribute to the possibility of multiple combinations of these subunits, which provide the basis for the functional diversity among the Ca^{2+} channel subtypes. Based on their range of activation, all Ca^{2+} channel subtypes can be classified into either low voltage activating threshold (LVA; T-type) or high voltage activating threshold (HVA; L-, N-, P/Q- and R- type) channels (Garcia et al., 2006) (Figure 4.2 B).

The only known type of LVA Ca^{2+} channel is the T-type channel (T for "transient"). These channels are characterized by their fast inactivation with a transient current at holding potentials between -50 and -60 mV. In addition to their low activation threshold, T channels also display a similar permeability to Ca^{2+} and Ba^{2+} with a single channel conductance of about 8 pS (Fox et al., 1987b, a). Although T-type channel mRNA has been detected in bovine ACCs (Garcia-Palomero et al., 2000), their currents are difficult to record. Nonetheless,

these currents have been reported in bovine (Diverse-Pierluissi et al., 1991) and rat ACCs (Hollins and Ikeda, 1996). It has been suggested that these channels may only be expressed in developing ACCs (Bournaud et al., 2001), which could account for their elusive detection in other species. On the other hand, it may be that these channels are disrupted by isololation. Interestingly, T-type channels can be up-regulated within a timeframe of hours to days following stress-mimicking conditions in isolated rat ACCs (Carbone et al., 2006).

HVA L-type, or "long-lasting" Ca^{2+} channels, have been characterized in ACCs of mouse (Hernandez-Guijo et al., 1998), rat (Prakriya and Lingle, 1999), cow (Artalejo et al., 1991; Bossu et al., 1991), cat (Albillos et al., 1994), human (Gandia et al., 1998) and pig (Kitamura et al., 1997). They display little inactivation during depolarizing steps and a lower sensitivity to depolarized holding potentials when Ba^{2+} is the charge carrier. In ACCs, if Ca^{2+} is used as a charge carrier instead, then these channels are completely inactivated (Hernandez-Guijo et al., 2001). The single channel conductance is between 18 and 25 pS in 100 mM Ba^{2+} (Garcia et al., 2006). These channels are highly characteristic of most excitable cells, serving as the main pathway for Ca^{2+} influx in heart, smooth muscle and neuroendocrine cells. The L-type current of each tissue is a consequence of differential expression of four α_1-subunits, α_{1C}, α_{1D}, α_{1F}, and α_{1S}. These channels are sensitive to 1,4-dihydropyridines (DHP), which

can act as agonists (e.g., BAY K 8644) (Nowycky et al., 1985) or antagonists (e.g., nifedipine, nitrendipine, nisoldipine, nimodipine, furnidipine) (Fleckenstein, 1983; Spedding, 1985).

HVA N-type or "neuronal" Ca^{2+} channels have been characterized in ACCs of mouse (Hernandez-Guijo et al., 1998), cow (Artalejo et al., 1992; Lopez et al., 1994), pig (Kitamura et al., 1997), cat (Albillos et al., 1994), rat (Prakriya and Lingle, 1999), and human (Gandia et al., 1998). They display faster inactivation than L-type channels, which is voltage-dependent (Fox et al., 1987a) and, they do not persist at less negative holding potentials (Villarroya et al., 1999). They have a single channel conductance between 11 – 15 pS (Tsien et al., 1987). At least in cow, N-type channels can also contain a non-inactivating component, called "non-classical N-type" (Artalejo et al., 1992). N-type channels are particularly sensitive to conotoxins. For example, they are irreversibly blocked by the *Conus geographus* toxin ω-conotoxin GVIA (Nowycky et al., 1985; Kasai et al., 1987) and reversibly blocked by the *Conus magus* toxin ω-conotoxin MVIIA (Valentino et al., 1993).

P-type or "Purkinje" Ca^{2+} channels are another type of HVA channel, but their expression levels in ACCs are low. For example, in mouse (Hernandez-Guijo et al., 1998) and rat ACCs (Gandia et al., 1995), P channels contribute only 10–15% to the total Ca^{2+} current. Nonetheless, P/Q-type channels are highly

coupled to catecholamine secretion in ACCs, most likely due to their close proximity to the release site *in situ* (Polo-Parada et al., 2006). These channels are relatively insensitive to changes in the holding potential and do not inactivate during depolarizing steps (Regan, 1991; Mintz et al., 1992). They can be selectively blocked by the funnel web spider toxin FTX, its synthetic analog sFTX, and by ω-agatoxin IVA at nanomolar concentrations. Since it is difficult to separate the α_{1A}-subunit into P- and Q-type channels (Sather et al., 1993), coupled with their low expression levels, P-type channels are generally grouped together with Q-type channels and referred to collectively as P/Q-type channels.

The characterization of HVA Q-type channels is based mostly on pharmacological properties. That is, Q channels are resistant to blockade by DHPs, ω-conotoxin GVIA, and low concentrations (<100 nM) of ω-agatoxin IVA, but are sensitive to ω-conotoxin MVIIC (1–3 μM) (Wheeler et al., 1994). In ACCs the P/Q component of the whole cell Ca^{2+} current is voltage inactivated (Villarroya et al., 1999), and can be pharmacologically isolated by 2 μM ω-conotoxin MVIIC, ω-conotoxin MVIID, or ω-agatoxin IVA (Gandia et al., 1997).

The last subtype of HVA Ca^{2+} channel is the R-type or “resistant” channel named for its insensitivity to blockade by DHPs, ω-conotoxin GVIA, ω-agatoxin IVA, and ω-conotoxin MVIIC (Randall and Tsien, 1995). This channel inactivates

rapidly, and is more sensitive to blockade by Ni^{2+} than by Cd^{2+}. There are reports of a selective R channel blocker SNX-482 in rat nerve terminals (Newcomb et al., 1998), but others have suggested that at least in the bovine ACC, that this toxin also blocks P/Q channels (Arroyo et al., 2003). While some studies employing whole cell recordings fail to report an R-type current component (Albillos et al., 1993; Gandia et al., 1993; Albillos et al., 1994; Artalejo et al., 1994; Kitamura et al., 1997; Gandia et al., 1998; Lukyanetz and Neher, 1999; Albillos et al., 2000), others using the perforated-patch configuration do find an R-type component (e.g., in mouse adrenal medullary slices and mouse and rat ACCs (Hollins and Ikeda, 1996; Albillos et al., 2000; Aldea et al., 2002; Carabelli et al., 2003; Cesetti et al., 2003)).

There are extreme interspecies differences in Ca^{2+} channel subtypes in primary cultures of ACCs (Figure 4.2 C) (Garcia et al., 2006). It also is worth noting that in mouse ACCs, which are employed in the studies of this dissertation, that even though L-type and N-type Ca^{2+} channels account for up to 80% of the whole cell Ca^{2+} channel current, the activation kinetics of secretion from these cells favor the R-type and N-type channels (Albillos et al., 2000; Chan et al., 2005; Polo-Parada et al., 2006). Furthermore, in freshly isolated mouse ACCs, we have found that the respective percentages that the L- and N-type components contribute to the total current can vary from ACC to ACC as well.

For example, the L-type fraction on average is about 40%, but some cells exhibit L-type fractions as low as 20 % and others up to 60%. The physiological relevance of these extreme inter-species and even intra-species differences may have specific consequences differentially controlling the exocytic release of epinephrine and norepinephrine according to variable stimulation.

Internal Ca^{2+} stores: Cytosolic [Ca^{2+}] in the ACC is constantly defined not only by influx and extrusion across the cell membrane, but also by uptake into and release from the Ca^{2+} storing organelles. In the ACC the ER, mitochondria and LDCGs account for the bulk of internal Ca^{2+} storage.

Similar to ER Ca^{2+} stores in other excitable cells, in ACCs the ER acts like a homogeneous thapsigargin-sensitive source whereby Ca^{2+} can be released via IP_3 or RYRs (Alonso et al., 1999; Inoue et al., 2003). Ca^{2+} entry through VGCCs can directly activate Ca^{2+} release from the ER. This phenomenon, termed Ca^{2+}-induced-Ca^{2+}-release (CICR) has been well documented in bovine (Alonso et al., 2002) and rat ACCs (Alonso et al., 1999), but in mouse ACCs CICR is presently a controversial topic, where CICR is thought to exist, but to a smaller extent (Rigual et al., 2002).

The mitochondria can act as a Ca^{2+}-sink in ACCs and is thought to play an important role in shaping cytosolic [Ca^{2+}] transients (Garcia-Sancho and Verkhratsky, 2008). Ca^{2+} is taken up by the mitochondria by the mitochondrial uniporter, which is a low affinity/high capacity system (Gunter and Pfeiffer, 1990; Trenker et al., 2007). The mitochondrial membrane potential, which is highly negative inside, creates a steep driving force capable of storing Ca^{2+} in the mitochondrial matrix at up to 5 - 6 orders of magnitude above the cytosolic [Ca^{2+}] (Bernardi, 1999). In bovine (Xu et al., 1997) and rat (Herrington et al., 1996; Babcock et al., 1997) ACCs, mitochondria have been shown to be essential to rapid clearance of cytosolic Ca^{2+} loads. For example, during conditions of maximal stimulation by depolarization with high K^+, mitochondria can take up Ca^{2+} at the same rate as Ca^{2+} entry through VGCCs (Montero et al., 2000; Montero et al., 2001; Villalobos et al., 2002).

Ca^{2+} release from the mitochondria occurs primarily via a Na^+/Ca^{2+} exchanger and to a lesser extent via a Na^+-independent system (Gunter and Pfeiffer, 1990; Gunter et al., 1994). On the other hand, under conditions when the mitochondria is completely depolarized, Ca^{2+} may be able to exit from the matrix through the uniporter, which usually only allows entry (Montero et al., 2001).

The LDCGs of the ACC occupy nearly 20% of the cell volume and have a $[Ca^{2+}]$ of about 40 μm (Mundorf et al., 2000). Therefore, LDCGs account for greater than 60% of all Ca^{2+} within the ACC, thus making these granules the largest source of stored Ca^{2+} (Mundorf et al., 2000). The majority of this Ca^{2+}, however, is not free. Instead it is tightly bound to chromogranins within the granule matrix. But chromogranin affinity for Ca^{2+} is sensitive to pH, which means that intra-granular changes in pH could affect the free $[Ca^{2+}]$ (Yoo and Albanesi, 1991). Furthermore, the granule membrane has IP_3 receptors (Yoo and Albanesi, 1990) and, it has been proposed that Ca^{2+} mobilization from LDCGs could serve a role in assisting exocytosis (Mundorf et al., 2000). It is also very worthwhile to note recent work whereby RYRs are strongly suggested to exist on the LDCGs of mouse neurohypophyseal nerve terminals (McNally, 2008). Interestingly, the intra-granular $[Ca^{2+}]$ can be decreased by stimulation with high K^+, caffeine, or ATP (Moreno et al., 2005).

Together, Ca^{2+} fluxes between cell membrane calcium channels and intracellular Ca^{2+}-storing organelles act in concert to provide a dynamic system by which Ca^{2+} signaling and homeostasis within the ACC is maintained (Figure 4.3). At rest, Ca^{2+} flux rates are low and cytosolic and mitochondrial $[Ca^{2+}]$ is about 100 nM. On the other hand, ER $[Ca^{2+}]$ is maintained within the range of 500 – 1000 μM at rest. The extracellular saline $[Ca^{2+}]$ is also very high, in the 1 –

2 mM range. Thus, steep electrochemical gradients favor diffusion of Ca^{2+} into the cytosol from the ER and through VGCCs in the cell membrane. Under conditions of minimal or low frequency stimulation, the Ca^{2+} signal within the ACC is almost exclusively determined by the rate of diffusion through the cytosol and binding by endogenous Ca^{2+} buffers (Neher, 1998b, a). In this case, global [Ca^{2+}] can rise to about 1 μM and Ca^{2+}-ATPases in the ER and cell membrane return the cytosolic [Ca^{2+}] to basal levels. During strong stimulation, however, global [Ca^{2+}] can rise to levels near 10 μM. In this case, mitochondria located proximal to release sites are thought to take up Ca^{2+} via the uniporter and most of the Ca^{2+} that enters the cytosol is accumulated in the mitochondria (Herrington et al., 1996; Park et al., 1996; Montero et al., 2000). This Ca^{2+} is released from the mitochondria post stimulation over a period ranging from seconds to minutes (Villalobos et al., 2002). It has been proposed that the slightly elevated global [Ca^{2+}] during this phase may contribute to the mobilization of LDCGs from the reserve pool to the readily releasable pool (Neher, 1998b, a). Again, release of Ca^{2+} from LDCGs may also occur during stimulation, but is controversial.

IP_3 and RYRs mediate Ca^{2+} release from internal stores

As mentioned earlier, Ca^{2+} can be released into the cytosol of the ACC from internal stores such as the ER via inositol 1, 4, 5-trisphosphate (IP_3) or ryanodine receptors (RYRs). The IP_3 and RYRs constitute two separate, but similar families of Ca^{2+} release channels. For example, all members of each family are comprised of a tetramer of homologous subunits with large n-terminal domains that include specific regulatory sites. Furthermore, the channels of both families are 46% identical in a 134 amino acid segment of their c-terminal domains (Gill, 1989).

Release of Ca^{2+} into the cytosol by the IP_3 receptor is initiated in response to cytosolic increases in the second messenger IP_3. This is generally triggered by the binding of certain ligands to G-protein coupled receptors on the cell membrane which in turn promote the hydrolysis of PIP2 and thereby generate intracellular IP_3. The activation of the IP_3 receptor by IP_3 is not dependent on extracellular Ca^{2+}. There are also various pharmacologic tools for the IP_3 receptor, but they are poor. For example, heparin is commonly used as a blocking agent, but there is evidence that it may also activate RYRs. Moreover, newer drugs such as xestospongin C and 2-APB are non-specific (Collin et al., 2005).

The RYR family has 3 known isoforms in mammals, type-1 (RYR1), type-2 (RYR2) and type-3 (RYR3) (Figure 4.4) RYR1 is primarily expressed in skeletal muscle, RYR2 in cardiac muscle and RYR3, while primarily expressed in the brain, is also present in multiple tissue types. The RYR subtypes are highly, but differentially expressed throughout the brain. (Non-mammalian vertebrate skeletal muscles express two isoforms in almost similar amount, α- and β-RYR which are homologues of mammalian isoforms RyR1 and 3, respectively (Ogawa et al., 2002).) These Ca^{2+} release channels all show high affinity to the plant alkaloid, ryanodine, for which they are named. Though the specific isoforms are usually associated with the distinct tissue type in which they are expressed, it should be noted that multiple isoforms can exist within the same cell. In the mouse ACC type-2 RYRs are highly expressed and are distributed evenly just below the cell membrane, while type-3 RYRs are expressed to a much lesser extent and their distribution lies about the perinuclear region in a punctuate fashion (ZhuGe et al., 2006).

The release of Ca^{2+} through RYRs expressed on the SR or ER is accomplished by different mechanisms according the RYR type. For example, RYR1 (skeletal muscle) activation occurs via a physical coupling to the dihydropyridine receptor, whereas, the primary mechanism of activation for RYR2 (cardiac) is CICR (Fabiato, 1983). RYR3 activation is also thought to

occur by a CICR mechanism, and has been suggested to play a role in amplifying the Ca^{2+} release signal from RYR1 (Yang et al., 2001). Furthermore, Ca^{2+} release from a number of RYRs in a cluster can result in a fast, transient, spatiotemporally-restricted rise in cytosolic [Ca^{2+}] termed a Ca^{2+} spark in muscle (Cheng et al., 1993) or a Ca^{2+} syntilla in nerve terminals (De Crescenzo et al., 2004) or ACCs (ZhuGe et al., 2006).

RYRs are the major cellular mediator of CICR, whereby stimulation by Ca^{2+} on the cytosolic side causes the channel to open and release stored Ca^{2+}, thus establishing a positive feedback mechanism to amplify Ca^{2+} signals (Zucchi and Ronca-Testoni, 1997). But Ca^{2+} is not the only second messenger that can activate RYRs. For example, in cardiac and pancreatic cells, cyclic ADP-ribose can also initiate the Ca^{2+} release. In addition, RYRs can participate in another positive feedback mechanism to amplify Ca^{2+} release by indirectly interacting with IP3 receptors to give rise to what is called a Ca^{2+} wave. This occurs when Ca^{2+} released by RYRs activates the phospholipase C pathway, thereby raising IP_3 levels.

In addition to ryanodine, which locks RYRs in a sub-conductance state at nanomolar concentrations, but completely blocks them at micromolar concentrations (Hille, 1992), RYRs are sensitive to a number of other pharmacologic agents. Known antagonists include dantrolene and ruthenium

red, both of which are reported to have poor specificity (Vites and Pappano, 1994; Collin et al., 2005). Both pharmacologic and physiologic agonists of RYRs have been reported. Pharmacologically, xanthines (e.g., caffeine and pentifylline) activate the RYR by potentiating its sensitivity to Ca^{2+} (Xu et al., 1998). Physiologically, cyclic ADP-ribose acts as a gating agent, possibly by making FKBP12.6 (12.6 kilodalton FK506 binding protein) dissociate from RYR2. Normally, FKBP12.6 binds to and blocks the RYR2 channel (Wang et al., 2004).

Ca^{2+} Syntillas

Ca^{2+} "syntillas" are highly localized, brief, spontaneous Ca^{2+} transients that resemble Ca^{2+} sparks in muscle cells and have been shown to arise from ryanodine-sensitive internal stores of both hypothalamic nerve terminals (De Crescenzo et al., 2004) and adrenal chromaffin cells (ZhuGe et al., 2006) (Figure 4.5). Our group initially discovered these Ca^{2+} transients in neurohypophyseal nerve terminals and later found them in ACCs. Thus, we have termed them "syntillas" (*scintilla*, Latin for spark; first found in nerve terminals, *syn*aptic structures).

Syntillas can be mediated by different isoforms of RYR according to cell type. In nerve terminals the frequency of syntillas can be modulated by a voltage-dependent mechanism, whereby the RYR1 is thought to directly interact

with L-type Ca^{2+} channels, in a process termed voltage induced Ca^{2+} release (VICaR) (De Crescenzo et al., 2006). On the other hand, in mouse ACCs, syntillas do not display voltage dependence and are most likely mediated by RYR2. This derives from RT-PCR and immunocytochemistry studies in these cells where high levels of RYR2, but only low levels of RYR3 and virtually no trace of RYR1 are detected. The RYR3 is distributed in a highly punctuate, perinuclear fashion about the center of the cell. RYR2 by contrast displays a subplasmalemmal distribution throughout the cell, which seems to be consistent with the localization of syntillas by imaging (ZhuGe et al., 2006).

Since discovered, the function of syntillas had become the subject of intense investigation within our group. It is well known that Ca^{2+} influx from outside the cell, through calcium channels, results in exocytosis. Therefore we first postulated that Ca^{2+} release from stores within the cell (syntillas) should also function to elicit exocytosis. But a previous study from our group had shown that this was not the case. That is, syntillas do not trigger exocytotic events, despite their release of sufficient Ca^{2+} to do so if released within several hundred nanometers of a docked, primed vesicle. Instead, we found that Ca^{2+} syntillas are released into microdomains distinct from the canonical exocytotic microdomains near the plasma membrane wherein docked, primed vesicles reside (ZhuGe et al., 2006).

The function of Ca^{2+} syntillas is now known. The following chapters of this dissertation describe in detail how syntillas function by exerting an inhibitory influence over spontaneous exocytosis in mouse ACCs and furthermore, how syntillas are modulated by physiologic stimulation of these cells.

References

Albillos A, Garcia AG, Gandia L (1993) omega-Agatoxin-IVA-sensitive calcium channels in bovine chromaffin cells. FEBS Lett 336:259-262.

Albillos A, Neher E, Moser T (2000) R-Type Ca2+ channels are coupled to the rapid component of secretion in mouse adrenal slice chromaffin cells. J Neurosci 20:8323-8330.

Albillos A, Artalejo AR, Lopez MG, Gandia L, Garcia AG, Carbone E (1994) Calcium channel subtypes in cat chromaffin cells. J Physiol 477 (Pt 2):197-213.

Aldea M, Jun K, Shin HS, Andres-Mateos E, Solis-Garrido LM, Montiel C, Garcia AG, Albillos A (2002) A perforated patch-clamp study of calcium currents and exocytosis in chromaffin cells of wild-type and alpha(1A) knockout mice. J Neurochem 81:911-921.

Alonso MT, Montero M, Carnicero E, Garcia-Sancho J, Alvarez J (2002) Subcellular Ca(2+) dynamics measured with targeted aequorin in chromaffin cells. Ann N Y Acad Sci 971:634-640.

Alonso MT, Barrero MJ, Michelena P, Carnicero E, Cuchillo I, Garcia AG, Garcia-Sancho J, Montero M, Alvarez J (1999) Ca2+-induced Ca2+ release in chromaffin cells seen from inside the ER with targeted aequorin. J Cell Biol 144:241-254.

Arroyo G, Aldea M, Fuentealba J, Albillos A, Garcia AG (2003) SNX482 selectively blocks P/Q Ca2+ channels and delays the inactivation of Na+ channels of chromaffin cells. Eur J Pharmacol 475:11-18.

Artalejo CR, Perlman RL, Fox AP (1992) Omega-conotoxin GVIA blocks a Ca2+ current in bovine chromaffin cells that is not of the "classic" N type. Neuron 8:85-95.

Artalejo CR, Adams ME, Fox AP (1994) Three types of Ca2+ channel trigger secretion with different efficacies in chromaffin cells. Nature 367:72-76.

Artalejo CR, Mogul DJ, Perlman RL, Fox AP (1991) Three types of bovine chromaffin cell Ca2+ channels: facilitation increases the opening probability of a 27 pS channel. J Physiol 444:213-240.

Augustine GJ, Santamaria F, Tanaka K (2003) Local calcium signaling in neurons. Neuron 40:331-346.

Aunis D (1998) Exocytosis in chromaffin cells of the adrenal medulla. Int Rev Cytol 181:213-320.

Babcock DF, Herrington J, Goodwin PC, Park YB, Hille B (1997) Mitochondrial participation in the intracellular Ca2+ network. J Cell Biol 136:833-844.

Bernardi P (1999) Mitochondrial transport of cations: channels, exchangers, and permeability transition. Physiol Rev 79:1127-1155.

Bossu JL, De Waard M, Feltz A (1991) Inactivation characteristics reveal two calcium currents in adult bovine chromaffin cells. J Physiol 437:603-620.

Bournaud R, Hidalgo J, Yu H, Jaimovich E, Shimahara T (2001) Low threshold T-type calcium current in rat embryonic chromaffin cells. J Physiol 537:35-44.

Carabelli V, Giancippoli A, Baldelli P, Carbone E, Artalejo AR (2003) Distinct potentiation of L-type currents and secretion by cAMP in rat chromaffin cells. Biophys J 85:1326-1337.

Carbone E, Marcantoni A, Giancippoli A, Guido D, Carabelli V (2006) T-type channels-secretion coupling: evidence for a fast low-threshold exocytosis. Pflugers Arch 453:373-383.

Cesetti T, Hernandez-Guijo JM, Baldelli P, Carabelli V, Carbone E (2003) Opposite action of beta1- and beta2-adrenergic receptors on Ca(V)1 L-channel current in rat adrenal chromaffin cells. J Neurosci 23:73-83.

Chan SA, Polo-Parada L, Smith C (2005) Action potential stimulation reveals an increased role for P/Q-calcium channel-dependent exocytosis in mouse adrenal tissue slices. Arch Biochem Biophys 435:65-73.

Cheek TR, Barry VA (1993) Stimulus-secretion coupling in excitable cells: a central role for calcium. J Exp Biol 184:183-196.

Cheng H, Lederer WJ, Cannell MB (1993) Calcium sparks: elementary events underlying excitation-contraction coupling in heart muscle. Science 262:740-744.

Chow RH, Klingauf J, Neher E (1994) Time course of Ca2+ concentration triggering exocytosis in neuroendocrine cells. Proc Natl Acad Sci U S A 91:12765-12769.

Collin T, Marty A, Llano I (2005) Presynaptic calcium stores and synaptic transmission. Curr Opin Neurobiol 15:275-281.

De Crescenzo V, ZhuGe R, Velazquez-Marrero C, Lifshitz LM, Custer E, Carmichael J, Lai FA, Tuft RA, Fogarty KE, Lemos JR, Walsh JV, Jr. (2004) Ca2+ syntillas, miniature Ca2+ release events in terminals of hypothalamic neurons, are increased in frequency by depolarization in the absence of Ca2+ influx. J Neurosci 24:1226-1235.

De Crescenzo V, Fogarty KE, Zhuge R, Tuft RA, Lifshitz LM, Carmichael J, Bellve KD, Baker SP, Zissimopoulos S, Lai FA, Lemos JR, Walsh JV, Jr. (2006) Dihydropyridine receptors and type 1 ryanodine receptors constitute the molecular machinery for voltage-induced Ca2+ release in nerve terminals. J Neurosci 26:7565-7574.

Diverse-Pierluissi M, Dunlap K, Westhead EW (1991) Multiple actions of extracellular ATP on calcium currents in cultured bovine chromaffin cells. Proc Natl Acad Sci U S A 88:1261-1265.

Fabiato A (1983) Calcium-induced release of calcium from the cardiac sarcoplasmic reticulum. Am J Physiol 245:C1-14.

Fleckenstein A (1983) History of calcium antagonists. Circ Res 52:I3-16.

Fox AP, Nowycky MC, Tsien RW (1987a) Kinetic and pharmacological properties distinguishing three types of calcium currents in chick sensory neurones. J Physiol 394:149-172.

Fox AP, Nowycky MC, Tsien RW (1987b) Single-channel recordings of three types of calcium channels in chick sensory neurones. J Physiol 394:173-200.

Gandia L, Albillos A, Garcia AG (1993) Bovine chromaffin cells possess FTX-sensitive calcium channels. Biochem Biophys Res Commun 194:671-676.

Gandia L, Borges R, Albillos A, Garcia AG (1995) Multiple calcium channel subtypes in isolated rat chromaffin cells. Pflugers Arch 430:55-63.

Gandia L, Lara B, Imperial JS, Villarroya M, Albillos A, Maroto R, Garcia AG, Olivera BM (1997) Analogies and differences between omega-conotoxins MVIIC and MVIID: binding sites and functions in bovine chromaffin cells. Pflugers Arch 435:55-64.

Gandia L, Mayorgas I, Michelena P, Cuchillo I, de Pascual R, Abad F, Novalbos JM, Larranaga E, Garcia AG (1998) Human adrenal chromaffin cell calcium channels: drastic current facilitation in cell clusters, but not in isolated cells. Pflugers Arch 436:696-704.

Garcia-Palomero E, Cuchillo-Ibanez I, Garcia AG, Renart J, Albillos A, Montiel C (2000) Greater diversity than previously thought of chromaffin cell Ca2+ channels, derived from mRNA identification studies. FEBS Lett 481:235-239.

Garcia-Sancho J, Verkhratsky A (2008) Cytoplasmic organelles determine complexity and specificity of calcium signalling in adrenal chromaffin cells. Acta Physiol (Oxf) 192:263-271.

Garcia AG, Garcia-De-Diego AM, Gandia L, Borges R, Garcia-Sancho J (2006) Calcium signaling and exocytosis in adrenal chromaffin cells. Physiol Rev 86:1093-1131.

Gill DL (1989) Calcium signalling: receptor kinships revealed. Nature 342:16-18.

Gunter TE, Pfeiffer DR (1990) Mechanisms by which mitochondria transport calcium. Am J Physiol 258:C755-786.

Gunter TE, Gunter KK, Sheu SS, Gavin CE (1994) Mitochondrial calcium transport: physiological and pathological relevance. Am J Physiol 267:C313-339.

Hernandez-Guijo JM, de Pascual R, Garcia AG, Gandia L (1998) Separation of calcium channel current components in mouse chromaffin cells superfused with low- and high-barium solutions. Pflugers Arch 436:75-82.

Hernandez-Guijo JM, Maneu-Flores VE, Ruiz-Nuno A, Villarroya M, Garcia AG, Gandia L (2001) Calcium-dependent inhibition of L, N, and P/Q Ca2+ channels in chromaffin cells: role of mitochondria. J Neurosci 21:2553-2560.

Herrington J, Park YB, Babcock DF, Hille B (1996) Dominant role of mitochondria in clearance of large Ca2+ loads from rat adrenal chromaffin cells. Neuron 16:219-228.

Hille B (1992) Ionic channels of excitable membranes, 2nd Edition. Sunderland, Mass.: Sinauer Associates.

Hollins B, Ikeda SR (1996) Inward currents underlying action potentials in rat adrenal chromaffin cells. J Neurophysiol 76:1195-1211.

Inoue M, Sakamoto Y, Fujishiro N, Imanaga I, Ozaki S, Prestwich GD, Warashina A (2003) Homogeneous Ca2+ stores in rat adrenal chromaffin cells. Cell Calcium 33:19-26.

Kasai H, Aosaki T, Fukuda J (1987) Presynaptic Ca-antagonist omega-conotoxin irreversibly blocks N-type Ca-channels in chick sensory neurons. Neurosci Res 4:228-235.

Kitamura N, Ohta T, Ito S, Nakazato Y (1997) Calcium channel subtypes in porcine adrenal chromaffin cells. Pflugers Arch 434:179-187.

Klingauf J, Neher E (1997) Modeling buffered Ca2+ diffusion near the membrane: implications for secretion in neuroendocrine cells. Biophys J 72:674-690.

Livett BG (1993) Chromaffin cells: roles for vesicle proteins and Ca2+ in hormone secretion and exocytosis. Trends Pharmacol Sci 14:345-348.

Lopez MG, Villarroya M, Lara B, Martinez Sierra R, Albillos A, Garcia AG, Gandia L (1994) Q- and L-type Ca2+ channels dominate the control of secretion in bovine chromaffin cells. FEBS Lett 349:331-337.

Lukyanetz EA, Neher E (1999) Different types of calcium channels and secretion from bovine chromaffin cells. Eur J Neurosci 11:2865-2873.

McNally JM (2008) Molecular mechanisms of neuropeptide secretion from neurohypophysial terminals : a dissertation / presented by James M. McNally. In: Physiology, pp xiv, 201 leaves (bound) : ill. (some col.) ; 229 cm. Worcester: University of Massachusetts Medical School.

Mintz IM, Venema VJ, Swiderek KM, Lee TD, Bean BP, Adams ME (1992) P-type calcium channels blocked by the spider toxin omega-Aga-IVA. Nature 355:827-829.

Montero M, Alonso MT, Albillos A, Garcia-Sancho J, Alvarez J (2001) Mitochondrial Ca(2+)-induced Ca(2+) release mediated by the Ca(2+) uniporter. Mol Biol Cell 12:63-71.

Montero M, Alonso MT, Carnicero E, Cuchillo-Ibanez I, Albillos A, Garcia AG, Garcia-Sancho J, Alvarez J (2000) Chromaffin-cell stimulation triggers fast millimolar mitochondrial Ca2+ transients that modulate secretion. Nat Cell Biol 2:57-61.

Moreno A, Lobaton CD, Santodomingo J, Vay L, Hernandez-SanMiguel E, Rizzuto R, Montero M, Alvarez J (2005) Calcium dynamics in catecholamine-containing secretory vesicles. Cell Calcium 37:555-564.

Mundorf ML, Troyer KP, Hochstetler SE, Near JA, Wightman RM (2000) Vesicular Ca(2+) participates in the catalysis of exocytosis. J Biol Chem 275:9136-9142.

Neher E (1998a) Vesicle pools and Ca2+ microdomains: new tools for understanding their roles in neurotransmitter release. Neuron 20:389-399.

Neher E (1998b) Usefulness and limitations of linear approximations to the understanding of Ca++ signals. Cell Calcium 24:345-357.

Newcomb R, Szoke B, Palma A, Wang G, Chen X, Hopkins W, Cong R, Miller J, Urge L, Tarczy-Hornoch K, Loo JA, Dooley DJ, Nadasdi L, Tsien RW, Lemos J, Miljanich G (1998) Selective peptide antagonist of the class E calcium channel from the venom of the tarantula Hysterocrates gigas. Biochemistry 37:15353-15362.

Nowycky MC, Fox AP, Tsien RW (1985) Three types of neuronal calcium channel with different calcium agonist sensitivity. Nature 316:440-443.

Ogawa Y, Murayama T, Kurebayashi N (2002) Ryanodine receptor isoforms of non-Mammalian skeletal muscle. Front Biosci 7:d1184-1194.

Park YB, Herrington J, Babcock DF, Hille B (1996) Ca2+ clearance mechanisms in isolated rat adrenal chromaffin cells. J Physiol 492 (Pt 2):329-346.

Penner R, Neher E (1988) The role of calcium in stimulus-secretion coupling in excitable and non-excitable cells. J Exp Biol 139:329-345.

Polo-Parada L, Chan SA, Smith C (2006) An activity-dependent increased role for L-type calcium channels in exocytosis is regulated by adrenergic signaling in chromaffin cells. Neuroscience 143:445-459.

Prakriya M, Lingle CJ (1999) BK channel activation by brief depolarizations requires Ca2+ influx through L- and Q-type Ca2+ channels in rat chromaffin cells. J Neurophysiol 81:2267-2278.

Randall A, Tsien RW (1995) Pharmacological dissection of multiple types of Ca2+ channel currents in rat cerebellar granule neurons. J Neurosci 15:2995-3012.

Regan LJ (1991) Voltage-dependent calcium currents in Purkinje cells from rat cerebellar vermis. J Neurosci 11:2259-2269.

Rigual R, Montero M, Rico AJ, Prieto-Lloret J, Alonso MT, Alvarez J (2002) Modulation of secretion by the endoplasmic reticulum in mouse chromaffin cells. Eur J Neurosci 16:1690-1696.

Sather WA, Tanabe T, Zhang JF, Mori Y, Adams ME, Tsien RW (1993) Distinctive biophysical and pharmacological properties of class A (BI) calcium channel alpha 1 subunits. Neuron 11:291-303.

Simon SM, Llinas RR (1985) Compartmentalization of the submembrane calcium activity during calcium influx and its significance in transmitter release. Biophys J 48:485-498.

Spedding M (1985) Activators and inactivators of Ca++ channels: new perspectives. J Pharmacol 16:319-343.

Trenker M, Malli R, Fertschai I, Levak-Frank S, Graier WF (2007) Uncoupling proteins 2 and 3 are fundamental for mitochondrial Ca2+ uniport. Nat Cell Biol 9:445-452.

Tsien RW, Hess P, McCleskey EW, Rosenberg RL (1987) Calcium channels: mechanisms of selectivity, permeation, and block. Annu Rev Biophys Biophys Chem 16:265-290.

Valentino K, Newcomb R, Gadbois T, Singh T, Bowersox S, Bitner S, Justice A, Yamashiro D, Hoffman BB, Ciaranello R, et al. (1993) A selective N-type calcium channel antagonist protects against neuronal loss after global cerebral ischemia. Proc Natl Acad Sci U S A 90:7894-7897.

Villalobos C, Nunez L, Montero M, Garcia AG, Alonso MT, Chamero P, Alvarez J, Garcia-Sancho J (2002) Redistribution of Ca2+ among cytosol and organella during stimulation of bovine chromaffin cells. Faseb J 16:343-353.

Villarroya M, Olivares R, Ruiz A, Cano-Abad MF, de Pascual R, Lomax RB, Lopez MG, Mayorgas I, Gandia L, Garcia AG (1999) Voltage inactivation of Ca2+ entry and secretion associated with N- and P/Q-type but not L-type Ca2+ channels of bovine chromaffin cells. J Physiol 516 (Pt 2):421-432.

Vites AM, Pappano AJ (1994) Distinct modes of inhibition by ruthenium red and ryanodine of calcium-induced calcium release in avian atrium. J Pharmacol Exp Ther 268:1476-1484.

Wang YX, Zheng YM, Mei QB, Wang QS, Collier ML, Fleischer S, Xin HB, Kotlikoff MI (2004) FKBP12.6 and cADPR regulation of Ca2+ release in smooth muscle cells. Am J Physiol Cell Physiol 286:C538-546.

Wheeler DB, Randall A, Tsien RW (1994) Roles of N-type and Q-type Ca2+ channels in supporting hippocampal synaptic transmission. Science 264:107-111.

Xu L, Tripathy A, Pasek DA, Meissner G (1998) Potential for pharmacology of ryanodine receptor/calcium release channels. Ann N Y Acad Sci 853:130-148.

Xu T, Naraghi M, Kang H, Neher E (1997) Kinetic studies of Ca2+ binding and Ca2+ clearance in the cytosol of adrenal chromaffin cells. Biophys J 73:532-545.

Yang D, Pan Z, Takeshima H, Wu C, Nagaraj RY, Ma J, Cheng H (2001) RyR3 amplifies RyR1-mediated Ca(2+)-induced Ca(2+) release in neonatal mammalian skeletal muscle. J Biol Chem 276:40210-40214.

Yoo SH, Albanesi JP (1990) Inositol 1,4,5-trisphosphate-triggered Ca2+ release from bovine adrenal medullary secretory vesicles. J Biol Chem 265:13446-13448.

Yoo SH, Albanesi JP (1991) High capacity, low affinity Ca2+ binding of chromogranin A. Relationship between the pH-induced conformational change and Ca2+ binding property. J Biol Chem 266:7740-7745.

Zhou Z, Neher E (1993) Mobile and immobile calcium buffers in bovine adrenal chromaffin cells. J Physiol 469:245-273.

ZhuGe R, DeCrescenzo V, Sorrentino V, Lai FA, Tuft RA, Lifshitz LM, Lemos JR, Smith C, Fogarty KE, Walsh JV, Jr. (2006) Syntillas release Ca2+ at a site different from the microdomain where exocytosis occurs in mouse chromaffin cells. Biophys J 90:2027-2037.

Zucchi R, Ronca-Testoni S (1997) The sarcoplasmic reticulum Ca2+ channel/ryanodine receptor: modulation by endogenous effectors, drugs and disease states. Pharmacol Rev 49:1-51.

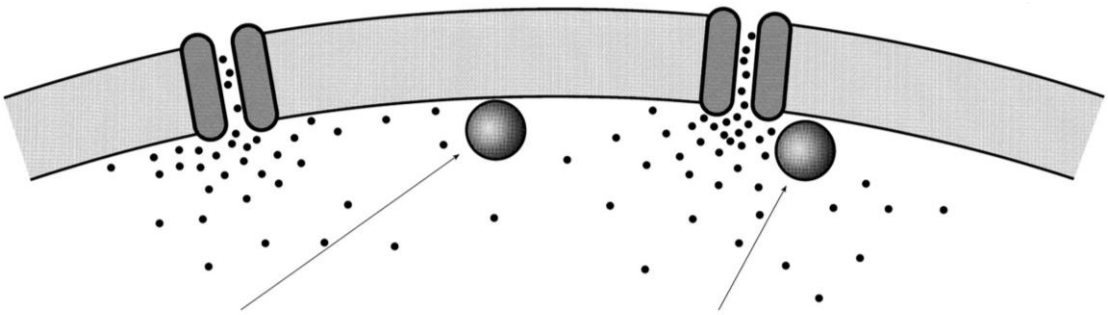

At 200 nm distance:

1.) $[Ca^{++}] \approx$ 5-10 µM
2.) Rises and falls in ≈ 10 msec
3.) Is at equilibrium with mobile buffers
4.) Strongly dependent on buffers; EGTA as effective as BAPTA
5.) $[Ca^{++}]$ determined by mean activity of several neighbouring channels

At 20 nm distance:

1.) $[Ca^{++}] \approx$ 100 µM
2.) Rises and falls within µsec
3.) Is not at equilibrium with mobile buffers
4.) Almost independent of Ca-buffers; EGTA totally ineffective
5.) $[Ca^{++}]$ predominantly determined by the local channel

Figure 4.1 **Ca^{2+} microdomains and nanodomains.** A separation between Ca^{2+} channel and target of the Ca^{2+} signal at about 200 nm (target lies within a Ca^{2+} *micro*domain) and another one in the range of 10 – 20 nm separation (target lies within a Ca^{2+} *nano*domain). **(Left)** The first one represents a mean distance for randomly mixed channels and release sites in the case of adrenal chromaffin cells. **(Right)** The second one is characteristic for the case that a Ca^{2+} channel is part of the release machinery.

(Adapted from Neher, 1998a)

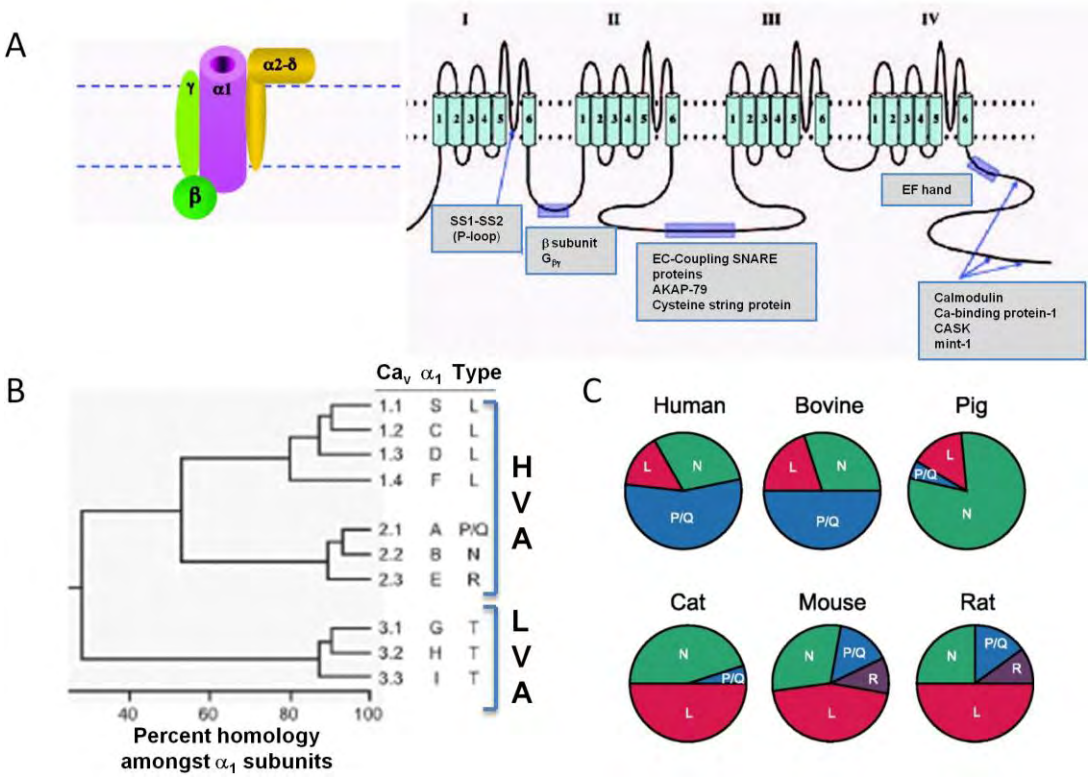
A
α2-δ
γ
α1
β
I
II
III
IV
SS1-SS2
(P-loop)
β subunit
$G_{\beta\gamma}$
EC-Coupling SNARE
proteins
AKAP-79
Cysteine string protein
EF hand
Calmodulin
Ca-binding protein-1
CASK
mint-1
B
Ca_V α_1 Type
1.1 S L
1.2 C L
1.3 D L
1.4 F L
2.1 A P/Q
2.2 B N
2.3 E R
3.1 G T
3.2 H T
3.3 I T
HVA
LVA
40
60
80
100
Percent homology
amongst α_1 subunits
C
Human
Bovine
Pig
Cat
Mouse
Rat
L
N
P/Q
R

Figure 4.2 Voltage gated calcium channels (VGCCs). A. Family composition of a VGCC complex and structure of the α_1 subunit. **(Left)** Diagram of a high-voltage-activated VGCC complex, indicating the α_1, α_2/δ, β, and γ subunits. The α_1 subunit forms the channel, comprising the voltage-sensing mechanism, the Ca^{2+} selective pore, and the target of identified pharmacological agents. **(Right)** Predicted structure and transmembrane topology of the α_1 subunit. Each domain possesses six putative membrane-spanning segments (1-6) and pore-forming P-loop (SS1-SS2). All high voltage-activated channel α_1 subunits possess a conserved region in the domain I-II linker that binds the Ca β subunit as well as a conserved EF hand motif in the carboxyl terminus. Other structural elements identified amongst the various types of high voltage-activated Ca^{2+} channels include: a high affinity G-protein βγ-subunit binding site in the I-II linker (Cav2.1 and Cav2.2); distinct regions in the domain II-III linker responsible for functional interaction with the synaptic release machinery (Cav2.1 and Cav2.2), binding to AKAP-79 (Cav1.2), cysteine string protein (Cav2.2) and the skeletal muscle excitation-contraction coupling machinery (Cav1.1); as well as carboxyl terminal regions shown to interact with calmodulin (Cav1.2, Cav2.1, Cav2.2, Cav2.3), Ca^{2+} -binding protein-1 (Cav1.2, Cav2.1), CASK (Cav2.2) and mint-1 (Cav2.2). **B.** Family classification of voltage-gated Ca^{2+} channels, based on biophysical properties, pharmacological sensitivity and sequence homology. The Ca_v1 and Ca_v2 subfamilies comprise the high-voltage-activated channels, while the Ca_v3 subfamily contains low-voltage-activated (T-type) channels. **C** Relative proportions of different neuronal calcium channel subtypes in primary cultures of chromaffin cells isolated from bovine, rat, mouse, cat, pig, and human adrenal medullary tissues.

(Adapted from Zamponi GW (2005) Voltage-gated calcium channels. Georgetown, Tex.New York, N.Y.: Landes Bioscience/Eurekah.com ; Kluwer Academic/Plenum Publishers. And Garcia et al., 2006)

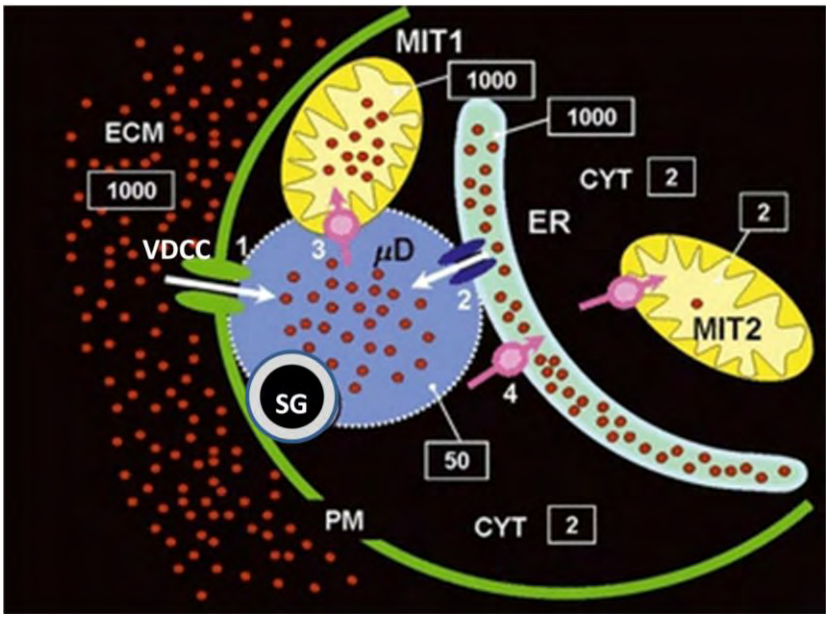

Figure 4.3 Functional triads responsible for the generation of subplasmalemmal high Ca^{2+} microdomains in chromaffin cells. The voltage-dependent Ca^{2+} channel (1, VDCC) of the plasma membrane (PM), the ryanodine receptor (2) from the endoplasmic reticulum (ER), the Ca^{2+} uniporter (3) from the surrounding mitochondria (MIT), and the secretory granule (SG) are all strategically located beneath the plasma membrane. Ca^{2+} entry through VDCC triggers Ca^{2+}-induced Ca^{2+}-release (CICR) from ER and generates a local $[Ca^{2+}]_{cyto}$ microdomain (μD) of about 50 μM. In the bulk of the cytosol (CYT), the $[Ca^{2+}]_{cyto}$ increase is much smaller, about 2 μM. The mitochondrion, placed at the triad, near the high Ca^{2+} microdomain (MIT1) quickly takes up Ca^{2+} and can eventually reach $[Ca^{2+}]$ of near 1000 μM. The mitochondrion placed far away from the high Ca^{2+} microdomain (MIT2), increases its $[Ca^{2+}]$ to only about 2 μM.

Adapted from Garcia et al. (2008)

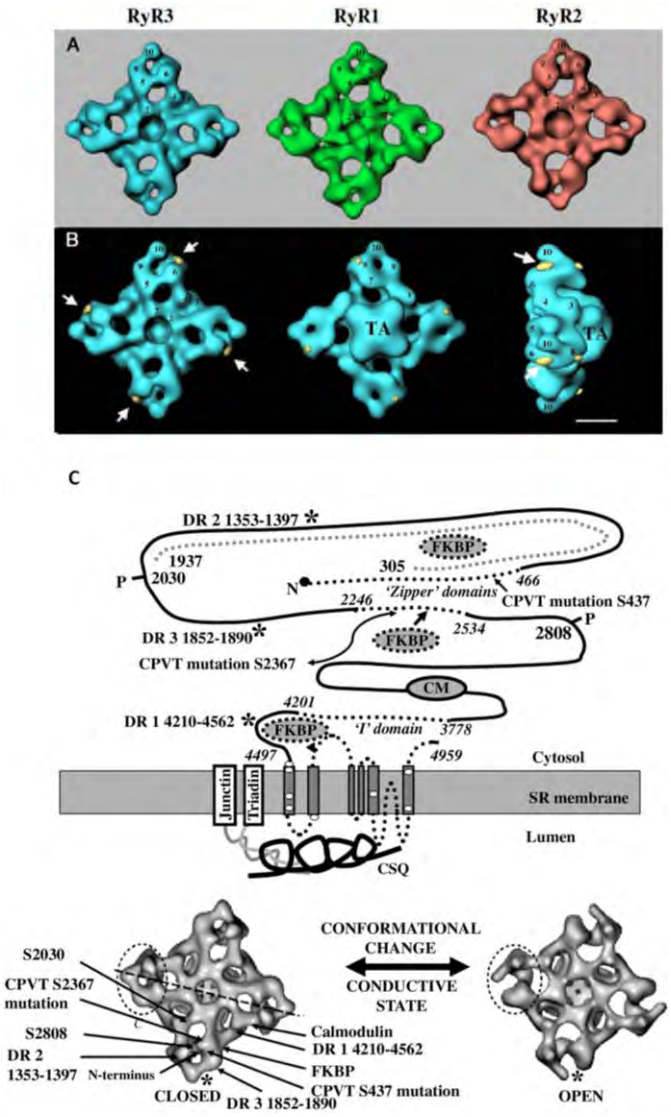
RyR3
RyR1
RyR2
A
B
TA
TA
C
DR 2 1353-1397 *
FKBP
1937
2030
P
305
N
'Zipper' domains
466
CPVT mutation S437
2246
2534
2808
P
DR 3 1852-1890*
FKBP
CPVT mutation S2367
CM
4201
DR 1 4210-4562 *
FKBP
'I' domain
3778
4497
4959
Cytosol
Junctin
Triadin
SR membrane
Lumen
CSQ
S2030
CPVT S2367 mutation
S2808
DR 2 1353-1397
N-terminus
CLOSED
DR 3 1852-1890
CONFORMATIONAL CHANGE
CONDUCTIVE STATE
Calmodulin
DR 1 4210-4562
FKBP
CPVT S437 mutation
OPEN

Figure 4.4 **3D reconstructions comparing RYR1, RYR2 and RYR3. A.** Solid body representations of cytoplasmic surface of RYR3 (blue), RYR1 (green), RYR2 (red). Domain architecture is conserved. **B.** RYR3 superimposed with the major differences (yellow) that are obtained when the reconstruction of RYR3 is subtracted from RYR1. Arrows indicate the main difference which is tentatively attributed to the D2 region which is absent from RYR3. **C.** RYR2 structure and the relationship to important domains associated with function, regulatory proteins and CPVT point mutations.

(Adapted from Wagenknecht and Samsó, 2002 and Blayney and Lai, 2009)

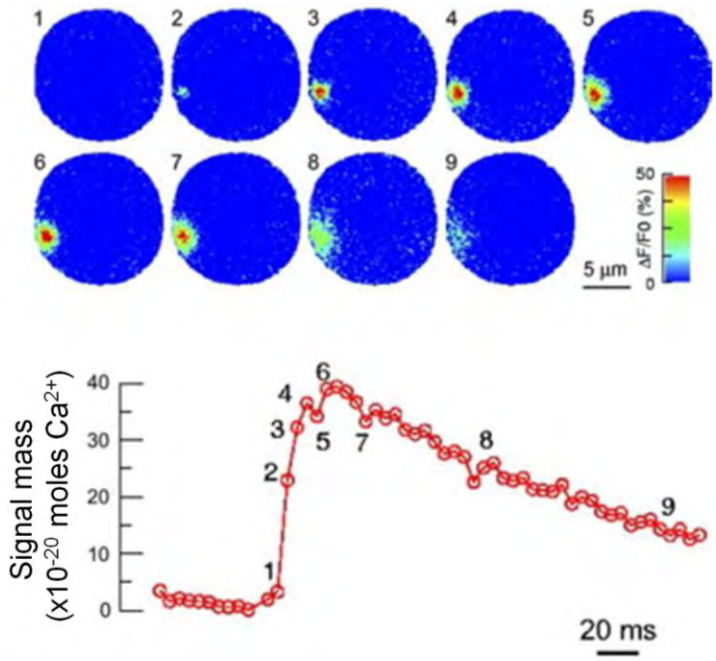

Figure 4.5 Evolution of a Ca^{2+} syntilla in a mouse adrenal chromaffin cell. (Top) Images display the evolution of a single Ca^{2+} syntilla resulting from the opening of RYRs. Changes in cytosolic Ca^{2+} were measured using fluo-3 (50 μM), which was introduced into the cell in the salt form through the patch pipette. The images were acquired at a rate of 200 Hz with an exposure time of 5 ms. The change in Ca^{2+} concentration in the images is expressed as $\Delta F/F_0$ (%) and displayed on a pseudo-color scale calibrated at the right of the second row of images. Numbers above the images correspond to the numbers in the top part of the panel below and indicate the time at which the image was obtained. Ca^{2+} syntillas were recorded with a high-speed imaging system from chromaffin cells that were voltage-clamped at a holding potential of −80 mV in the absence of extracellular Ca^{2+} in this case. **(Bottom)** The time course of the signal mass or the total moles of Ca^{2+} released in the syntilla shown in panel above.

Adapted from ZhuGe et al., (2006)

Chapter 5

Suppression of calcium syntillas increases spontaneous exocytosis in mouse adrenal chromaffin cells

Abstract: **A central concept in the physiology of neurosecretion is that a rise in cytosolic [Ca^{2+}] in the vicinity of plasmalemmal Ca^{2+} channels due to Ca^{2+} influx, elicits exocytosis. Here we examine the effect on spontaneous exocytosis of a rise in focal cytosolic [Ca^{2+}] in the vicinity of ryanodine receptors (RYRs) due to release from internal stores in the form of Ca^{2+} syntillas. Ca^{2+} syntillas are focal cytosolic transients mediated by RYRs, which we first found in hypothalamic magnocellular neuronal terminals. (*Scintilla*, Latin for spark, found in nerve terminals, normally synaptic structures.) We have also observed Ca^{2+} syntillas in mouse adrenal chromaffin cells. Here we examine the effect of Ca^{2+} syntillas on exocytosis in chromaffin cells. In such a study on elicited exocytosis, there are two sources of Ca^{2+}, that due to influx from the cell exterior through voltage-gated Ca^{2+} channels and that due to release from intracellular stores. To eliminate complications arising from Ca^{2+} influx, we have examined spontaneous exocytosis where influx is not activated. We report here that decreasing syntillas leads to an increase in spontaneous exocytosis measured amperometrically. Two independent lines of experimentation each lead to this conclusion. In one case release from stores was blocked by ryanodine; in another, stores were partially emptied using thapsigargin plus caffeine after which syntillas were decreased. We conclude that Ca^{2+} syntillas act to inhibit spontaneous exocytosis, and we propose a simple model to account quantitatively for this action of syntillas.**

Introduction

Since the work of Katz, Douglas and their collaborators almost half a century ago (Katz, 1969) a central concept in the physiology of neurosecretion is that a rise in cytosolic [Ca^{2+}], resulting from Ca^{2+} influx, triggers exocytosis. More recently it has become clear that the rise in [Ca^{2+}] occurs in a microdomain within the vicinity (i.e., at a distance of 200-300 nm in chromaffin cells) of plasmalemmal Ca^{2+} channels (Garcia et al., 2006; Neher and Sakaba, 2008). This finding raises the possibility of other microdomains where a rise in focal [Ca^{2+}] might mediate other processes, allowing Ca^{2+} to subserve a number of functions without crosstalk. This possibility receives further support from the study of Ca^{2+} sparks in smooth muscle cells. Ca^{2+} sparks are focal Ca^{2+} transients found in striated and smooth muscle and mediated by Ryanodine Receptors (RYRs) (Cheng and Lederer, 2008). In striated muscle they are the quanta or building blocks that make up a global increase in [Ca^{2+}] to trigger contraction (Csernoch, 2007). However, in smooth muscle Ca^{2+} sparks have quite a different function. They activate large conductance Ca^{2+}-activated K^+ channels (BK channels) located within 150-300 nm of the spark site (Zhuge et al., 2002); the resulting K^+ efflux and hyperpolarization deactivates voltage-gated Ca^{2+} channels and thus terminates contraction. Hence in smooth muscle sparks have quite the opposite

function from that in striated muscle and the opposite of a global [Ca^{2+}] in smooth muscle. In smooth muscle sparks cause a relaxation (Nelson et al., 1995; ZhuGe et al., 1998).

Ca^{2+} syntillas are brief (on the order of tens of milliseconds), focal cytosolic Ca^{2+} transients due to release from intracellular stores and mediated by RYRs (De Crescenzo et al., 2004; Collin et al., 2005). They were first found in freshly isolated neurohypophyseal terminals of magnocellular neurons (De Crescenzo et al., 2004). Because the transients resembled Ca^{2+} sparks found in muscle, we designated them Ca^{2+} syntillas (*scintilla*, Latin for spark; from a nerve terminal, normally a synaptic structure). In a previous study (ZhuGe et al., 2006), we also found such focal transients in freshly isolated mouse adrenal chromaffin cells, which resemble in their magnitude, time course and spontaneous frequency those found in neurohypophyseal nerve terminals. That study established two main points: 1. syntillas in chromaffin cells arise from intracellular stores, as indicated by their occurrence in the absence of extracellular Ca^{2+}; and 2. syntillas do not trigger exocytotic events, despite their releasing sufficient Ca^{2+} to do so if the release were to occur within several hundred nm of a docked, primed large dense core granule (LDCG). Hence we proposed that Ca^{2+} syntillas arise in a different microdomain from that of the

docked, primed granule. However we did not uncover the function of Ca^{2+} syntillas, the topic addressed here.

Here we examine the effects of Ca^{2+} syntillas on exocytosis in mouse adrenal chromaffin cells. We have begun by studying spontaneous exocytosis in the form of individual exocytotic events as measured amperometrically. (We use the term “spontaneous” rather than “basal” exocytosis since a low level of stimulation is sometimes designated “basal” stimulation, e.g., Fulop et al, 2005.) There are three reasons for studying spontaneous exocytosis. First elicited exocytosis demands Ca^{2+} influx through voltage-gated Ca^{2+} channels, and so there are two sources of cytosolic Ca^{2+}, that from influx and that from intracellular stores. The examination of spontaneous exocytosis allows us to examine the latter without activating the former and hence circumvents the complication of two Ca^{2+} sources. Second, the study of spontaneous exocytosis has, since the time of Katz (Katz, 1969), contributed valuable insights into the general process, most notably establishing the quantal or vesicular nature of exocytosis. Third, in neurons it is increasingly apparent that spontaneous exocytosis is not simply a byproduct of synaptic transmission but has a physiological role and is worth studying in its own right (see (Glitsch, 2008)) for the following reasons. In hippocampal CA1 pyramidal cells spontaneous glutamate release maintains dendritic spines via AMPA receptor activation (McKinney et al., 1999). Moreover,

spontaneous neurotransmitter release may regulate dendritic protein synthesis and thus influence expression of receptors on postsynaptic cells (Sutton and Carew, 2000). Furthermore, spontaneous neurotransmitter release can influence the processing of synaptic inputs in small interneurons and affect the interneuron's ability to fire action potentials (Carter and Regehr, 2002). Finally, short-term potentiation of mEPSCs regulates excitability of postsynaptic supraoptic neurons in the hypothalamus (Kombian et al., 2000). Hence, in a number of neurons, spontaneous exocytosis has its own function.

In this study we find that preventing Ca^{2+} release from intracellular stores in the form of Ca^{2+} syntillas, in two different and independent ways, results in an increase in frequency and magnitude of spontaneous exocytotic events as measured by amperometry. The syntillas were monitored by using a unique high temporal and spatial resolution optical imaging system which permits monitoring of the entire cell and a "signal mass" analysis which measures the total *amount* of Ca^{2+} released per individual syntilla (See Methods). Contrary to expectation, we conclude that Ca^{2+} syntillas *inhibit* spontaneous exocytosis of LDCGs.

Materials and methods

Tight-seal, whole cell recordings on chromaffin cells, freshly dissociated from adult male Swiss Webster mice as described previously (ZhuGe et al., 2006), were performed with a HEKA EPC10 amplifier (HEKA Electronics, Lambrecht, Germany) on the same day as isolation. Mice (6–8 weeks) were sacrificed by cervical dislocation in accordance with the IACUC guidelines at the University of Massachusetts Medical School. Patch pipette solution (mM) was: 0.05 K_5fluo-3 (Molecular Probes, Eugene, OR), 135 KCl, 2 $MgCl_2$, 30 Hepes, 4 MgATP, 0.3 Na-GTP, pH 7.3. The pipette solution buffered at 150 nM [Ca^{2+}] (mM) was: 0.025 K_5fura-2 (Molecular Probes) or 0.05 K_5fluo-3, 0.25 EGTA, 0.175 $CaCl_2$, 135 KCl, 2 $MgCl_2$, 30 Hepes, 4 MgATP, 0.3 Na-GTP, pH 7.3. The pipette solution buffered at 500 nM [Ca^{2+}] (mM) was: 0.025 K_5fura-2 (Molecular Probes) or 0.05 K_5fluo-3, 0.1 EGTA, 0.1 $CaCl_2$, 135 KCl, 2 $MgCl_2$, 30 Hepes, 4 MgATP, 0.3 Na-GTP, pH 7.3. EGTA, fura-2 or fluo-3 and $CaCl_2$ values were predicted with the free- Ca^{2+} and Mg^{2+} program within IGOR Pro (Wavemetrics, Lake Oswego, Oregon) to achieve a free- [Ca^{2+}] of 150 nM or 500 nM, then adjusted based on measurements of global $[Ca^{2+}]_i$ with fura-2. Bath solution: 135 NaCl, 5 KCl, 10 Hepes, 10 glucose, 1 $MgCl_2$, and 2.2 $CaCl_2$, pH 7.2. Except when otherwise indicated, all reagents came from Sigma (Saint Louis, MO).

Fluorescence images using fluo-3 as a Ca^{2+} indicator were obtained using a custom-built wide-field digital imaging system described previously (ZhuGe et al., 2006). To assess the properties of individual Ca^{2+} syntillas quantitatively, the signal mass approach was used, as conceptualized by Sun et al. (Sun et al., 1998) and developed for wide-field microscopy of Ca^{2+} sparks by ZhuGe et al (ZhuGe et al., 2000). The purpose of this approach is to obtain a measure of the total *amount* of Ca^{2+} (as opposed to concentration of Ca^{2+}) released by a focal Ca^{2+} transient. Global $[Ca^{2+}]_i$ was measured by fluorescence with cell-impermeant fura-2 (25 μM) that was loaded into cells through the patch pipette and measured as previously described (Grynkiewicz et al., 1985; Becker and Fay, 1987; Drummond and Tuft, 1999).

Corrections for buffers in the calculations of signal mass, simulations for Figure 5.6 and amperometric measurements are as follows. For the syntillas recorded in control and ryanodine experiments, where the only exogenous Ca^{2+} buffers were fluo-3 (50 μM) and ATP (4 mM), we corrected the signal mass value, as determined from the fluo-3 signal, for competition by endogenous Ca^{2+} buffer, as described previously (De Crescenzo et al., 2004; ZhuGe et al., 2006). Briefly, a correction factor of 2.15 was calculated from the binding ratios at resting Ca^{2+} of the fluo-3, ATP and the endogenous buffer. For the syntillas recorded in experiments where the resting $[Ca^{2+}]$ was buffered to normal resting

values with the addition of 250 μM EGTA and 175 μM Ca^{2+}, the fluo-3 signal mass was multiplied by 4.38 to account for the added competition by the EGTA. This number was determined empirically using computer simulations of the "typical" chromaffin syntilla (ZhuGe et al., 2006) with the addition of 250 μM EGTA, Kd=180 nM, koff=0.45/s (Naraghi and Neher, 1997), and increasing the syntilla Ca^{2+} current magnitude until the fluo-3 signal mass equaled that in simulation without the EGTA. Note that this is much less than the factor of 17.46 that is predicted by equilibrium buffering, where the binding ratio of the EGTA is > 600:1. The binding of Ca^{2+} by EGTA is too slow to significantly compete with fluo-3 over the few tens of milliseconds duration of a syntilla. Additionally, the simulations demonstrate that the effect of this amount of EGTA on the free [Ca^{2+}] spatiotemporal profile is negligible in the syntilla microdomain where high (>> 1μM) [Ca^{2+}] occurs.

Experimental protocols

1. Fluo-3 Ca^{2+} imaging and amperometry. After the patch is ruptured to provide the whole cell configuration, we waited at least two minutes for the fluo-3 to reach equilibrium in the cell. In a typical experiment, when the fluorescence was stable, we began to record two 4-second image sequences in a row (200 images separated by 20ms, with an exposure time of 10ms). Then we started to record

the amperometry for 4 to 6 minutes (2 to 3 segments of two minutes each). After the amperometric recording, two more 4-second image sequences of fluo-3 fluorescence were recorded. These two image sequences and the ones recorded earlier were used to establish the syntilla frequency for that cell. These data show no difference between the frequency at the beginning and the frequency at the end of the experiments. So in a typical cell, both amperometry and fluo-3 fluorescence were recorded.

2. Ryanodine protocol. Ryanodine stock was first prepared in DMSO at 100mM. Just before the experiments, ryanodine was dissolved in the physiological solution at 1/1000 to reach the 100 μM concentration used. The cells were bathed in the 100 μM ryanodine solution in the dark for 30 minutes before recordings started.

In control, a caffeine pulse increased the basal $[Ca^{2+}]_i$ on average by 316 $\pm$ 91 % (N=3). $[Ca^{2+}]_i$ always returned to basal levels after the pulse. We found that after 30 minutes in ryanodine, the response to caffeine was minimal, inducing a mean increase of only 10 $\pm$ 2% above baseline (N=3). Increasing the incubating time to 60 minutes in ryanodine in two cells did not further decrease the caffeine response (11% and 18% above baseline in response to caffeine).

3. Reserpine protocol. The cells were bathed in the 100 μM ryanodine solution (for control) or in 100 μM ryanodine plus 1μM reserpine, in the dark for 30 minutes, before experiments commenced (Mundorf et al., 2000; Gong et al., 2003). Preliminary experiments show that 1 μM reserpine alone compared to control (normal saline solution, in the absence of ryanodine) gave a significant decrease in mean charge of amperometric spikes (0.21 ± 0.04 pC, N=6, in control solution versus 0.10 ± 0.01 pC, N=17, in presence of reserpine, p= 0.012). This 50% decrease is comparable to the reserpine effects (30% decrease) reported previously in adrenal chromaffin cells (Mundorf et al., 2000; Gong et al., 2003).

4. Thapsigargin and caffeine protocols. (See legend of Figure 5.4 and Results.)

Data Analysis

Statistical analyses and plots were performed in OriginPro 8.0 (Origin, Northampton, MA). In all cases except for syntilla frequency and signal mass, data was first averaged per cell and is reported as mean ±SE of all cells. Data from syntilla frequency and signal mass is reported, as previously (ZhuGe et al., 2006), as mean ±SE of individual records and mean ±SE of individual syntillas,

respectively. Statistical analysis of difference was made with a Student's t-test (log-transformed, for charge data) or a Mann-Whitney test (for syntilla frequencies) and the p-values are presented in the Figure captions, as appropriate. A p-value less than 0.05 is significant except in multiple comparisons, where the Bonferroni corrected p values must be less than 0.02 (significance is indicated by an asterisk). N indicates the number of cells and n the number of events, i.e., syntillas or amperometric spikes.

Modeling the relationship between syntillas and exocytosis.

We modeled the relationship between syntillas and the frequency of amperometric events, in Figure 5.6B as a simple two-state system: granules that are able to release their catecholamines, and granules that are inhibited from releasing them by a process caused by a rise in $[Ca^{2+}]$ in a Ca^{2+} microdomain, which for purposes of fitting the data as seen in Figure 5.6B we define as a volume where free $[Ca^{2+}]$ generated by a syntilla was > 10 μM. The two state model is represented as:

$$R \underset{\alpha}{\overset{\beta}{\leftarrow\!\rightarrow}} I$$

where α is the rate of inhibition due to syntillas and β is reverse rate to the releasable state. (We note that the syntilla microdomain could be set for any level of free [Ca^{2+}], but 10 μM was chosen because it gave a slightly better fit to the data in Figure 5.6B and for a number of other reasons enumerated in Results. However, in Figure 5.6A we show the contour lines delimiting volumes corresponding to values of free [Ca^{2+}] for 1, 3, 10 and 30 μM.) The number of releasable granules R, and therefore the observed frequency of amperometric events in this case is:

$$f_{amp} \propto \left(\frac{\beta}{\beta + \alpha} \right) \qquad \text{(eq. 1)}$$

We modeled α as proportional to the product of the syntilla frequency and the volume of the syntilla microdomain, which we call the Syntilla Index or SI:

$$SI = f_{syn} \cdot V_{syn} \qquad \text{(eq. 2)}$$

where f_{syn} is the syntilla frequency, and V_{syn} is the volume of the syntilla microdomain exceeding 10 μM free [Ca^{2+}]. The units of SI are $\mu m^3/s$. Each of the four experimental conditions shown in Figure 5.6A (control, ryanodine, buffered control, buffered Tg+caffeine) has a corresponding SI value.

We can simplify by combining equations 1 and 2 to obtain:

$$f_{amp} \propto \left(\frac{1}{1 + k * SI} \right) \qquad \text{(eq. 3)}$$

where k*SI is equal to the ratio α/β.

The equation describing the frequency of amperometric events in granules/s at equilibrium is:

$$f_{amp} = F_0 * \left(\frac{1}{1 + k * SI} \right) \qquad \text{(eq. 4)}$$

where F_0 is the frequency of events when syntillas are completely abolished (SI=0). Assuming that the carbon fiber monitors ~10% of the cell surface (Haller et al., 1998; Grabner et al., 2005), whole-cell, amperometric frequencies were plotted against their corresponding SI's as seen in Figure 5.6B.

Determining syntilla microdomain volume.

To determine the SI it was first necessary to find the volume of the syntilla microdomain as defined above. To do this we used the same approach as in ZhuGe et al. (2006) where we determined the spatiotemporal profile of free

$[Ca^{2+}]$ using as input the I_{Ca} of the average chromaffin cell syntilla as derived from the first derivative of the average signal-mass over time. We determined I_{Ca} from the average peak signal mass for each experimental condition in Figure 5.6 (control, ryanodine, buffered control, buffered Tg+caffeine) using the time course found in ZhuGe et al (2006). A computer simulation with the I_{Ca} for each condition as input was carried out, and the resulting spatiotemporal profile of free $[Ca^{2+}]$ was established (Figure 5.6A). (The ordinate in Figure 5.6A represents one spatial dimension with the other two being identical to the first. Together they make up a hemisphere rather than a sphere since the type two RYRs and hence the syntillas are in a subplasmalemmal space where diffusion can only occur in a hemispherical volume.) The free $[Ca^{2+}]$ used to compute the volumes were 30, 10, 3 and 1 μM at their maximum spatial extent. For the SI we used 10 μM free $[Ca^{2+}]$. The volumes were 0.02895, 0.00045, 0.0194, and 0.01435 μm^3 for control, ryanodine, buffered control, and buffered Tg+caffeine respectively. The corresponding syntilla frequencies were 0.81, 0.28, 0.78, and 0.42 s^{-1}, as shown in the lower panel of Figure 5.6A. By equation 2, these gave SI values of 0.0235, 0.000126, 0.015, and 0.006 $\mu m^3/s$.

Amperometric measurements.

Quantal release of catecholamine from single chromaffin cells was monitored electrochemically using carbon fiber electrodes with a tip diameter of 5.8 μm (ALA Scientific Instruments, Westbury, NY), as described before (ZhuGe et al., 2006). Amperometric signals, i.e., oxidation currents, were monitored with a VA-10 amplifier (NPI Electronic, Tamm, Germany), filtered at 0.5 kHz, digitized at 1 kHz with a Digidata 1200B acquisition system, and acquired with Patchmaster software from HEKA. Amperometric spikes were identified and analyzed using the Mini Analysis Program (Synaptosoft, Decatur, GA). Each event was visually inspected so that artifacts could be rejected from the analysis. The root mean square noise in acquired traces was typically < 0.25 pA as determined by the Mini Analysis program. The detection threshold for an event was set to 2.5 times the baseline root mean square. Overlapping events were rare, and were excluded from analysis. To minimize errors due to possible variation in exocytosis among cells from different animals, cells from each animal were divided into two groups: one as control and the other treated with agents such as ryanodine. SAFs were separated from spikes based on criteria somewhat similar to (Wang et al., 2006), where an index of event shape was used to evaluate the "rectangularity" of a putative SAF. In the present study, to qualify as an SAF an event had to meet the criteria of an amplitude less than 2.5 pA and a ratio of full-

width at half-height to event duration greater than 0.25. Event durations for spikes and SAFs are defined as the duration between the time when the event signal exceeds, and the time when it returns to, the detection threshold amplitude as defined above.

Results

For all experiments reported here, except for those of Figure 5.3, freshly dissociated mouse adrenal chromaffin cells were studied in whole cell voltage-clamp mode with the membrane potential held at -80 mV. Calcium indicator dyes were introduced through the patch pipette in the salt form, favoring its confinement to the cytosol and ensuring the same concentration from cell to cell; fluo-3 was used for detection of Ca^{2+} syntillas and fura-2 for measurement of global cytosolic [Ca^{2+}]. Amperometry was used to monitor individual exocytotic events.

Blocking ryanodine receptors

To examine the effect of Ca^{2+} stores on spontaneous exocytosis, we first employed 100 μM ryanodine (See Methods for protocol), which, as we have shown previously, blocks Ca^{2+} syntillas in mouse adrenal chromaffin cells (ZhuGe et al., 2006). Figure 5.1 illustrates the fundamental findings of this first set of experiments. In panel A, a cell is shown from a single image under control conditions (left) with a typical Ca^{2+} syntilla and another cell bathed for 30 minutes in ryanodine (right), with syntillas decreased in frequency and amplitude (De

Crescenzo et al., 2004; ZhuGe et al., 2006). This is due to block of RYRs, the Ca^{2+} channels embedded in the ER membrane which are responsible for Ca^{2+} syntillas (De Crescenzo et al., 2004 ; ZhuGe et al., 2006) as well as Ca^{2+} sparks (Cheng and Lederer, 2008). In panel B, typical amperometric traces are shown from a control (left) and ryanodine treated (right) cell where individual events are more frequent and of larger amplitude. The Ca^{2+} syntillas decreased in frequency whereas, quite surprisingly, the amperometric events increased in frequency upon treatment with ryanodine (Figure 5.1C, left). Moreover, the average magnitude of the individual Ca^{2+} syntilla, as measured by its signal mass was decreased whereas the mean charge per amperometric event increased (Figure 5.1C, right). (Simply put, the signal mass is a measure of the total *amount* of Ca^{2+} released per individual syntilla and hence it is given in units of moles of Ca^{2+}. See methods.)

The total charge per single spontaneous amperometric event (i.e., its magnitude) in the presence and absence of ryanodine is given in the distribution of Figure 5.2A, with the inset showing the difference between the two distributions, that is, the additional events in the presence of ryanodine. These distributions count all events, and show an increase in both their frequency and magnitude in the presence of ryanodine. When the events are separated into spikes and stand-alone feet (SAF) (Figure 5.2B and C), the frequency of the

spikes, but not of the stand-alone feet, is increased by ryanodine. Thus, the increase in frequency of spikes is not due to a shift from SAFs to spikes. (SAFs are taken to represent partial granule emptying or "kiss and run" events, whereas spikes may represent either full fusion *or* "kiss and run" events (Wang et al., 2003; Gong et al., 2007).) What accounts for the increase in the magnitude of the SAFs and spikes in the presence of ryanodine? In the case of the SAF's, which are approximated by a square wave, the amplitude alone is increased and not the duration. In the case of the spikes, the amplitude, rise time and duration are all increased (Table 5.1).

A change in global cytosolic Ca^{2+} concentration might be invoked to explain these results. However, global cytosolic Ca^{2+} concentration, as determined ratiometrically with fura-2, did not change in the presence of ryanodine [133.0 ± 28.4 nM (n=11)] versus [140.0 ± 35.0 nM in control (n=5, p=0.89)]. Furthermore 100 μM ryanodine caused a decrease in the global calcium transient evoked by 20mM caffeine (See ryanodine protocol in Methods) as expected, showing that ryanodine was indeed blocking Ca^{2+} release via RYRs. Hence, there was no increase in global cytosolic [Ca^{2+}] to explain the increase in amplitude and frequency of the spontaneous amperometric events. In sum, both the frequency and the magnitude of the amperometric spikes increased upon a decrease in the frequency and signal mass of the Ca^{2+} syntillas in the presence of ryanodine.

Blocking ryanodine receptors in the presence of reserpine

The ryanodine-induced increase in *frequency* of exocytotic events is not readily explained by an inhibitory effect of syntillas on the vesicular monoamine transporter (VMAT). Nevertheless we examined the exocytotic events in the presence of reserpine to block the VMAT – with and without ryanodine. 1 μM reserpine was applied for at least 30 minutes (Mundorf et al., 2000; Gong et al., 2003) before recording, a standard protocol which was sufficient to exert the expected effects. (See Methods.) However, reserpine did not block the effects of ryanodine on the frequency of amperometric events (0.12 ± 0.03 (N = 17) and 0.40 ± 0.13 S^{-1} (N=12, $p<0.02$) for reserpine and reserpine plus ryanodine, respectively) nor the mean charge increase (0.09 ± 0.01 (N = 17) and 0.26 ± 0.03 pC (N= 12, $p<0.00001$) for reserpine and reserpine plus ryanodine, respectively).

Blocking ryanodine receptors in unpatched intact cells

In unpatched cells, we observed much the same spontaneous exocytotic activity as in whole cell recording. Furthermore, the same effects of ryanodine on amperometric events observed under conditions of whole cell recording are also seen in unpatched cells where the cytosol is not disturbed (Figure 5.3 and Table

5.2). Thus, the effect on spontaneous exocytosis extends beyond conditions of whole-cell recording to intact cells.

Decreasing Ca^{2+} levels in ryanodine-sensitive internal stores

To examine the effect of Ca^{2+} stores in a way that did not depend on ryanodine blockade and that would provide another, independent line of evidence, we employed thapsigargin (Tg) to deplete the Ca^{2+} stores. Tg, which blocks the sarco-endoplasmic reticulum Ca^{2+} ATPase (SERCA) pump that returns Ca^{2+} to the ER, by itself did not appear to cause substantial store depletion in the chromaffin cells, since syntilla frequency did not decrease under this condition compared to its control (0.37 ± 0.11 vs 0.46 ± 0.06) (Figure 5.4A). This is to be expected when the stores have a minimal leak, as found, for example, in smooth muscle (ZhuGe et al., 1999). In that situation, not only is it necessary to prevent reuptake of Ca^{2+} into stores by blocking the SERCA pump, but caffeine also has to be employed transiently to elicit release from the stores. Therefore, we treated the cells with Tg and then delivered a brief pulse of caffeine. Subsequently, after a one minute pause to allow the cells to recover from the transient Ca^{2+} release, syntillas and exocytosis were monitored over 4 to 6 minutes (Figure 5.4A). Neither Tg alone nor caffeine alone had an effect on syntillas or amperometric events as compared to the data under control conditions as shown in Figures 5.1

and 5.2. Tg+caffeine decreased the frequency of syntillas compared to Tg alone or caffeine alone (Figure 5.4B). In the second case, that is, when caffeine was puffed in the absence of Tg, syntillas were recorded after 1 minute. Only with the Tg+caffeine protocol did we find a corresponding increase in the frequency of both Spikes and SAFs (5.4C). The charge of amperometric events was not significantly altered (Figure 5.4D). However, when we measured *global* $[Ca^{2+}]$ in each condition, we found that Tg+caffeine caused a rise in mean global cytosolic $[Ca^{2+}]$ to about 500 nM (Figure 5.4E). This rise in global $[Ca^{2+}]$ was a confounding condition since it has been reported that elevation of global calcium can facilitate the spontaneous release of granules in cultured bovine adrenal chromaffin cells (Augustine and Neher, 1992) over a range of $[Ca^{2+}]_i$ levels above 200 nM and saturating at 10 μM.

To distinguish the possible effect of the elevated global $[Ca^{2+}]$ from that of syntillas, we experimentally separated them in two ways. First we buffered the internal solution to 500 nM to study only the effect of a higher global $[Ca^{2+}]$. Second we buffered the internal solution to 150nM, the approximate resting level (see below) and applied Tg+caffeine, to study the effect of lower Ca^{2+} syntilla frequency alone without a global increase.

Internal solution buffered to 500nM

To do this we buffered the internal solution with Ca^{2+} and EGTA to mimic the increased global Ca^{2+} levels in the Tg+caffeine experiments and monitored both syntillas and amperometric events. The results are shown in Figure 5.4, rightmost column in green. We detected no difference in the frequency of syntillas when global Ca^{2+} was elevated to 500nM (Figure 5.4B). Nor did we find an increase in the frequency or charge of amperometric events when resting global Ca^{2+} was raised from 135 nM to 500 nM (Figure 5.4C and D). This was to be expected, however, since significant facilitation of granule release was not achieved until $[Ca^{2+}]_i$ reached levels near 1 μM in Augustine et al. (1992).

Internal solution buffered to 150nM along with treatment with Tg+caffeine. We buffered the internal cytosolic $[Ca^{2+}]$ to 150 nM with EGTA introduced through the patch pipette (Figure 5.5). With this buffering the global $[Ca^{2+}]$ in control cells versus Tg alone or Tg+caffeine treated cells was not different ($p>0.025$), as determined with ratiometric fura-2 measurements. (Control: 106 ± 9 nM, (n=4) versus Tg alone: 127±30 (n=6; p=0.53l); and control versus Tg+caffeine: 176.4 ±38 nM (n=5; p=0.14).) Moreover, these levels were well below the 500 nM concentration which itself was without detectable effect on the amperometric events (See previous paragraph.) Upon Tg+caffeine treatment in the buffered condition, we again saw a decrease in the syntilla frequency and an

increase in frequency and magnitude of amperometric events as we did when RYRs were blocked with ryanodine (Figure 5.5A). The distribution of the total charge per amperometric event in control and treated cells is shown in Figure 5.5B. The distribution of the amperometric events suppressed by release of Ca^{2+} from stores is shown in the inset of Figure 5.5B. As with the experiments using ryanodine, there was an increase in spike frequency without change in SAF frequency (Figure 5.5C). There was an increase in the mean magnitude of all the amperometric events, which was evident when the spikes and SAFs were grouped together (Figure 5.5A), although this was not as marked as that observed with ryanodine (Figure 5.1C). However, there was no increase in rise time of spikes, nor in SAF amplitude (Table 5.3), in contrast to the experiments with ryanodine. (Hence the change in amplitude of amperometric events seen in Figure 5.5A appears to simply be a consequence of an increase in spike frequency without a change in SAF frequency (Figure 5.5C).) Finally, the amplitude of the syntillas in these experiments did not change (Figure 5.5A), again in contrast to the experiments with ryanodine (Figure 5.1C). The mean signal mass of the syntillas as given in Figure 5.5A has been corrected for the EGTA buffering as outlined in Methods. With this correction the signal mass does not differ from the signal mass in unbuffered solution (Figure 5.1C), whereas the frequency of syntillas has decreased. This is reminiscent of the finding with Ca^{2+} sparks in smooth muscle where a partial depletion of the ER

results in a decrease in spark frequency without a change in amplitude. The reason appears to be that a small reduction of [Ca^{2+}] in the ER regulates spark frequency even when that reduction is not sufficient to result in a substantially smaller driving force on the Ca^{2+} (ZhuGe et al., 1999). The results from the experiments using buffered internal solutions show that the global [Ca^{2+}] in the range of 150 to 500 nM has no detectable effect on spontaneous exocytosis.

The results with Tg and caffeine, taken together with those of ryanodine above, argue against an effect mediated by the level of the [Ca^{2+}] in the ER, for example an effect on the store operated channels, since in one case the stores are depleted while in the other they are not. The results with Tg and caffeine also indicate that the effect on release is an acute effect. The effect occurs within minutes after the application of caffeine, a time too short for granule synthesis or recycling. (Wakade et al., 1988; von Grafenstein and Knight, 1992).

Relationship between exocytotic events and syntillas

The data from the experiments reported here were used to construct a plot of the relationship between Ca^{2+} syntillas and frequency of spontaneous amperometric events (Figure 5.6B). We devised a “syntilla index” (SI), which is the product of the syntilla rate and the volume of the syntilla microdomain, as defined in

Methods and shown in Figure 5.6A. We show four spatiotemporal contour lines delimiting volumes of four [Ca^{2+}]'s within the syntillas microdomain (from 1 to 30 μM) (Figure 5.6A). We do not provide a contour line for lower [Ca^{2+}], since buffering the global [Ca^{2+}] to 500 nM was without effect on spontaneous amperometric events. Similarly a target which can only be affected by a [Ca^{2+}] an order of magnitude higher than 30 μM has no precedent so far as we know. The syntilla rate for each experimental condition is summarized directly below the contour lines in Figure 5.6A. The relationship between Ca^{2+} syntillas and amperometric event frequency (Figure 5.6B) was fitted by assuming that the granules reached a state where they could be exocytosed and the action of a syntilla, directly or indirectly, resulted in the inhibition of that state.

Discussion

The central finding of this study is that decreasing the frequency of Ca^{2+} syntillas leads to an increase in the frequency and magnitude of spontaneous exocytosis. We therefore propose, as the simplest explanation, that syntillas exert an inhibitory influence over spontaneous exocytosis. The result cannot easily be explained by hitherto unknown effects of the agents used to produce the decrease in syntilla frequency since we used two quite different sets of agents in separate experiments, whose effects have been studied in considerable detail over decades. Our results also rule out two explanations for the findings. First, the increase in magnitude of the amperometric events observed upon blocking syntillas does not seem to be due to a change in granule filling since it is not affected by reserpine (See Results). Second, a trivial explanation for the increase in frequency of amperometric events might be that an increase in magnitude improves detection, thus making it appear that the frequency has risen. For this to be the case, there would need to be smaller undetected events in the control condition. But when we lowered the threshold for inclusion in the data from 0.5 pA to 0.2 pA we found only 21 more events in addition to the 918 in Figure 5.2A which would increase the frequency by about 2.3%. This is far from sufficient to account for the 450% increase observed in the

presence of ryanodine (Figure 5.2C). Moreover, in the experiments with Tg+caffeine, the frequency of spikes increases but the charge apparently does not. Finally the same effects on amperometric events are found when ryanodine is applied to intact, unpatched cells.

A second Ca^{2+} microdomain

The increase in exocytotic frequency and magnitude upon blocking syntillas is quite unexpected, given the usual role attributed to Ca^{2+} in the exocytotic process. Nevertheless, at least one precedent exists for such a result, and that is the effect of the analogue of syntillas, Ca^{2+} sparks, in smooth muscle. In that case sparks, by activating Ca^{2+}-sensitive, large conductance K^+ channels *within the spark microdomain,* elicit current which hyperpolarizes the membrane, thus turning off voltage-activated Ca^{2+} channels and causing relaxation. This effect is precisely the opposite of what might be expected of cytosolic Ca^{2+} in muscle (Nelson et al., 1995). This mechanism of relaxation depends on the action of Ca^{2+} in a distinct microdomain, calculated to be within a radius of 150-300 nm from the Ca^{2+} release site (Zhuge et al., 2002). We suggest that in adrenal chromaffin cells, the syntillas act in a different microdomain from that where the final exocytotic step occurs. This conclusion is borne out by a previous study, as well as the present one, in which Ca^{2+} syntillas, despite their ability to raise $[Ca^{2+}]$

to supermicromolar levels within their microdomain, do not elicit exocytosis (ZhuGe et al., 2006). One microdomain might be termed the exocytotic domain where the voltage-gated Ca^{2+} channels responsible for elicited exocytosis are found and where the final exocytotic steps are triggered by Ca^{2+}; and the other the syntilla microdomain where RYR2s are present and where Ca^{2+} has an inhibitory effect on spontaneous exocytosis.

Physiological role of spontaneous exocytosis and its regulation by syntillas.

Is the spontaneous exocytosis examined here of physiological significance? And is the regulation exerted by the syntillas on catecholamine release of quantitative importance? We can gain some insight into these questions by comparing our results with recent work from the Smith laboratory (Fulop et al (2005), Doreian et al 2008, 2009) on physiological levels of stimulation of mouse chromaffin cells. These investigators call attention to two different physiological types of stimulation – a low frequency (0.5 Hz) and a high frequency (15 Hz) corresponding, respectively to resting sympathetic tone and "stress-associated" sympathetic activation (Brandt et al., 1976; Kidokoro and Ritchie, 1980).

Fulop et al (Fulop et al., 2005) found a rate of approximately 0.93 amperometric events per second per amperometric site per cell for both stimulus

paradigms, the difference in the two conditions being primarily the magnitude of the individual events. In our study the rate was 0.16 ± 0.03 s^{-1} in control conditions and 0.73 ± 0.15s^{-1} in the presence of ryanodine when virtually all syntillas were blocked. Thus the rate when syntillas are suppressed is 66% of that at physiological levels of stimulation. (If the plot in Figure 5.6 is extrapolated to zero syntilla rate, then the rate of amperometric events achieved by a physiological stimulation level (0.93 s^{-1}) and the rate achieved by syntilla suppression (0.78 s^{-1}) are of the same magnitude.)

Physiologically, in terms of relevance to the whole organism, it is of some interest to examine the rate of catecholamine release, i.e., moles s^{-1} of catecholamines. At the lower physiological stimulation rate of 0.5 Hz Fulop et al (2005) measured 200 pC of catecholamines, for a mean rate of 1.73 aM s^{-1} of catecholamine per amperometric site per cell. (At their higher rate of 15 Hz, Fulop et al (2005) found that the amount of catecholamine released per second (M s^{-1}) approximately doubled.) We measured 0.06 aM s^{-1} of catecholamine per amperometric site per cell under control conditions and 1.06 aM s^{-1} of catecholamine) in the presence of ryanodine, which almost completely suppressed the syntillas. Several points deserve mention. First, the effect of suppressing syntillas on the rate of spontaneous catecholamine release is not trivial, amounting to more than a 10-fold increase. In fact it is greater than that of

increasing the stimulation from 0.5 to 15 Hz, which results in an approximate 2-fold increase in rate of catecholamine release. Second, the rate of catecholamine release when syntillas are almost completely suppressed (1.06 aM s^{-1}) is 62% of that at 0.5 Hz (1.73 aM s^{-1}). That is, the two values are of the same order of magnitude, the intriguing implications of which have not eluded our notice. From these considerations we suggest that syntillas may well be a potent physiological regulator of catecholamine release.

The parameters of individual exocytotic events at the two levels of physiological stimulation have also been measured (Doreian et al 2008, 2009; supplementary data) and can be compared to spontaneous events in the present study. First, the mean amperometric amplitude and magnitude with basal stimulation at 0.5Hz (4.0 ± 0.43 pA, 0.08 ± 0.01pC) are the same as spontaneous release (5.4 ± 1. 3 pA, 0.08 ± 0.01pC). Moreover, when spontaneous syntillas are suppressed with ryanodine, the mean amplitude and charge (14.5 pA, 0.28 pC) are the same as reported for stimulation at 15Hz (16.3 pA, 0.31 pC). In sum, when the amplitude and magnitude of individual amperometric events are considered, suppression of syntillas with ryanodine yields the same increase as stimulation at 15 Hz. Therefore Ca^{2+} store modulation of spontaneous release may involve the mechanisms invoked by the Smith group to describe differences in 0.5 vs. 15Hz stimulation, i.e, a change in mode of release from kiss and run to

full fusion. This points to the possible relevance of the mechanisms affecting spontaneous release for understanding elicited release at physiological levels of stimulation.

Dual effect of syntillas on spontaneous exocytosis

The two effects of suppressing syntillas on spontaneous exocytosis, increasing the frequency and increasing the magnitude, might be linked or independent. If the increase in frequency and the increase in charge are indeed distinct effects, how might this happen? We propose that some LDCG's exposed to the syntilla microdomain are simply removed temporarily from the releasable pool, and so the frequency of spontaneous exocytosis goes down. Other granules exposed to Ca^{2+} in the syntilla microdomain would have their pore machinery modified resulting in less catecholamine release. This effect is reminiscent of the findings of Ales et al. (Ales et al., 1999), where greater Ca^{2+} influx caused a shift away from full fusion and toward kiss and run events. The larger Ca^{2+} influx in that study, resulting from extracellular Ca^{2+} concentrations as high as 90 mM, might have impinged on the Ca^{2+} syntilla microdomain and thus mimicked the effects of syntillas.

A second hypothesis is that block of Ca^{2+} syntillas causes greater recruitment of a population of larger LDCGs. Such a population has been observed in mouse chromaffin cells both morphologically and physiologically (Grabner et al., 2005). In this case the observed changes in the parameters of the amperometric spikes are consistent with a larger dense core granule being exocytosed through a pore of the same size as that of the smaller LDCGs which is opening at the same rate. On the one hand such a shift from a population of smaller LDCGs to larger ones is attractive because it explains both changes in frequency and magnitude of amperometric events by a single mechanism. On the other hand the effects of blocking syntillas on magnitude and frequency of amperometric events seem separable so that they may indeed be different effects.

Speculation into the molecular components involved in the regulation of spontaneous exocytosis by syntillas are discussed in the final Chapter 7.

References

Ales E, Tabares L, Poyato JM, Valero V, Lindau M, Alvarez de Toledo G (1999) High calcium concentrations shift the mode of exocytosis to the kiss-and-run mechanism. Nat Cell Biol 1:40-44.

Augustine GJ, Neher E (1992) Calcium requirements for secretion in bovine chromaffin cells. J Physiol 450:247-271.

Becker PL, Fay FS (1987) Photobleaching of fura-2 and its effect on determination of calcium concentrations. Am J Physiol 253:C613-618.

Brandt BL, Hagiwara S, Kidokoro Y, Miyazaki S (1976) Action potentials in the rat chromaffin cell and effects of acetylcholine. J Physiol 263:417-439.

Carter AG, Regehr WG (2002) Quantal events shape cerebellar interneuron firing. Nat Neurosci 5:1309-1318.

Cheng H, Lederer WJ (2008) Calcium sparks. Physiol Rev 88:1491-1545.

Collin T, Marty A, Llano I (2005) Presynaptic calcium stores and synaptic transmission. Curr Opin Neurobiol 15:275-281.

Csernoch L (2007) Sparks and embers of skeletal muscle: the exciting events of contractile activation. Pflugers Arch 454:869-878.

De Crescenzo V, ZhuGe R, Velazquez-Marrero C, Lifshitz LM, Custer E, Carmichael J, Lai FA, Tuft RA, Fogarty KE, Lemos JR, Walsh JV, Jr. (2004) Ca2+ syntillas, miniature Ca2+ release events in terminals of hypothalamic neurons, are increased in frequency by depolarization in the absence of Ca2+ influx. J Neurosci 24:1226-1235.

Drummond RM, Tuft RA (1999) Release of Ca2+ from the sarcoplasmic reticulum increases mitochondrial [Ca2+] in rat pulmonary artery smooth muscle cells. J Physiol 516 (Pt 1):139-147.

Fulop T, Radabaugh S, Smith C (2005) Activity-dependent differential transmitter release in mouse adrenal chromaffin cells. J Neurosci 25:7324-7332.

Garcia AG, Garcia-De-Diego AM, Gandia L, Borges R, Garcia-Sancho J (2006) Calcium signaling and exocytosis in adrenal chromaffin cells. Physiol Rev 86:1093-1131.

Glitsch MD (2008) Spontaneous neurotransmitter release and Ca2+--how spontaneous is spontaneous neurotransmitter release? Cell Calcium 43:9-15.

Gong LW, de Toledo GA, Lindau M (2007) Exocytotic catecholamine release is not associated with cation flux through channels in the vesicle membrane but Na+ influx through the fusion pore. Nat Cell Biol 9:915-922.

Gong LW, Hafez I, Alvarez de Toledo G, Lindau M (2003) Secretory vesicles membrane area is regulated in tandem with quantal size in chromaffin cells. J Neurosci 23:7917-7921.

Grabner CP, Price SD, Lysakowski A, Fox AP (2005) Mouse chromaffin cells have two populations of dense core vesicles. J Neurophysiol 94:2093-2104.

Grynkiewicz G, Poenie M, Tsien RY (1985) A new generation of Ca2+ indicators with greatly improved fluorescence properties. J Biol Chem 260:3440-3450.

Haller M, Heinemann C, Chow RH, Heidelberger R, Neher E (1998) Comparison of secretory responses as measured by membrane capacitance and by amperometry. Biophys J 74:2100-2113.

Katz B (1969) The release of neural transmitter substances. Springfield, Ill.,: Thomas.

Kidokoro Y, Ritchie AK (1980) Chromaffin cell action potentials and their possible role in adrenaline secretion from rat adrenal medulla. J Physiol 307:199-216.

Kombian SB, Hirasawa M, Mouginot D, Chen X, Pittman QJ (2000) Short-term potentiation of miniature excitatory synaptic currents causes excitation of supraoptic neurons. J Neurophysiol 83:2542-2553.

McKinney RA, Capogna M, Durr R, Gahwiler BH, Thompson SM (1999) Miniature synaptic events maintain dendritic spines via AMPA receptor activation. Nat Neurosci 2:44-49.

Mundorf ML, Troyer KP, Hochstetler SE, Near JA, Wightman RM (2000) Vesicular Ca(2+) participates in the catalysis of exocytosis. J Biol Chem 275:9136-9142.

Naraghi M, Neher E (1997) Linearized buffered Ca2+ diffusion in microdomains and its implications for calculation of [Ca2+] at the mouth of a calcium channel. J Neurosci 17:6961-6973.

Neher E, Sakaba T (2008) Multiple roles of calcium ions in the regulation of neurotransmitter release. Neuron 59:861-872.

Nelson MT, Cheng H, Rubart M, Santana LF, Bonev AD, Knot HJ, Lederer WJ (1995) Relaxation of arterial smooth muscle by calcium sparks. Science 270:633-637.

Sun XP, Callamaras N, Marchant JS, Parker I (1998) A continuum of InsP3-mediated elementary Ca2+ signalling events in Xenopus oocytes. J Physiol 509 (Pt 1):67-80.

Sutton MA, Carew TJ (2000) Parallel molecular pathways mediate expression of distinct forms of intermediate-term facilitation at tail sensory-motor synapses in Aplysia. Neuron 26:219-231.

von Grafenstein H, Knight DE (1992) Membrane recapture and early triggered secretion from the newly formed endocytotic compartment in bovine chromaffin cells. J Physiol 453:15-31.

Wakade AR, Wakade TD, Malhotra RK (1988) Restoration of catecholamine content of previously depleted adrenal medulla in vitro: importance of synthesis in maintaining the catecholamine stores. J Neurochem 51:820-829.

Wang CT, Bai J, Chang PY, Chapman ER, Jackson MB (2006) Synaptotagmin-Ca2+ triggers two sequential steps in regulated exocytosis in rat PC12 cells: fusion pore opening and fusion pore dilation. J Physiol 570:295-307.

Wang CT, Lu JC, Bai J, Chang PY, Martin TF, Chapman ER, Jackson MB (2003) Different domains of synaptotagmin control the choice between kiss-and-run and full fusion. Nature 424:943-947.

Zhuge R, Fogarty KE, Tuft RA, Walsh JV, Jr. (2002) Spontaneous transient outward currents arise from microdomains where BK channels are exposed to a mean Ca(2+) concentration on the order of 10 microM during a Ca(2+) spark. J Gen Physiol 120:15-27.

ZhuGe R, Sims SM, Tuft RA, Fogarty KE, Walsh JV, Jr. (1998) Ca2+ sparks activate K+ and Cl- channels, resulting in spontaneous transient currents in guinea-pig tracheal myocytes. J Physiol 513 (Pt 3):711-718.

ZhuGe R, Tuft RA, Fogarty KE, Bellve K, Fay FS, Walsh JV, Jr. (1999) The influence of sarcoplasmic reticulum Ca2+ concentration on Ca2+ sparks and spontaneous transient outward currents in single smooth muscle cells. J Gen Physiol 113:215-228.

ZhuGe R, Fogarty KE, Tuft RA, Lifshitz LM, Sayar K, Walsh JV, Jr. (2000) Dynamics of signaling between Ca(2+) sparks and Ca(2+)- activated K(+) channels studied with a novel image-based method for direct intracellular measurement of ryanodine receptor Ca(2+) current. J Gen Physiol 116:845-864.

ZhuGe R, DeCrescenzo V, Sorrentino V, Lai FA, Tuft RA, Lifshitz LM, Lemos JR, Smith C, Fogarty KE, Walsh JV, Jr. (2006) Syntillas release Ca2+ at a site different from the microdomain where exocytosis occurs in mouse chromaffin cells. Biophys J 90:2027-2037.

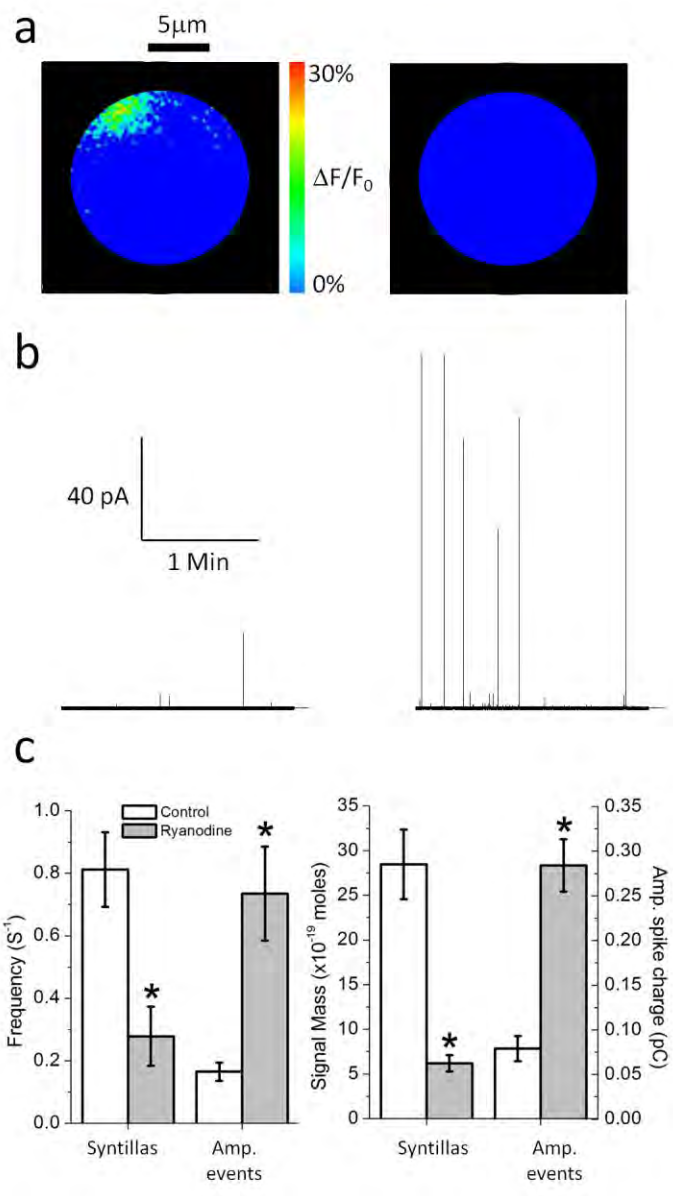
a
5µm
30%
ΔF/F0
0%
b
40 pA
1 Min
c
Control
Ryanodine
Frequency (S-1)
Signal Mass (x10-19 moles)
Amp. spike charge (pC)
Syntillas
Amp. events
Syntillas
Amp. events

Figure 5.1 **Effect of 100 μM ryanodine.** **A.** Changes in cytosolic [Ca^{2+}] measured with the Ca^{2+}–indicator dye, Fluo-3, and expressed on a pseudo-color scale as the change in fluorescence over the baseline fluorescence ($\Delta F/F_0$). Image threshold is 15% of $\Delta F/F_0$. Syntillas are larger and more frequent under normal conditions **(left)** and they are smaller, less frequent or completely blocked in the presence of ryanodine **(right)**. **B.** Representative amperometric trace from a cell in absence **(left)** and presence **(right)** of ryanodine. In the presence of syntillas **(left,** control**)** amperometric events are smaller and less frequent. When syntillas are blocked or decreased (**right**, 100 μM ryanodine) amperometric events are larger and more frequent. **C.** Left panel: 100μM ryanodine decreases syntilla frequency (**left bar graph**) from 0.81 ± 0.12 (n = 4) to 0.28 ± 0.09 s^{-1} (N = 18) ($p < 0.02$). Conversely, ryanodine increases exocytotic frequency (**right bar graph**) from 0.16 ±0.03 (N = 12) to 0.73 ± 0.15 s^{-1} (N =13) ($p < 0.002$). Error bars ± S.E.M. Right panel: 100 μM ryanodine also decreases the mean signal mass of the individual syntilla from 28.5 ± 3.9 (N = 13) to 6.2 ± 0.9 $x10^{-20}$ moles (n = 18) ($p < 0.00001$) and increases the mean charge per amperometric event from 0.08 ± 0.01 (N =12) to 0.28 ± 0.03 pC (N =13) ($p < 0.0003$).

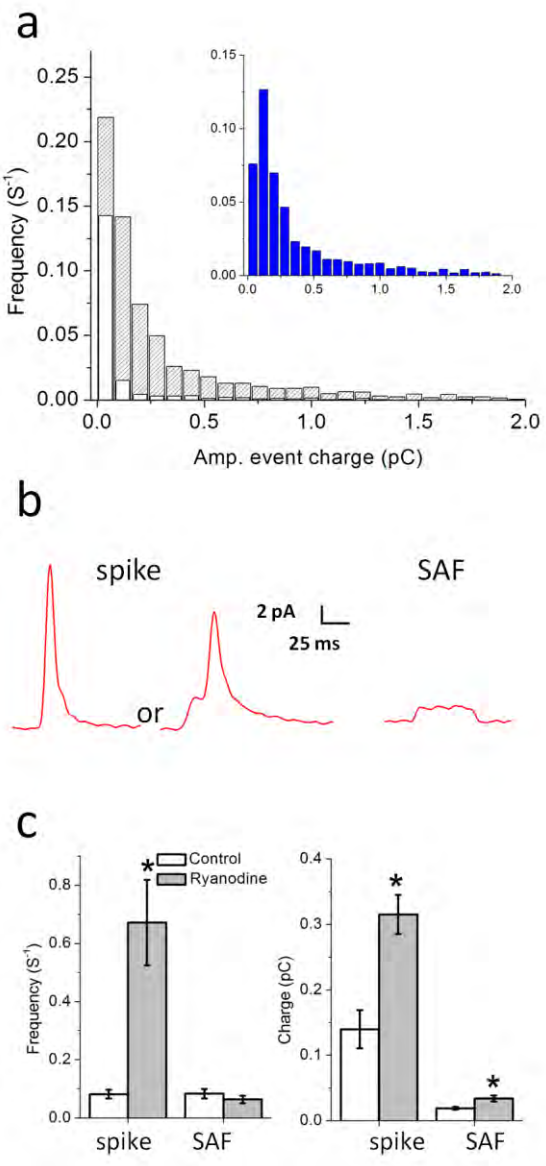
a
Frequency (S-1)
Amp. event charge (pC)
b
spike
SAF
2 pA
25 ms
or
c
Control
Ryanodine
Frequency (S-1)
Charge (pC)
spike
SAF

Figure 5.2 **Population of LDCGs blocked by ryanodine.** **A.** Frequency distribution of individual amperometric events according to charge (pC) in control (white, 918 events) and ryanodine treated cells (stripes, 2536 events). The difference between the two distributions is shown on an expanded x-axis in the inset. **B.** Examples of amperometric events recorded from mouse chromaffin cells. The first two traces show a spike, the second one with a pre-spike foot. The third one represents a stand alone foot (SAF). (Panel A includes all events, both SAFs and spikes. The criteria for classifying an event as an SAF are given in Methods.) **C.** Left panel shows the frequency of the spikes and the SAFs in control solution (0.08 ± 0.01 s^{-1} for both, N=12). Spike frequency increases in presence of ryanodine (0.67 ± 0.14 s^{-1}, $p < 0.0008$, N=13). Right panel shows that ryanodine increases the mean charge of spikes (0.14 ± 0.03 to 0.31 ± 0.03 pC, $p<0.0003$, N = 12 for control and N = 13 for treated cells) and SAFs (0.02 ± 0.00 to 0.04 ± 0.01 pC, $p<0.01$, N = 12 for control and N = 13 for treated cells).

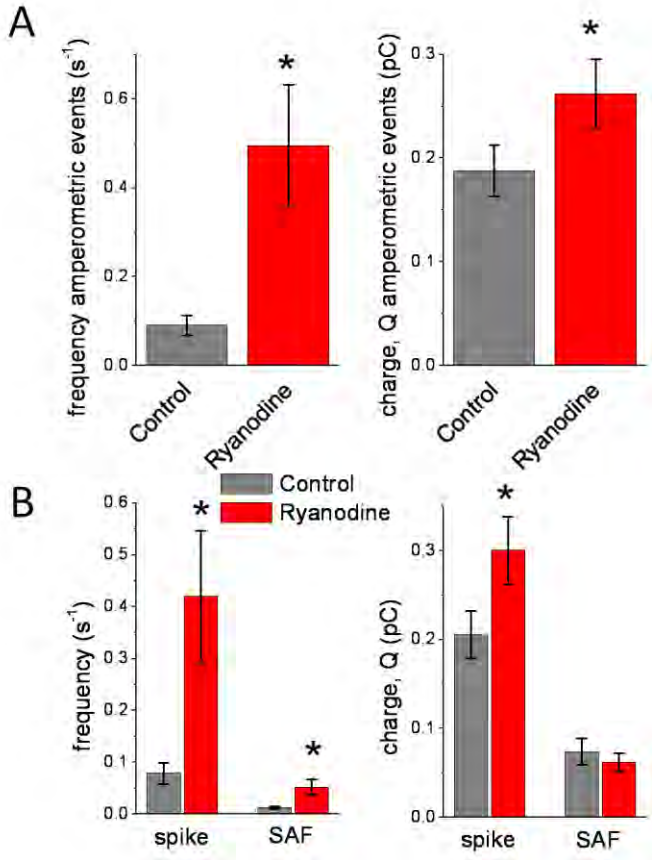
A
frequency amperometric events (s-1)
0.0
0.2
0.4
0.6
*
Control
Ryanodine
charge, Q amperometric events (pC)
0.0
0.1
0.2
0.3
*
Control
Ryanodine
B
Control
Ryanodine
frequency (s-1)
0.0
0.1
0.2
0.3
0.4
0.5
0.6
*
*
spike
SAF
charge, Q (pC)
0.0
0.1
0.2
0.3
*
spike
SAF

Figure 5.3 **Effect of 100 μM ryanodine in unpatched cells.** In the results shown here the same protocol was used as in Figures 5.1 and 5.2, except that the cells were not patched and hence the cytosol was left undisturbed. **A.** All amperometric events. **(Left)** frequency of all events in control (0.09 ± 0.02 s^{-1}, N = 28) vs. ryanodine (0.49 ± 0.14 s^{-1}, N = 9), $p<0.0002$. **(Right)** magnitude of all events for control (0.18 ± 0.2 pC, N = 28) vs. ryanodine (0.26 ± 0.03 pC, N = 9), $p<0.02$. **B.** Amperometric events separated into spikes and SAFs. **(Left)** control frequency of spikes (0.08 ± 0.02 s^{-1}, N = 28) and SAFs (0.01 ± 0.00 s^{-1}, N = 28) vs. ryanodine (0.42 ± 0.13 s^{-1}, N = 9) for spikes, $p<0.03$; and (0.05 ± 0.02 s^{-1}, N = 9) for SAFs, $p<0.02$. **(Right)** magnitude of spikes (0.20 ± 0.03 pC, N = 28) and SAFs (0.07 ± 0.01 pC, N = 21) in control vs. ryanodine (0.30 ± 0.04 pC, N = 9) for spikes, $p<0.02$ and (0.06 ± 0.01 pC, N = 9) for SAFs, $p=0.6$.

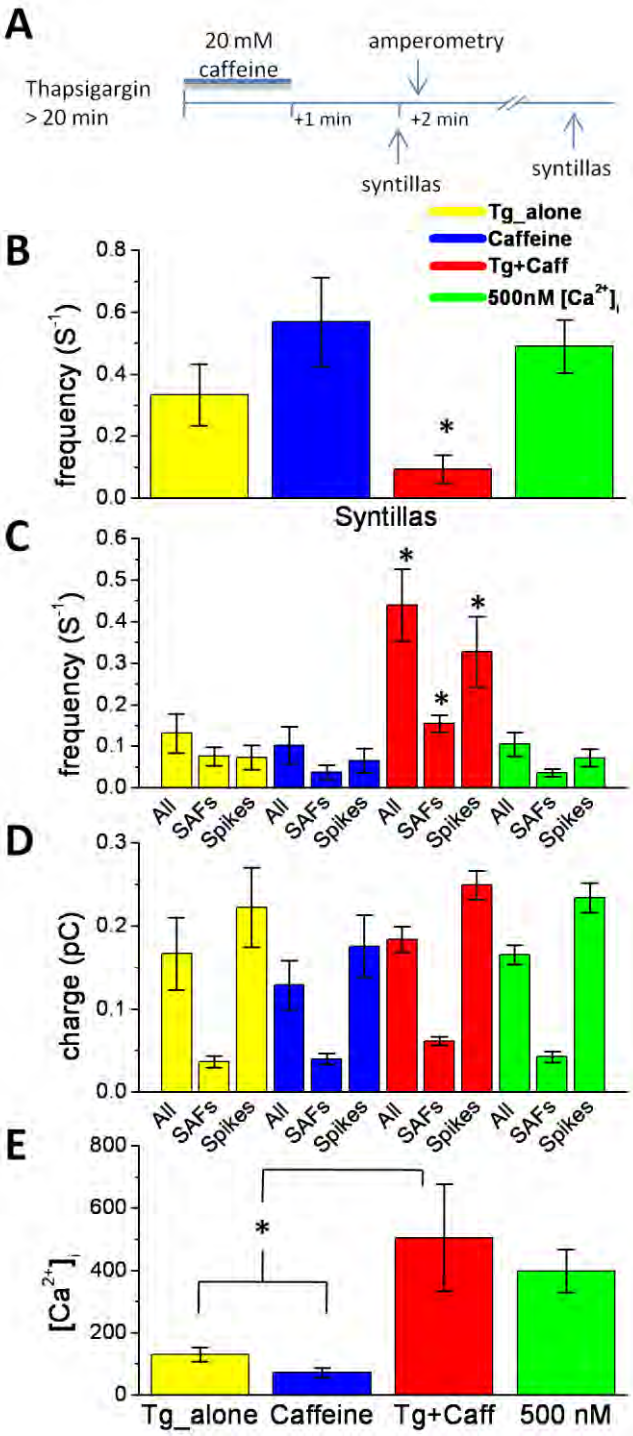
A
20 mM
caffeine
amperometry
Thapsigargin
> 20 min
+1 min
+2 min
syntillas
syntillas
Tg_alone
Caffeine
Tg+Caff
500nM [Ca2+]i
B
frequency (S-1)
0.0
0.2
0.4
0.6
0.8
*
Syntillas
C
frequency (S-1)
0.0
0.1
0.2
0.3
0.4
0.5
0.6
*
*
*
All
SAFs
Spikes
D
charge (pC)
0.0
0.1
0.2
0.3
E
[Ca2+]i
0
200
400
600
800
*
Tg_alone
Caffeine
Tg+Caff
500 nM

Figure 5.4 Effect of 2 μM thapsigargin plus 20 mM caffeine and buffering free $[Ca^{2+}]_i$ at 500nM with EGTA and $CaCl_2$.

A. Diagram representing the protocol to decrease the stores with thapsigargin and caffeine. **B.** Thapsigargin and caffeine decrease syntilla frequency to 0.09 ± 0.04 s^{-1} (N = 8) compared with thapsigargin alone, 0.33 ± 0.09 s^{-1} (N = 15) ($p < 0.04$); with caffeine alone, 0.57 ± 0.14 s^{-1} (N = 12) ($p < 0.01$); and with the free $[Ca^{2+}]_i$ buffered at 500nM, 0.49 ± 0.08 s^{-1} (N = 23) ($p < 0.001$). **C.** Thapsigargin and caffeine increase the frequency of all amperometric events to 0.44 ± 0.09 s^{-1} (N = 8), SAFs to 0.15 ± 0.02 s^{-1} (N = 8) and spikes to 0.33 ± 0.09 s^{-1} (N = 8) when compared with thapsigargin alone 0.13 ± 0.05 s^{-1} (N = 9) ($p < 0.01$) for all events, 0.08 ± 0.02 s^{-1} (N = 7) ($p < 0.02$) for SAFs, 0.07 ± 0.03 s^{-1} (N = 9) ($p < 0.02$) for spikes, caffeine alone 0.10 ± 0.04 s^{-1} (N = 10) ($p < 0.01$) for all events, 0.04 ± 0.02 s^{-1} (N = 10) ($p < 0.001$) for SAFs, 0.07 ± 0.03 s^{-1} (N = 10) ($p < 0.02$) for spikes, and when the free $[Ca^{2+}]_i$ is buffered at 500nM 0.10 ± 0.03 s^{-1} (N = 10) ($p < 0.01$) for all events, 0.04 ± 0.01 s^{-1} (N = 9) ($p < 0.001$) for SAFs, 0.07 ± 0.02 s^{-1} (N = 10) ($p < 0.02$) for Spikes. **D.** Thapsigargin and caffeine do not alter the quantal charge of amperometric events compared to thapsigargin alone, caffeine alone or when the free $[Ca^{2+}]_i$ is buffered at 500nM. **E.** Thapsigargin and caffeine increase global $[Ca^{2+}]_i$ to 505.3 ± 172 nM (N = 5) compared with typical basal global $[Ca^{2+}]_i$ in thapsigargin alone 130.0. ± 23 nM (N = 7) ($P < 0.03$) and caffeine alone 71.4 ± 16 nM (N = 7) ($P < 0.02$). When free $[Ca^{2+}]_i$ is buffered at 500nM the mean basal global $[Ca^{2+}]_i$, 397.8 ± 69 nM (N = 6) is not significantly different compared to thapsigargin and caffeine ($P = 0.59$). Error bars ± S.E.M.

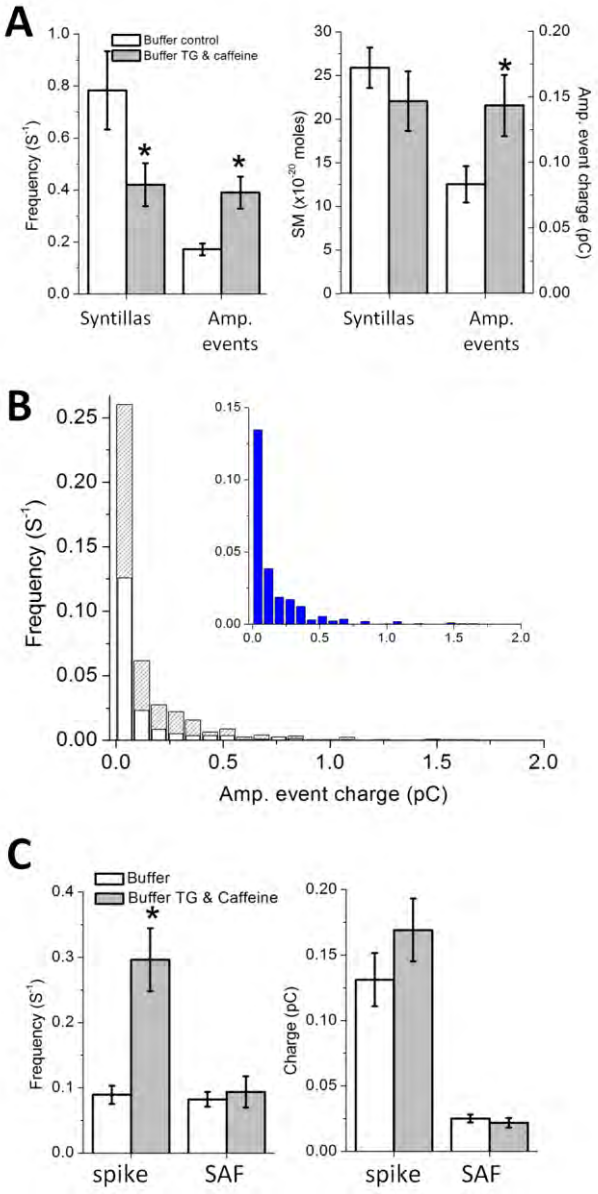
A
Buffer control
Buffer TG & caffeine
Frequency (S-1)
SM (x10-20 moles)
Amp. event charge (pC)
Syntillas
Amp. events
B
Frequency (S-1)
Amp. event charge (pC)
C
Buffer
Buffer TG & Caffeine
Frequency (S-1)
Charge (pC)
spike
SAF

Figure 5.5 Effect of 2 μM thapsigargin with caffeine. Chromaffin cells were treated with the SERCA inhibitor thapsigargin (2μM) for 20 min or longer and briefly exposed to caffeine by picospritzer (1 min, 20mM) to reduce internal Ca^{2+} stores. **A.** When Ca^{2+} stores are reduced and cytosolic Ca^{2+} is buffered with EGTA as described in Methods, the mean frequency of syntillas is reduced from 0.78 ± 0.15 (N = 15) to 0.42 ± 0.01 (N = 23) ($p<0.03$), and the amperometric event frequency is increased from 0.17 ± 0.02 (N = 20) to 0.39 ± 0.06 s^{-1} (N = 10) ($p < 0.0003$), left panel. When the stores are reduced, there is no detectable change in the mean syntilla signal mass (25.9 ± 2.3 (n = 47) and 22.1 ± 3.4 (n = 36), control and treated, respectively); but the mean charge of amperometric events increases (0.083 ± 0.014 (N = 20) and 0.143 ± 0.023 pC (N = 10) ($p < 0.026$), right panel). (Panels A and B include both spikes and SAFs.) **B.** Frequency distribution of individual amperometric events according to charge (pC) in control (white, 731 events) and when stores are reduced by thapsigargin and caffeine treatment (stripes, 908 events). The difference between the two distributions is shown on an expanded x-axis in the inset in blue. **C.** Left panel shows that the frequency in control solution with buffer (0.09 ± 0.01 s^{-1} for spikes and 0.08 ± 0.01 s^{-1} for SAFs is the same as in control solution without buffer as given in figure 5.2C). After treatment with thapsigargin and caffeine, the spike frequency increases to 0.30 ± 0.05 s^{-1} ($p<0.00002$ and N = 10). Right panel shows the mean charge of spikes (0.13 ± 0.02 vs 0.17 ± 0.02 pC) or SAFs (0.02 ± 0.00 for control and treatment) in control and after thapsigargin plus caffeine treatment.

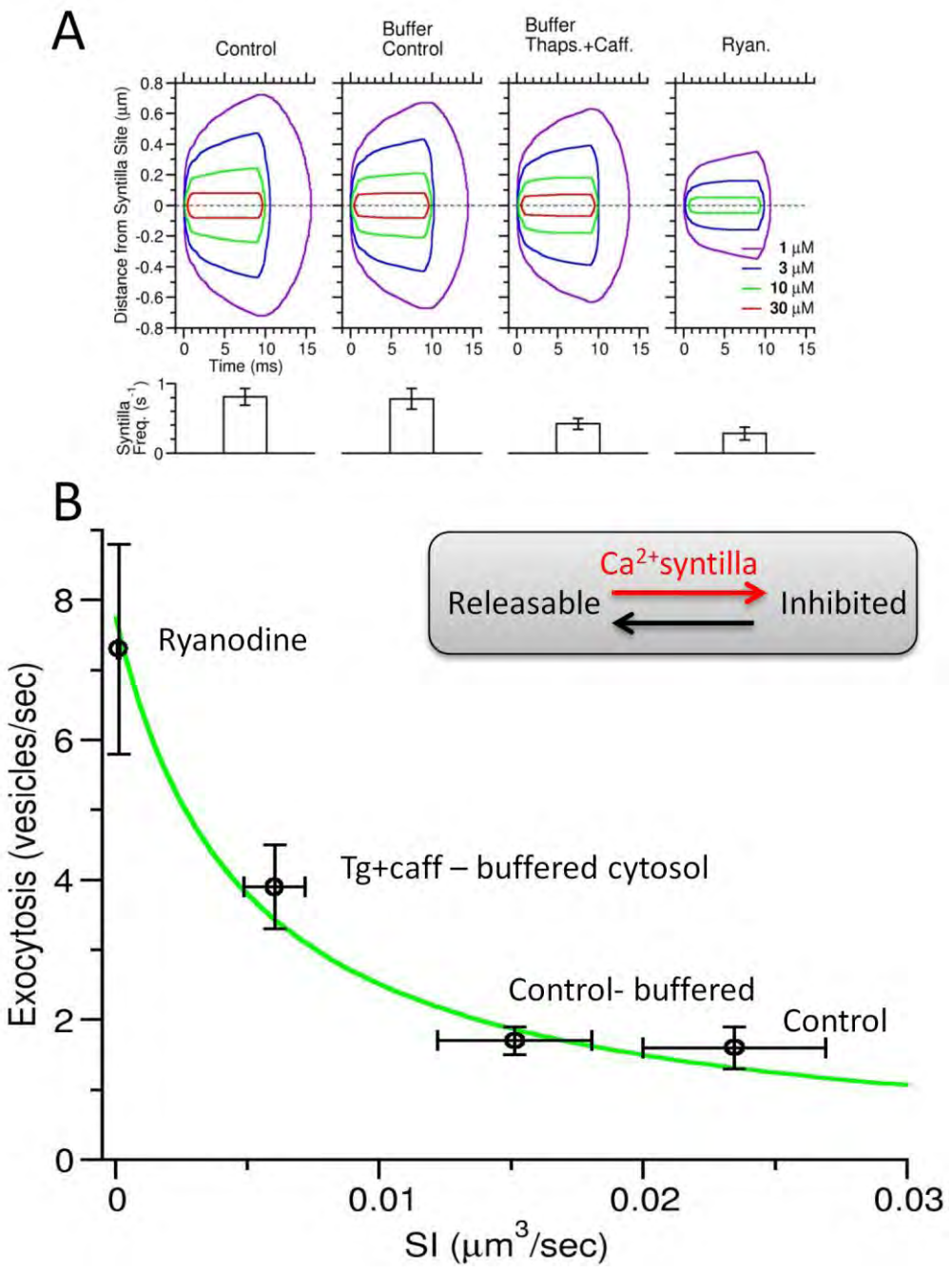
A
Control
Buffer Control
Buffer Thaps.+Caff.
Ryan.
Distance from Syntilla Site (µm)
Time (ms)
Syntilla Freq. (s-1)
1 µM
3 µM
10 µM
30 µM
B
Ca2+syntilla
Releasable
Inhibited
Ryanodine
Tg+caff – buffered cytosol
Control- buffered
Control
Exocytosis (vesicles/sec)
SI (µm3/sec)

<u>Figure 5.6</u> Relationship between Ca^{2+} released into the syntilla microdomain and exocytotic events. **A. Upper.** Spatio-temporal profiles of the Ca^{2+} syntilla arising from RYR2s near the plasma membrane for each experimental condition. Concentric curves represent different [Ca^{2+}]'s within the syntilla microdomain. Note that the ordinate presents one of the spatial axes, the other two being the same as the one shown and together constituting a hemisphere (See Methods). **Lower.** Syntilla frequency for each of the four experimental conditions listed above the upper panel. **B.** Relationship of the SI for the entire cell versus frequency of exocytotic events from the entire cell surface. The plot shows that the frequency of amperometric events declines to a baseline level as the (SI) increases. The relationship drawn here is based on a 10 μM syntilla microdomain (see panel A above – green line. The equation of the curve to which the data is fit:

$$f_{amp} = F_0 * \left(\frac{1}{1 + k * SI} \right) \qquad \text{(eq. 4)}$$

is based on a two state model as described in Methods, where LDCGs are either in an inhibited or releasable state. A least-squares fit of equation 4 to the data points in panel B was performed, resulting in F_0 = 7.75 and k = 104.10. The correlation coefficient (R^2) of the fit is 0.993.

Table 5.1 Spike and SAF parameters: control vs 100 μM ryanodine

	Control	100 μM Ryanodine	
Spikes	mean ± sem	mean ± sem	p value
Amplitude(pA)	9.20 ± 2.3	15.90 ± 1.6	*0.026
†Risetime (ms)	6.78 ± 0.65	10.83 ± 0.95	*0.002
Halfwidth (ms)	11.79 ± 0.89	15.23 ± 1.5	0.068
‡Tau (ms)	11.45 ± 0.87	14.23 ± 1.38	0.099
Duration (ms)	62.99 ± 4.86	84.49 ± 7.56	*0.027
SAFs			
Amplitude (pA)	1.09 ± 0.03	1.84 ± 0.06	*0.000
Duration (ms)	32.68 ± 3.6	33.55 ± 4.3	0.877

p values are from two sample students t-tests.

†Risetime is 10 – 90%.

‡Tau is 67% decay

Table 5.2 Spike and SAF parameters: control vs 100 μM ryanodine in unpatched mouse chromaffin cells

	Control	100 μM Ryanodine	
Spikes	mean ± sem	mean ± sem	p value
Amplitude(pA)	6.9 ± 2.0	14.2 ± 2.1	*0.019
†Risetime (ms)	19.8 ± 1.3	12.1 ± 0.9	*0.00005
Halfwidth (ms)	21.2 ± 1.5	19.8 ± 1.2	0.47
‡Tau (ms)	23.2 ± 1.5	18.3 ± 0.9	*0.008
Duration (ms)	119.9 ± 11.0	89.2 ± 5.6	*0.018
SAFs			
Amplitude (pA)	1.7 ± 0.11	1.8 ± 0.08	0.53
Duration (ms)	68.5 ± 11.8	59.7 ± 8.79	0.56

p values are from two sample students t-tests.

†Risetime is 10 – 90%.

‡Tau is 67% decay.

Table 5.3 Spike and SAF parameters: control vs Tg + caffeine buffered

	Control	Tg + Caff	
Spikes	mean ± sem	mean ± sem	p value
Amplitude(pA)	8.56 ± 1.9	9.71 ± 2.6	0.726
†Risetime (ms)	9.41 ± 0.93	8.63 ± 0.88	0.552
Halfwidth (ms)	12.72 ± 0.84	12.1 ± 0.89	0.615
‡Tau (ms)	13.22 ± 1.2	12.0 ± 1.2	0.462
Duration (ms)	69.79± 4.0	65.00 ± 4.3	0.424
SAFs			
Amplitude (pA)	1.15 ± 0.06	1.31 ± 0.13	0.306
Duration (ms)	38.81 ± 4.0	33.10 ± 5.5	0.414

p values are from two sample students t-tests.

†Risetime is 10 – 90%.

‡Tau is 67% decay.

Chapter 6

Physiologically relevant stimulation differentially regulates Ca^{2+} syntillas

Abstract: **Catecholamine and neuropeptide release from adrenal chromaffin cells (ACCs) into the circulation is controlled by the sympathetic division of the Autonomic Nervous System (ANS). To ensure proper homeostasis tightly controlled exocytic mechanisms must exist both in resting conditions, where minimal output is desirable and under stress, where maximal, but not total release is necessary. It is thought that sympathetic discharge accomplishes this task by regulating the frequency of Ca^{2+} influx through VGCCs, which serves as a direct trigger for exocytosis. But studies on spontaneous release in ACCs have revealed the presence of Ca^{2+} syntillas, brief, focal cytosolic Ca^{2+} transients released from internal stores and mediated by RYRs which have the opposite effect of inhibiting release. Therefore, assuming CICR via RYRs due to Ca^{2+} influx through VGCCs, we are confronted with a contradiction. Sympathetic discharge should increase syntilla frequency and that in turn should *decrease* exocytosis, a paradox. A simple "explanation" might be that the increase in syntillas would act as a brake to prevent an overly great exocytic release. But upon investigation of this question a different finding emerged. We examined the role of syntillas under varying levels of physiologic stimulation in ACCs using simulated action potentials (sAPs) designed to mimic native input at frequencies associated with stress, 15 Hz, and the basal sympathetic tone, 0.5 Hz. Surprisingly, we found that sAPs delivered at 15 Hz or 0.5 Hz were able to completely *abolish* Ca^{2+} syntillas within a time frame of two minutes. This was not expected. Further, a single sAP is all that was necessary to initiate suppression of syntillas. Syntillas remained inhibited after 0.5 Hz stimulation but were only temporarily suppressed (for 2 minutes) by 15 Hz stimulation, where global $[Ca^{2+}]_i$ was raised to 1 – 2 µM. Thus we propose that CICR, if present in these cells, is overridden by other processes. Hence it appears that inhibition of syntillas by action potentials in ACCs is due to a new process**

which is the opposite of CICR. This process needs to be investigated, and that will be one of the very next steps in the future. Finally we conclude that syntilla suppression by action potentials is part of the mechanism for elicited exocytosis, resolving the paradox.

Introduction

The adrenal chromaffin cell (ACC) is a major peripheral output of the sympathetic nervous system. Catecholamine and neuropeptide release from ACCs into the circulation is controlled by the sympathetic tone (Kidokoro and Ritchie, 1980). At basal levels of stimulation associated with tone, the ACC receives input from the splanchnic nerve and fires action potentials (APs) at a rate of 0.5 Hz which is thought to result in kiss-and-run style exocytosis, whereby small fusion pores allow only catecholamines to be released. At supertonic rates of stimulation, consistent with a sympathetic stress response, ACCs can fire APs at a rate of 15 Hz and release both catecholamines and larger neuropeptides by full fusion exocytosis (Fulop et al., 2005; Fulop and Smith, 2006). A striking feature of the autonomic nervous system is that only a low stimulation frequency is required for the activation of autonomic effectors. For example, one nerve impulse every other second is sufficient to maintain the basal sympathetic and parasympathetic effect known as “rest and digest” (Guyton and Hall, 2000).

Up to this point, it had been assumed that the normal resting rate of catecholamine secretion by the adrenal medulla is directly determined by voltage-gated Ca^{2+} channels in response to action potentials the ACC fires based on sympathetic input from the splanchnic nerve (Douglas and Poisner, 1962,

1963; Baker and Knight, 1978). In other words, Ca^{2+} influx every other second, serving as a direct trigger for exocytosis, is responsible for basal catecholamine release.

As shown above, however, Ca^{2+} released from within the ACC from internal stores in the form of Ca^{2+} syntillas, brief (on the order of tens of milliseconds), focal cytosolic Ca^{2+} transients due to release from intracellular stores and mediated by RYRs, has a counterintuitive and opposite effect. Instead of triggering large dense core granule (LDCG) release, this Ca^{2+} inhibits spontaneous release (Lefkowitz et al., 2009). Based on this finding, we wondered what role syntillas could serve in elicited release. Could they also inhibit elicited exocytosis during physiologic stimulation matching tonic (0.5 Hz) and supertonic (15 Hz) input? While the presence of syntillas during conditions of spontaneous release could serve as a guard to prevent mass catecholamine output during rest, certainly their presence during intense stimulation underscoring a stress response would not be so beneficial.

Here we examine the role of syntillas under varying levels of physiologic stimulation. Simulated action potentials (sAP) designed to mimic native input were used to stimulate ACCs at frequencies associated with stress, 15 Hz and the basal sympathetic tone, 0.5 Hz (Brandt et al., 1976; Chan and Smith, 2001; Fulop et al., 2005). We find that physiologic input serves as an upstream

regulator of syntillas. Quite surprisingly sAPs are able to completely abolish Ca^{2+} syntillas within a time frame of a few minutes, depending on the stimulation frequency. Over time this suppression of syntillas leads to increases in frequency and amplitude of LDCG release. A single sAP is all that is necessary to initiate syntilla suppression. Furthermore, syntillas return after high frequency stimulation where rises in global [Ca^{2+}] are high. On the other hand, strikingly, syntillas remain suppressed long term (> 30 minutes) after stimulation with a single sAP.

We propose that this action potential induced syntilla suppression may be triggered by Ca^{2+} influx or Ca^{2+} -mediated 2^{nd} messenger interactions with RYR2. This syntilla suppression which would serve to relieve the inhibition that syntillas normally exert on exocytosis, instead of direct Ca^{2+} influx triggering of LDCGs, could provide the basis of long term catecholamine release into the general circulation. Such a paradigm would allow for an energetically efficient, high fidelity mechanism where the ACC would not need to receive frequent input or generate APs at regular intervals to provide consistent basal release and normal catecholamine serum levels. Whether the ACC fires one AP every other second or every 10 minutes is sufficient to suppress syntillas and maintain a basal rate of exocytosis. Thus, syntilla suppression by action potentials may be an important part of the mechanism in elicited exocytosis.

This work implies that *in vivo* syntillas are basically absent or suppressed most of the time, since the animal spends the majority of its time in the resting state. Accordingly, Ca^{2+} syntillas are only present after intense stimulation, when the stress response is initiated – where they are highly desirable to quickly punctuate exocytic release. During this condition, when global $[Ca^{2+}]_i$ reaches levels that are high enough to persistently release all LDCGs available, it is necessary to quickly activate a brake such that the total amount catecholamines and peptides within the ACC would not be released and kill the animal.

Materials and Methods

Tight-seal, whole cell recordings on adrenal chromaffin cells (ACCs) held at -60 mV, freshly dissociated from adult male Swiss Webster mice as described previously (ZhuGe et al., 2006), were performed with a HEKA EPC10 amplifier (HEKA Electronics, Lambrecht, Germany) on the same day as isolation. Mice (6–8 weeks) were sacrificed by cervical dislocation in accordance with the IACUC guidelines at the University of Massachusetts Medical School. Patch pipette solution (mM) was: 0.05 K_5fluo-3 or 0.025 K_5fura-2 (Molecular Probes, Eugene, OR), 135 KCl, 2 $MgCl_2$, 30 Hepes, 4 MgATP, 0.3 Na-GTP, pH 7.3. Bath solution (mM): 135 NaCl, 5 KCl, 10 Hepes, 10 glucose, 1 $MgCl_2$, and 2.2 $CaCl_2$, pH 7.2. Except when otherwise indicated, all reagents came from Sigma (Saint Louis, MO).

Fluorescence images using fluo-3 as a Ca^{2+} indicator were obtained using a custom-built wide-field digital imaging system described previously (ZhuGe et al., 2006). To assess the properties of individual Ca^{2+} syntillas quantitatively, the signal mass approach was used, as conceptualized by Sun et al. (Sun et al., 1998) and developed for wide-field microscopy of Ca^{2+} sparks by ZhuGe et al. (ZhuGe et al., 2000). The purpose of this approach is to obtain a measure of the total *amount* of Ca^{2+} (as opposed to concentration of Ca^{2+}) released by a focal

Ca^{2+} transient. Global $[Ca^{2+}]_i$ was measured by fluorescence with cell-impermeant fura-2 (25 μM) that was loaded into cells through the patch pipette and measured as previously described (Grynkiewicz et al., 1985; Becker and Fay, 1987; Drummond and Tuft, 1999). Corrections for buffers in the calculations of signal mass have been described previously (Lefkowitz et al., 2009).

Experimental recording protocols

Fluo-3 Ca^{2+} imaging and amperometry. After the patch is ruptured to provide the whole cell configuration, we waited at least two minutes for the fluo-3 to reach equilibrium in the cell. In a typical experiment, when the fluorescence was stable, we began to record two 4-second image sequences in a row (200 images separated by 20ms, with an exposure time of 10ms). Single 4-second recordings were made thereafter over time as indicated in each experiment. Amperometric recordings were made in 2 or 4 minute segments over time as indicated in each experiment. In some cases the data was binned into 15 second intervals to follow amperometric effects over time.

Simulated Action Potentials (sAPs). Patched cells with access resistances less than 20 MΩ and leak conductances below 30 pA were selected for stimulation experiments where they received trains of sAPs at either 15 Hz or 0.5 Hz and in

some cases just a single sAP. Simulated action potential waveforms consisted of a 3-step ramp as follows (start potential (mV), end potential (mV), duration (ms)): 1) -80, 50, 2.5; 2) 50, -90, 2.5; 3) -90, -80, 2.5. This waveform evoked Ca^{2+} and Na^{+} currents statistically identical to native action potentials and, thus, are considered functionally equivalent (Chan and Smith, 2001). We found that our K-Cl based internal solution produced similar Ca^{2+} and Na^{+} currents to those reported by Chan and Smith, (2001) where they employed a Cs-glutamate based internal solution.

Amperometric measurements.

Quantal release of catecholamine from single chromaffin cells was monitored electrochemically using carbon fiber electrodes with a tip diameter of 5.8 μm (ALA Scientific Instruments, Westbury, NY), as described before (ZhuGe et al., 2006). Amperometric signals, i.e., oxidation currents, were monitored with a VA-10 amplifier (NPI Electronic, Tamm, Germany), filtered at 0.5 kHz, digitized at 1 kHz with a Digidata 1200B acquisition system, and acquired with Patchmaster software from HEKA. Amperometric spikes were identified and analyzed using the Mini Analysis Program (Synaptosoft, Decatur, GA). Each event was visually inspected so that artifacts could be rejected from the analysis. The root mean square noise in acquired traces was typically < 0.25 pA as determined by the

Mini Analysis program. The detection threshold for an event was set to 2.5 times the baseline root mean square. Overlapping events were rare, and were excluded from analysis. To minimize errors due to possible variation in exocytosis among cells from different animals, cells from each animal were divided into two groups: one as control and the other treated with agents such as ryanodine. SAFs were separated from spikes based on criteria somewhat similar to (Wang et al., 2006), where an index of event shape was used to evaluate the "rectangularity" of a putative SAF. In the present study, to qualify as an SAF an event had to meet the criteria of an amplitude less than 2.5pA and a ratio of full-width at half-height to event duration greater than 0.25. Event durations for spikes and SAFs are defined as the duration between the time when the event signal exceeds, and the time when it returns to, the detection threshold amplitude as defined above.

Statistical analyses

Statistical analyses and plots were performed in OriginPro 8.0 (Origin, Northampton, MA). In all cases except for syntilla frequency and signal mass, data was first averaged per cell and is reported as mean ±SE of all cells. Data from syntilla frequency and signal mass is reported, as previously (ZhuGe et al., 2006), as mean ±SE of individual records and mean ±SE of individual syntillas,

respectively. Statistical analysis of difference was made using a Student's t-test, one-way ANOVA or Mann-Whitney test as indicated in the figure captions. A p-value less than 0.05 is significant except in multiple comparisons, where the appropriated correction was applied. Significance is indicated by an asterisk. N indicates the number of cells and n the number of events, i.e., syntillas or amperometric spikes.

Results

Under conditions whereby an ACC receives no input stimulation, these cells still participate in a form of spontaneous exocytosis, whereby LDCGs are released in a non-concerted manner (i.e., spontaneous release). Our group has recently shown that Ca^{2+} released from ryanodine-sensitive internal stores in the form of Ca^{2+} syntillas, serves to inhibit this spontaneous release, an unusual role for Ca^{2+} in exocytosis (Lefkowitz et al., 2009). Based on this finding, we wondered what role syntillas could serve in elicited release. That is, the presence of syntillas during conditions of spontaneous release seems to make sense from a physiologic perspective in that syntillas could serve as a guard to prevent mass catecholamine output when the cell is at rest. But what role, if any, could syntillas play in elicited release where at times massive catecholamine output is not only desirable but crucial? To examine this question, freshly dissociated mouse ACCs were patched in the whole cell voltage-clamp configuration, held at -60 mV and stimulated by 15 Hz or 0.5 Hz trains of simulated action potential (sAP) waveforms designed to mimic native physiologic electrical firing patterns associated with stress-like sympathetic activation or basal sympathetic tone (Brandt et al., 1976; Kidokoro and Ritchie, 1980). Also, in a set of preliminary experiments, unpatched cells were stimulated with the ACC's native stimulant,

acetylcholine (ACh), designed to induce a single action potential. The Ca^{2+} indicator dyes fluo-3 and fura-2 were used to detect Ca^{2+} syntillas and monitor global cytosolic [Ca^{2+}], respectively. Amperometry was used to follow the effects on individual exocytotic events.

Stress-associated elicited release, 15 Hz

To examine the role of Ca^{2+} stores during elicited release, patched ACCs were stimulated at 15 Hz and Ca^{2+} syntillas were monitored over time according the protocol depicted in Figure 6.1 A. Strikingly, stressful stimulation completely abolishes the presence of syntillas by 2 minutes (Figure 6.1 A, Left). Equally interesting, the syntillas begin to return 3 minutes into stimulation and the syntilla frequency is restored to near pre-stimulus levels 2 minutes after the stimulation has ceased. In addition to the frequency of syntillas, we also monitored the average magnitude of Ca^{2+} syntillas by the signal mass approach (see Methods) (Figure 6.1 A, Right). Briefly, the signal mass is a measure of the total amount of Ca^{2+} released per individual syntilla, given in units of moles of Ca^{2+}. During the initial 60 seconds of stimulation the average magnitude of Ca^{2+} syntillas showed a decreasing trend, with a significant difference detected at 60 seconds. Halfway through the 15 Hz stimulation, as the frequency of syntillas began to return to pre-stimulus levels, the signal mass of these recovering syntillas showed no

significant difference from those recorded before stimulation. Thus, 15 Hz stimulation seems to temporarily suppress both the frequency and signal mass of Ca^{2+} syntillas.

To examine the effect of temporary syntilla suppression caused by 15 Hz stimulation on elicited exocytosis, we next made amperometric recordings from the ACCs before, during and after stimulation and followed the effect over time. Figure 6.1 B, (Top) shows that the frequency of amperometric events initially undergoes a dramatic, nearly 8-fold increase during the first 30 seconds of stimulation, then tapers off to a more moderate, but sustained 2- to 3-fold increase about halfway through the stimulation. The amperometric frequency returns to baseline at the end of stimulation. The effect on the magnitude of individual amperometric events, measured by the quantal charge, Q is shown in Figure 6.1 B, (Bottom).

During 15 Hz stimulation there is obviously another source of Ca^{2+} in addition to release from stores, that of Ca^{2+} influx. Thus, as a next step we examined the intracellular global [Ca^{2+}] level profile during 15 Hz stimulation. That is, if influx over the course of a 4 minute 15 Hz stimulation could lead to sustained, increased intracellular Ca^{2+} levels, then it would be more likely that Ca^{2+} influx, as opposed to suppression of Ca^{2+} release from stores, accounts for the increase in exocytosis during elicited release. Figure 6.2 shows the results of

these experiments where global $[Ca^{2+}]_i$ is indeed increased to super micromolar levels throughout stimulation. While we observed an initial transient increase in $[Ca^{2+}]_i$ upon stimulation that might be explained by CICR (see Discussion), there was also a curious spike-like increase in $[Ca^{2+}]_i$ immediately before or just as stimulation ceased, which could not be explained.

Sympathetic tone associated elicited release, 0.5 Hz

The ability of 15 Hz stimulation to suppress syntillas would seem to make sense, given that the function of syntillas serves to decrease exocytosis. That is, during stressful stimulation which demands high levels of catecholamine output, it would be desirable not only to invoke Ca^{2+} influx, but also to relieve the braking mechanism that syntillas exert on exocytosis. But what about conditions of elicited release that begin to approximate spontaneous release, where we know syntillas to be present? Do syntillas persist under low levels of stimulation that are associated with the sympathetic tone? To answer this question we stimulated ACCs at 0.5 Hz and monitored the effects on both syntillas and exocytosis in the same manner as we did in the 15 Hz stimulation experiments (Figure 6.3). Stimulation at 0.5 Hz led to a complete suppression of syntillas by 2 minutes, similar to that observed during 15 Hz stimulation. But unlike the 15 Hz stimulation, the syntillas never recovered, even after stimulation ceased (Figure

6.3 A, (Left)). This was an overall surprising result to us. We expected syntilla suppression to be less during low stimulation, hypothesizing that a consistent braking system could moderate the exocytic output under basal conditions. In contrast, the syntilla suppression was more complete. The mean signal mass of the residual syntillas during the first minute 0.5 Hz stimulation was not significantly different than before stimulation (Figure 6.3 A, (Right)).

As expected, the effect of 0.5 Hz stimulation on exocytosis was less dramatic, leading to a sustained 3 – fold increase in amperometric frequency during the first 2 minutes of stimulation (Figure 6.3 B, (Top)). Interestingly, stimulation beyond the first 2 minutes had no further effect on amperometric frequency. On the other hand, the amperometric frequency began to rise again between one and two minutes post stimulation, a point in time where there is no external stimulation and syntillas have been suppressed for about 5 minutes. This may offer a first hint at the timeframe in which the absence of syntillas could result in exocytic increases (see Discussion). The mean quantal charge of amperometric events showed a rising trend upon 0.5 Hz stimulation, similar to that observed during 15 Hz stimulation (Figure 6.3 B, (Bottom)). The difference was, however, that after 0.5 Hz stimulation stopped, the amperometric charge continued to rise. It is worthwhile noting at this point, that the continued rise in charge correlates well with a prolonged absence of syntillas after 0.5 Hz

stimulation. This is in contrast to 15 Hz stimulation, where once the syntillas returned to near control levels, the amperometric charge also returned to control levels. The implications of this are significant, suggesting that during 0.5 Hz levels of stimulation associated with sympathetic tone, occasional stimulatory input may only serve to override the default state of inhibition which syntillas exert on exocytosis.

To be sure of our interpretation of these results it was necessary to look at the effect of low frequency stimulation on global cytosolic [Ca^{2+}] over the same time frame. Figure 6.4 A shows a representative global $[Ca^{2+}]_i$ recording with fura-2 from an individual ACC stimulated at 0.5 Hz. During the first 30 seconds of stimulation the $[Ca^{2+}]_i$ rises transiently to levels near 300 nM, then returns to near resting levels until stimulation ceases. Again, we observed an unexplainable transient spike in $[Ca^{2+}]_i$ at the end of stimulation. Averaged fura-2 recordings show that throughout most of the 0.5 Hz stimulation, $[Ca^{2+}]_i$ levels linger around 200 nM (Figure 6.4 B). This concentration of $[Ca^{2+}]_i$ is not sufficient to induce exocytotic release, as demonstrated in a previous study where global $[Ca^{2+}]_i$ was artificially raised to 500 nM with $CaCl_2$ and EGTA without a concomitant increase in basal amperometric frequency examined after a 2 – 5 minute period for $[Ca^{2+}]_i$ equilibration (Lefkowitz et al., 2009).

A single action potential

Low frequency stimulation at 0.5 Hz, which is associated with basal sympathetic tone, can significantly suppress syntillas within 1 minute. In other words, roughly 30 sAPs are capable of causing this inhibition. Therefore, toward elucidating a mechanism by which sAPs could suppress syntillas, we next examined what the minimal stimulation was necessary to cause the inhibition. We performed experiments where ACCs were given only a single sAP and followed the effects on syntillas and exocytosis (Figure 6.5). We found that a single sAP caused near complete suppression of syntillas by 5 minutes and that this suppression persisted for 20 minutes, the entire length of the experiment (Figure 6.5 A).

Figure 6.5 B shows the amperometry recording protocol we used in these experiments. Basically a 4 minute amperometric recording was performed starting 5 minutes after the ACC received a sAP. The 5 minute pause was chosen based on the accompanying syntilla data which showed that syntillas were almost completely suppressed by this point in time. Syntilla suppression between 5 – 9 minutes resulted in significant increases in both the frequency and charge of all amperometric events (Figure 6.5 C). The effect on amperometric charge was further examined by sorting the events into stand alone foot events (SAFs), which are taken to represent kiss-and-run exocytic events and spike events, which represent more full release either though full fusion or kiss-and-run

modes of exocytosis (Wang et al., 2006; Gong et al., 2007). We found a significant increase in the charge of SAFs, but not in spikes. In fact, though the overall effects on amperometry were significant, they were not very dramatic. For example, the mean charge of all amperometric events was only slightly increased from 0.12 ± 0.01 pC to 0.16 ± 0.04 pC, only half the value that prolonged syntilla suppression for 30 minutes or more is capable of (See below and +ryanodine in Table A1 of Appendix A).

Preliminary Results and Discussion

The following experiments, which are preliminary data only, have been included in this chapter due to their usefulness in advancing speculation about mechanisms regarding the syntilla process and its effects on exocytosis

0.5 Hz stimulation after blocking RYRs for 30+ minutes

If the absence of syntillas were to account for the long term exocytosis of catecholamines under basal conditions, then blocking syntillas for a prolonged period of time with ryanodine and then stimulating the ACCs at 0.5 Hz should yield similar results to blocking the syntillas with ryanodine alone, since both treatments decrease syntillas. For example, since increases in amperometric frequency stop after the first 2 minutes of 0.5 Hz stimulation (Figure 6.3 B), then syntilla suppression should be the only acting mechanism by which to increase exocytosis thereafter.

To test this idea we performed experiments where ACCs were stimulated at 0.5 Hz after syntillas were first blocked for 30 minutes or longer using 100 μM ryanodine, a concentration known to be a potent inhibitor of syntillas in mouse ACCs (ZhuGe et al., 2006; Lefkowitz et al., 2009). We then recorded Ca^{2+}

syntillas and amperometry and compared these results with experiments where syntillas were blocked with ryanodine long term, without additional stimulation (Figure 6.6). As expected, both syntilla frequency and signal mass were significantly suppressed compared to those normally observed in untreated ACCs (Figure 6.6 A). In the experiment with 0.5 Hz stimulation on top of long term ryanodine treatment, syntillas were recorded immediately after the 0.5 Hz stimulation ceased. At this point, syntilla frequency was essentially completely suppressed, 0.028 ± 0.018 Hz compared to normally observed frequencies around 0.8 Hz.

There are multiple points to consider in the amperometry data from these experiments (Figure 6.6 B). Figure 6.7 has been created to make comparisons with the previous 0.5 Hz data in Figure 6.3 easier.

First, 0.5 Hz stimulation after ryanodine treatment yields a generally higher, almost 2-fold increase in amperometric frequency compared to 0.5 Hz stimulation alone (Figure 6.7 B, light blue boxes).

Second, the increased amperometric frequency lasts throughout the duration of the 0.5 Hz stimulation when ryanodine is present, whereas during 0.5 Hz stimulation alone the frequency increase is gone after 2 minutes (Figure 6.7 B, light blue boxes). The two dark blue shaded boxes superimposed on the amperometric frequency data in Figure 6.7 B represent the timeframe during

which 0.5 Hz stimulation causes a nominal rise in global [Ca^{2+}] above resting levels, to about 200 - 250 nM. As shown in the amperometric data with 0.5 Hz stimulation alone, this transient rise in $[Ca^{2+}]_i$ can at best produce an increase in frequency for up to 2 minutes. Therefore the prolonged increase in amperometric frequency observed when ryanodine is present must be due to the absence of syntillas, since we have previously shown that 100 μM ryanodine does not alter resting $[Ca^{2+}]_i$ levels (Lefkowitz et al., 2009).

Third, during 0.5 Hz stimulation on top of ryanodine, both the amperometric frequency and charge data are on average decreased compared to ryanodine alone (Figure 6.7 B and C). This is especially noticeable in the amperometric charge data where there is a decreasing trend from around 0.3 pC to about 0.15 pC over the course of the stimulation. A possible explanation for this could be that Ca^{2+} influx during the 0.5 Hz stimulation has impinged on the syntilla microdomain, partially restoring the inhibitory influence that Ca^{2+} within this microdomain normally exerts over exocytosis. It would indeed have been interesting to see if 0.5 Hz stimulation for a longer period of time could restore the amperometric parameters back to normal levels, before syntillas were blocked. Alternatively, if the effects on frequency and charge are separable, then the re-release of partially loaded granules due to local recycling during 0.5 Hz stimulation could account for the decreasing trend in charge.

Fourth, the combined data from the experiments with 0.5 Hz alone, ryanodine alone and then ryanodine + 0.5 Hz reveal a time frame for which the absence of Ca^{2+} within the syntilla microdomain can lead to a maximal effect on exocytosis. The superimposed yellow boxes in Figure 6.7 B and C represent the point at which syntillas have been completely or near completely blocked for at least 5 minutes and up to more than 30 minutes. The point where syntillas have been suppressed for about 5 minutes (Figure 6.7 A, Left) seems to roughly correlate with the point where the amperometric frequency and charge begin to increase (Figure 6.7 B, Left). By 30 minutes or longer without sufficient Ca^{2+} release into the syntilla microdomain (e.g., the data with ryanodine alone), the amperometric data have reached maximum values. For example, in mouse ACCs the mean charge of amperometric events seems to be maximal around 0.35 pC (See Table A1 in Appendix A). Together this suggests that the absence of Ca^{2+} release into the syntilla microdomain for 30 minutes or longer is enough to exert a maximal effect on exocytosis. The fact that 0.5 Hz stimulation provided after syntillas have been suppressed long term can depress amperometric values back toward normal levels also suggests a mechanism by which occasional Ca^{2+} influx through VGCCs entering into the syntilla microdomain could balance out the effect of syntilla absence (See Discussion).

Eliciting a single action potential with ACh in unpatched ACCs

The previous experiments seemed to indicate that it was necessary for Ca^{2+} release into the syntilla microdomain to be absent for a period of time to relieve the inhibitory effect that syntillas normally exert on exocytic output. For example, in the single sAP experiments, if syntillas were suppressed for 5 – 9 minutes, then there was only a moderate increase in amperometric frequency and charge. On the other hand, if syntillas were suppressed for 30 minutes or more (e.g., the ryanodine experiments), then there was a maximal effect on exocytosis. Therefore we next wanted to establish an actual time frame in which syntillas had to be absent to relieve the inhibition of exocytosis. We hypothesized that the longer syntillas are suppressed, the further exocytosis should increase in frequency and charge.

To test this, we followed the effects on amperometry over a much longer period of time, up to 30 minutes after syntillas were suppressed. But to monitor amperometry constantly over 30 minutes or more we needed to switch to unpatched cells, since we found it to be technically very difficult to record from patched ACCs beyond 20 minutes. Moreover, we had previously shown that blocking syntillas in unpatched ACCs has the same effect on amperometry as in patched cells (Lefkowitz et al., 2009). Of course, in unpatched cells we could not stimulate the cell with sAPs. Instead, we used an ultra brief, 25 ms puff of ACh,

the native stimulant of the ACC, which has been demonstrated to elicit single action potentials in ACCs (Cuchillo-Ibanez et al., 2002; de Diego et al., 2008). We have found in our own current clamp recordings that this protocol works quite well to elicit single and occasionally double or triple action potentials in mouse ACCs. From our own voltage clamp recordings, we further find that these brief puffs of ACh result in currents similar to those of sAPs. We did not use high concentrations of ryanodine to block syntillas since our experience has shown that full blockade of RYRs with 100 μM ryanodine can occur anywhere between 17 – 30 minutes. Therefore we would have no way of knowing at what point in time syntilla blockade actually began.

Figure 6.8 A depicts a diagram of the protocol used to record amperometry before and after a brief ACh puff was used to elicit an action potential and presumably block syntillas. The effects on amperometry followed over time are shown both for ACCs that were treated with an ACh puff and those that were not (Figure 6.8 B and C, red and black, respectively). In untreated cells there was no significant increase in amperometric frequency or charge throughout the duration of recording. On the other hand, ACCs that were administered a brief puff of ACh experienced an increase in both amperometric frequency and charge that was significantly different from pre-treatment basal levels by around 15 minutes. Note that these are repeated measures

experiments, such that comparisons should be made within each group between points in time after the ACh puff to the point in time before the ACh puff (e.g., basal is the control). Statistical comparisons are not made between groups; the treated and untreated groups are merely overlaid for comparison.

The effects on SAF and spike events were also examined over time (Figure 6.8 D). By plotting a ratio of the mean spike frequency over the mean SAF frequency we can get a quantitative index of the effects of syntilla suppression on the mode release over time. For example, a ratio below 1.0 is interpreted as a preference for the kiss-and-run mode of exocytosis while a ratio above 1.0 represents a preference for more complete release (Wang et al., 2006). In ACCs treated with an ACh puff these cells seem to switch to a more full release mode between 10 – 19 minutes, a time frame during which syntillas would have been suppressed for 8 – 17 minutes (Figure 6.8 D, Left). Consistent with this observation, the ACh puff has no effect on the amperometric charge of SAFs over time (Figure 6.8 D, Right - Top), while syntilla suppression does cause a significant increase in the amperometric charge of spikes (Figure 6.8 D, Right - Bottom). This is similar to our previous findings, where prolonged syntilla blockade with 100 μM ryanodine primarily affected spikes and not SAFs (Lefkowitz et al., 2009).

Discussion

It would be lethal if the entire catecholamine content of the ACC were to be released at once. To prevent this, the sympathoadrenal system must employ tightly controlled mechanisms to fine tune exocytic output. This study finds that physiologically relevant forms of stimulation are able to regulate Ca^{2+} syntillas in the ACC, which have previously been found to inhibit spontaneous exocytosis in these cells. Thus, physiological regulation of Ca^{2+} syntillas could importantly add to the mechanisms by which the cell can fine tune output, based on input.

15 Hz

High frequency stimulation with sAPs, a condition matched to the true sympathetic stress response (i.e., "fight or flight"), was able to temporarily suppress Ca^{2+} syntillas. The temporary syntilla suppression, however, is unable to account for the immediate increase in exocytic output as measured by amperometry. That is*, prima facie,* it appears that as syntillas are depressed the frequency of exocytotic events is increased and as the syntillas return, the frequency of amperometric events goes back down (Figure 6.1). But if syntilla suppression were responsible for the increase in exocytosis during elicited

release, then there would seem to be some inconsistencies. For example, amperometric frequency does not peak at 2 minutes, the time where syntillas are completely abolished. Instead, amperometric frequency is highest during the first 30 seconds of stimulation, when syntillas are actually still present, albeit at a lower frequency. Moreover, the amperometric charge continues to increase throughout stimulation, even as syntillas begin to return to basal levels. Therefore, it is unlikely that syntilla suppression alone could account for elicited release during 15 Hz stimulation. Instead, increased global $[Ca^{2+}]_i$, in the 1 – 2 μM range, most likely produces the amperometric increase. Examination of global $[Ca^{2+}]_i$ levels in individual ACCs over time before, during and after the 15 Hz stimulation reveals $[Ca^{2+}]_i$ profiles bearing remarkable resemblance to the amperometric frequency profile during 15 Hz stimulation over the same time course (compare Figure 6.2 A (Left) to 6.1 B (Top)). During the first 15 – 30 seconds of intense stimulation, global $[Ca^{2+}]_i$ consistently spiked to levels between 5 and 10 μM, the same timeframe in which the amperometric frequency profile spiked to 8 – fold basal levels. Furthermore, global $[Ca^{2+}]_i$ was sustained at levels between 1 – 2 μM throughout the duration of the 15 Hz stimulation, well above the levels known to induce exocytosis ACCs (Augustine and Neher, 1992; Neher and Augustine, 1992), and returned to basal $[Ca^{2+}]_i$ levels immediately after stimulation stopped, again consistent with the amperometric frequency profile (Figure 6.2 B). Therefore, it is most likely that syntilla suppression does

not account for immediate increases in exocytosis elicited by 15 Hz stimulation – instead increased $[Ca^{2+}]_i$ does.

The fact that syntillas come back during the second half of the 15 Hz stimulation, where $[Ca^{2+}]_i$ remains high, and are restored to near basal levels after stimulation, may provide some insight into the mechanism by which different levels of stimulation can differentially regulate the Ca^{2+} syntilla. This is discussed below and in detail in the final chapter.

0.5 Hz

On the other hand, low frequency stimulation, a condition matched to that set by the sympathetic tone under basal conditions (i.e., "rest and digest"), was able to completely suppress Ca^{2+} syntillas. What's more, the syntilla suppression persisted even after stimulation ceased. It is very interesting that any increases in exocytic output as measured by amperometry under this condition were gone by 2 minutes, which implies that 0.5 Hz input associated with the sympathetic tone can only account for exocytic increases in the short term. That is, Ca^{2+} influx serving as a direct trigger for exocytosis during basal levels of stimulation is probably not the controlling factor for long term output, since it was only the first

two minutes of 0.5 Hz stimulation that induced an increase in exocytic output above that which was already present under spontaneous release conditions.

This, however, creates a paradox, since the ACC constantly receives stimulation and low levels of catecholamine are constantly secreted at basal levels enough to maintain blood pressure, enteric activity and insulin secretion. In other words, *in vivo*, secretion does not just stop after 2 minutes. But, this only seems paradoxical when thinking in terms of Ca^{2+} influx only as a direct trigger for exocytosis. For example, it may be that the moderate Ca^{2+} influx occurring approximately every other second during resting conditions serves multiple purposes. By suppressing Ca^{2+} release from internal stores in the form of Ca^{2+} syntillas, moderate stimulation could additionally serve to relieve the inhibitory pathway of exocytosis that Ca^{2+} released into the syntilla microdomain normally activates. Therefore, the major driving force of long term exocytic output under resting conditions may be accomplished by syntilla suppression. Of course, it is unclear which component of stimulation leads to syntilla suppression. But for reasons discussed below and in the final chapter, it is tempting to speculate that direct exposure of RYR2's to low levels of Ca^{2+} or Ca^{2+} -activated 2^{nd} messengers could be responsible.

Single sAP

The time frame for syntilla suppression after a single sAP was only slightly slower than in the experiments with 0.5 Hz stimulation, with 1 sAP causing near complete suppression by 2 minutes and lasting at least 20 minutes thereafter. The prolonged syntilla inhibition in these experiments was not an artifact due to run down as a result of long term whole cell patch clamping, since syntillas could be recorded at normal frequencies up to 25 minutes after conversion to the whole cell configuration in ACCs that were not given a sAP.

Though the ability of a single action potential to completely abolish Ca^{2+} syntillas was a surprising finding to us, the phenomenon is not entirely without precedent. That is, in bullfrog sympathetic neurons, the sister cells of ACCs, stimulation with a 50 ms depolarizing pulse was found to inactivate Ca^{2+}-induced Ca^{2+} release (CICR) via RYRs within a time frame of 10 – 20 ms (Akita and Kuba, 2008). The faster inactivation time could be explained by the much higher amounts of Ca^{2+} influx encountered during a 50 ms depolarizing square pulse, versus a simulated action potential (de Diego et al., 2008). It is also worth noting that in this study, recovery from inactivation was based on global $[Ca^{2+}]_i$ levels.

Ca^{2+} influx into the syntilla microdomain

If basal stimulation were to physiologically serve the purpose of suppressing syntillas long term, then how do we explain our preliminary experiments with ryanodine and ACh which show that syntilla suppression for more 30 minutes can lead to maximal exocytic output? In other words, why don't we observe maximal catecholamine output *in vivo* under resting conditions where ACCs are thought to fire APs at a frequency around 0.5 Hz? Again, the answer may be that Ca^{2+} influx through VGCCs during low frequency stimulation serves multiple purposes in addition to a direct exocytic trigger; First, as discussed above, to inhibit Ca^{2+} release from RYRs into the syntilla microdomain, this serves to increase exocytosis and; Second, to provide at spaced out intervals a nominal amount of Ca^{2+} influx sufficient to impinge upon the syntilla microdomain and thereby activate the same inhibitory process on exocytosis (see ryanodine + 0.5 Hz experiments in Preliminary Results). Thus, low frequency Ca^{2+} entry could provide the perfect balance between syntilla suppression and activation of the syntilla-mediated exocytic inhibition pathway.

CICR in Mouse ACCs?

Both of the fura-2 experiments showed a transient spike in the $[Ca^{2+}]_i$ upon stimulation, with 15 Hz stimulation producing a much larger spike than 0.5 Hz. Whether the initial spike shape in $[Ca^{2+}]_i$ was caused exclusively by Ca^{2+} influx, followed by Ca^{2+} channel inactivation or Ca^{2+}-induced-Ca^{2+}-release (CICR) followed by inhibition of CICR (see (Rios et al., 2008)) is unknown. Though CICR is prevalent in rat ACCs (Alonso et al., 1999; Inoue et al., 2003), at least one group has suggested that CICR does not play a significant role in mouse ACCs (Rigual et al., 2002). On the other hand, we find that if a mouse ACC is stimulated at 15 Hz and then stimulated at 15 Hz again after a period of rest, then the initial spike in $[Ca^{2+}]_i$ is much smaller in the later stimulation (Figure 6.2 A, (Right)). This could be more easily explained by a CICR mechanism where stores were depleted or RYRs were inactivated after the first stimulus, versus the alternative explanation where Ca^{2+} channels remained inactivated over the course of minutes. Further experiments monitoring the levels of store Ca^{2+} with mag-fura-2 will provide insight into this and may be useful in elucidating the mechanism by which stimulation is able to operate/suppress syntillas.

How does physiologic stimulation regulate Ca^{2+} syntillas?

How different levels of physiologically relevant stimulation can differentially regulate Ca^{2+} syntillas is still unknown. This study does, however, offer some clues for speculation into the mechanism, which are addressed in Preliminary Results and Discussion and discussed in detail in the final chapter.

How do Ca^{2+} syntillas regulate exocytosis?

We propose that the entry of Ca^{2+} into the syntilla microdomain activates an inhibitory path capable of suppressing exocytosis. The time frame for exocytic inhibition by the syntilla, about 2 – 4 minutes (see preliminary experiments with ryanodine + 0.5 Hz), is much faster than the time frame to relieve this inhibition (i.e., the absence of Ca^{2+} in the syntilla microdomain), which begins around 5 minutes and can take up to 30 minutes to achieve complete relief of exocytic inhibition. This implies a period of time necessary between the syntilla target and the eventual suppression of LDCG exocytosis.

Accordingly, the regulation of LDCG movement from a reserve pool to the readily releasable pool could satisfy these time restrictions. In this case the Ca^{2+} syntilla would target the F-actin network which is thought to serve as a barrier to LDCG movement. In one case, Ca^{2+} entry into the syntilla microdomain

would directly or indirectly promote actin polymerization and maintenance of the barrier, which could be accomplished within a time frame of minutes. The absence of Ca^{2+} in the syntilla microdomain for a prolonged period of time would lead to destabilization and breakdown of the actin barrier, a process that would seem to be consistent with the progressive increase in exocytosis over the course of 30 minutes of syntilla suppression. On the other hand, not only does F-actin serve as a barrier to LDCG movement, but it also provides the tracks for LDCG transport to the membrane. Thus, in another case, syntillas could serve to block the movement of LDCGs to the membrane by removing F-actin tracks. These mechanisms as well as those involving other molecular targets such as synaptotagmin1 and synapsin are considered more detail in the final chapter.

Ca^{2+} syntillas in vivo

The Ca^{2+} syntilla can be seen as a brake on exocytosis. Once the brake is relieved, exocytic output begins to increase. Thus, during normal resting conditions, Ca^{2+} influx must intermittently enter the syntilla microdomain and reapply the brake to ensure steady and slow release. This type of system, where exocytic output is largely driven not by constant activation of a trigger, but rather by intermittent suppression of an inhibitory pathway is very attractive from an energetic point of view. That is, the ACC does not need to receive frequent input

or generate action potentials at regular intervals (as evidenced by the fact that a single action potential can initiate the suppression) to provide consistent basal release and normal catecholamine output.

References

Akita T, Kuba K (2008) Ca2+-dependent inactivation of Ca2+-induced Ca2+ release in bullfrog sympathetic neurons. J Physiol 586:3365-3384.

Alonso MT, Barrero MJ, Michelena P, Carnicero E, Cuchillo I, Garcia AG, Garcia-Sancho J, Montero M, Alvarez J (1999) Ca2+-induced Ca2+ release in chromaffin cells seen from inside the ER with targeted aequorin. J Cell Biol 144:241-254.

Augustine GJ, Neher E (1992) Calcium requirements for secretion in bovine chromaffin cells. J Physiol 450:247-271.

Baker PF, Knight DE (1978) Calcium-dependent exocytosis in bovine adrenal medullary cells with leaky plasma membranes. Nature 276:620-622.

Becker PL, Fay FS (1987) Photobleaching of fura-2 and its effect on determination of calcium concentrations. Am J Physiol 253:C613-618.

Brandt BL, Hagiwara S, Kidokoro Y, Miyazaki S (1976) Action potentials in the rat chromaffin cell and effects of acetylcholine. J Physiol 263:417-439.

Chan SA, Smith C (2001) Physiological stimuli evoke two forms of endocytosis in bovine chromaffin cells. J Physiol 537:871-885.

Cuchillo-Ibanez I, Olivares R, Aldea M, Villarroya M, Arroyo G, Fuentealba J, Garcia AG, Albillos A (2002) Acetylcholine and potassium elicit different patterns of exocytosis in chromaffin cells when the intracellular calcium handling is disturbed. Pflugers Arch 444:133-142.

de Diego AM, Arnaiz-Cot JJ, Hernandez-Guijo JM, Gandia L, Garcia AG (2008) Differential variations in Ca2+ entry, cytosolic Ca2+ and membrane capacitance upon steady or action potential depolarizing stimulation of bovine chromaffin cells. Acta Physiol (Oxf) 194:97-109.

Douglas WW, Poisner AM (1962) On the mode of action of acetylcholine in evoking adrenal medullary secretion: increased uptake of calcium during the secretory response. J Physiol 162:385-392.

Douglas WW, Poisner AM (1963) The influence of calcium on the secretory response of the submaxillary gland to acetylcholine or to noradrenaline. J Physiol 165:528-541.

Drummond RM, Tuft RA (1999) Release of Ca2+ from the sarcoplasmic reticulum increases mitochondrial [Ca2+] in rat pulmonary artery smooth muscle cells. J Physiol 516 (Pt 1):139-147.

Fulop T, Smith C (2006) Physiological stimulation regulates the exocytic mode through calcium activation of protein kinase C in mouse chromaffin cells. Biochem J 399:111-119.

Fulop T, Radabaugh S, Smith C (2005) Activity-dependent differential transmitter release in mouse adrenal chromaffin cells. J Neurosci 25:7324-7332.

Gong LW, de Toledo GA, Lindau M (2007) Exocytotic catecholamine release is not associated with cation flux through channels in the vesicle membrane but Na+ influx through the fusion pore. Nat Cell Biol 9:915-922.

Grynkiewicz G, Poenie M, Tsien RY (1985) A new generation of Ca2+ indicators with greatly improved fluorescence properties. J Biol Chem 260:3440-3450.

Guyton AC, Hall JE (2000) Textbook of medical physiology, 10th Edition. Philadelphia: Saunders.

Inoue M, Sakamoto Y, Fujishiro N, Imanaga I, Ozaki S, Prestwich GD, Warashina A (2003) Homogeneous Ca2+ stores in rat adrenal chromaffin cells. Cell Calcium 33:19-26.

Kidokoro Y, Ritchie AK (1980) Chromaffin cell action potentials and their possible role in adrenaline secretion from rat adrenal medulla. J Physiol 307:199-216.

Lefkowitz JJ, Fogarty KE, Lifshitz LM, Bellve KD, Tuft RA, ZhuGe R, Walsh JV, Jr., De Crescenzo V (2009) Suppression of Ca2+ syntillas increases spontaneous exocytosis in mouse adrenal chromaffin cells. J Gen Physiol 134:267-280.

Neher E, Augustine GJ (1992) Calcium gradients and buffers in bovine chromaffin cells. J Physiol 450:273-301.

Rigual R, Montero M, Rico AJ, Prieto-Lloret J, Alonso MT, Alvarez J (2002) Modulation of secretion by the endoplasmic reticulum in mouse chromaffin cells. Eur J Neurosci 16:1690-1696.

Rios E, Zhou J, Brum G, Launikonis BS, Stern MD (2008) Calcium-dependent inactivation terminates calcium release in skeletal muscle of amphibians. J Gen Physiol 131:335-348.

Sun XP, Callamaras N, Marchant JS, Parker I (1998) A continuum of InsP3-mediated elementary Ca2+ signalling events in Xenopus oocytes. J Physiol 509 (Pt 1):67-80.

Wang CT, Bai J, Chang PY, Chapman ER, Jackson MB (2006) Synaptotagmin-Ca2+ triggers two sequential steps in regulated exocytosis in rat PC12 cells: fusion pore opening and fusion pore dilation. J Physiol 570:295-307.

ZhuGe R, Fogarty KE, Tuft RA, Lifshitz LM, Sayar K, Walsh JV, Jr. (2000) Dynamics of signaling between Ca(2+) sparks and Ca(2+)- activated K(+) channels studied with a novel image-based method for direct intracellular measurement of ryanodine receptor Ca(2+) current. J Gen Physiol 116:845-864.

ZhuGe R, DeCrescenzo V, Sorrentino V, Lai FA, Tuft RA, Lifshitz LM, Lemos JR, Smith C, Fogarty KE, Walsh JV, Jr. (2006) Syntillas release Ca2+ at a site different from the microdomain where exocytosis occurs in mouse chromaffin cells. Biophys J 90:2027-2037.

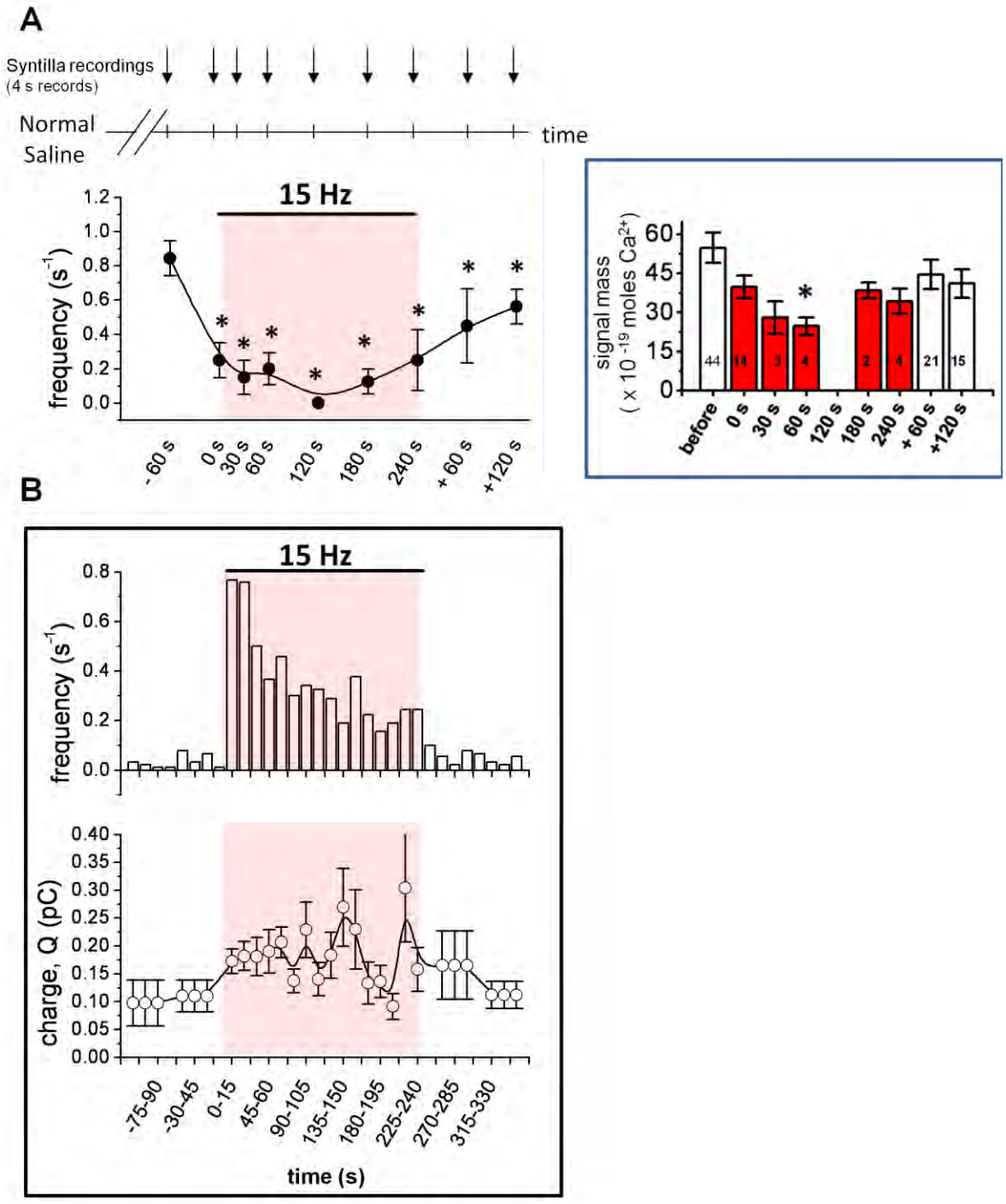
A
Syntilla recordings
(4 s records)
Normal
Saline
time
15 Hz
frequency (s-1)
- 60 s
0 s
30 s
60 s
120 s
180 s
240 s
+ 60 s
+120 s
signal mass
(x 10 -19 moles Ca2+)
before
B
15 Hz
frequency (s-1)
charge, Q (pC)
-75-90
-30-45
0-15
45-60
90-105
135-150
180-195
225-240
270-285
315-330
time (s)

Figure 6.1 Effects of stressful stimulation on Ca^{2+} syntillas and exocytosis. **A.** 15 Hz stimulation temporarily suppresses syntillas. **(Left)** Simulated action potentials (sAPs) were applied to the ACC at a frequency of 15 Hz for 4 minutes and syntilla recordings were made before, during and after stimulation as indicated in the figure. The frequency of syntillas is completely suppressed after 2 minutes of stimulation but begins to return by 3 minutes (N=12cells, 54 records). **(Right)** The mean signal mass of individual syntillas is decreased after 1 minute of stimulation and begins to return to pre-stimulus levels 3 minutes into stimulation. Red bars indicate period of stimulation and numbers inside bars indicate number of records. Asterisks represent statistical significance at the $P<0.05$ level compared to -60 s (or pre-stimulus) using a one ANOVA and Fisher's LSD test for pair-wise multiple means comparisons. **B.** To follow the effect of 15 Hz stimulation on exocytosis over time, amperometric recordings were made before, during and after stimulation and the data was binned into 15 s intervals. **(Top)** The frequency of amperometric events immediately increases upon stimulation and gradually tapers off to near basal levels as stimulation continues. **(Bottom)** Oppositely, the amperometric charge shows a gradually increasing trend over time. Due to low event frequencies, charge data was divided into 30 s intervals before and after stimulation (N = 8 cells, 32 events before, 630 during and 39 after stimulus).

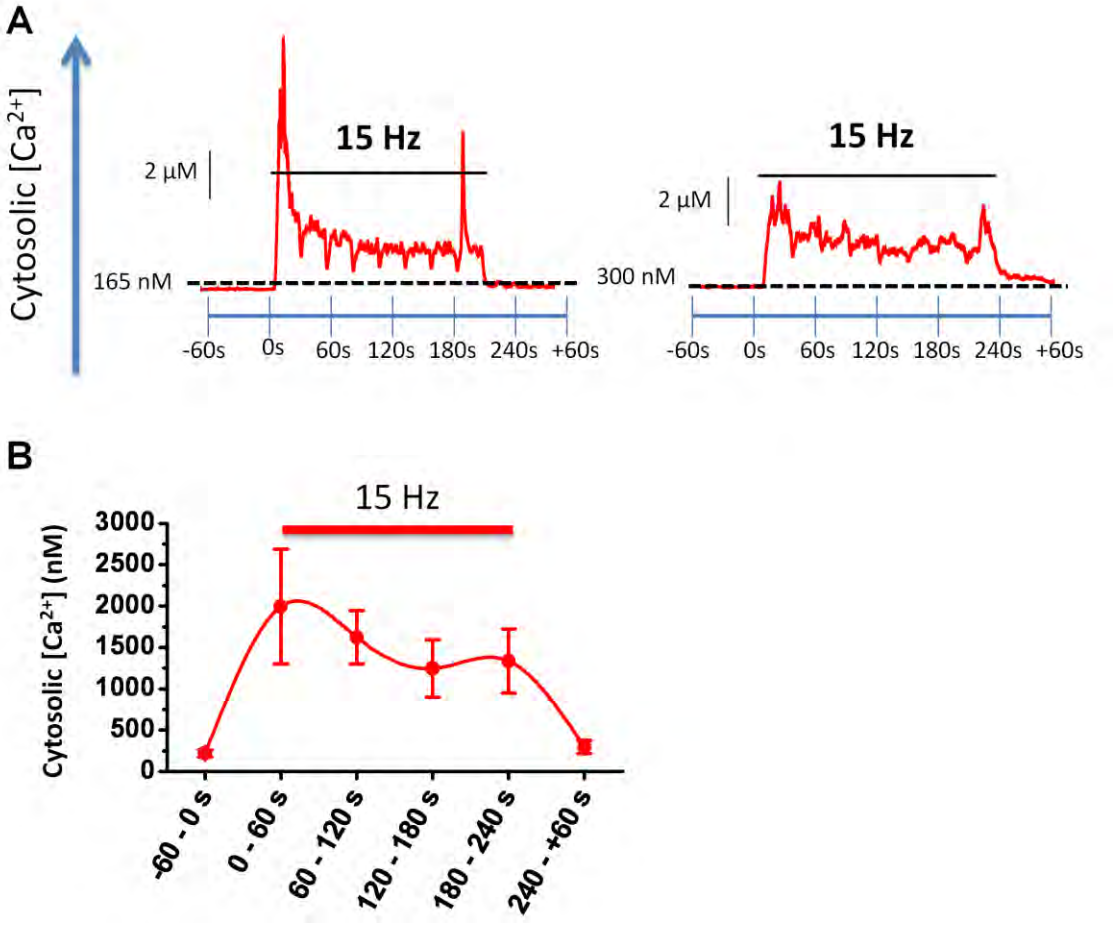

Figure 6.2 Global $[Ca^{2+}]_i$ during 15 Hz stimulation. The Ca^{2+} indicator dye Fura-2 was used to assay changes in global intracellular $[Ca^{2+}]$ before, during and after stimulation by sAP's delivered at 15 Hz. **A. (Left)** Representative recording from an individual ACC stimulated at 15 Hz. **(Right)** Another representative recording from a cell that was stimulated at 15 Hz after first being stimulated at 0.5 Hz with 2 minutes of rest in between shows a smaller initial transient increase. **B.** Mean $[Ca^{2+}]_i$ for each 60 s interval is shown before, during and after stimulation. (N= 4 cells).

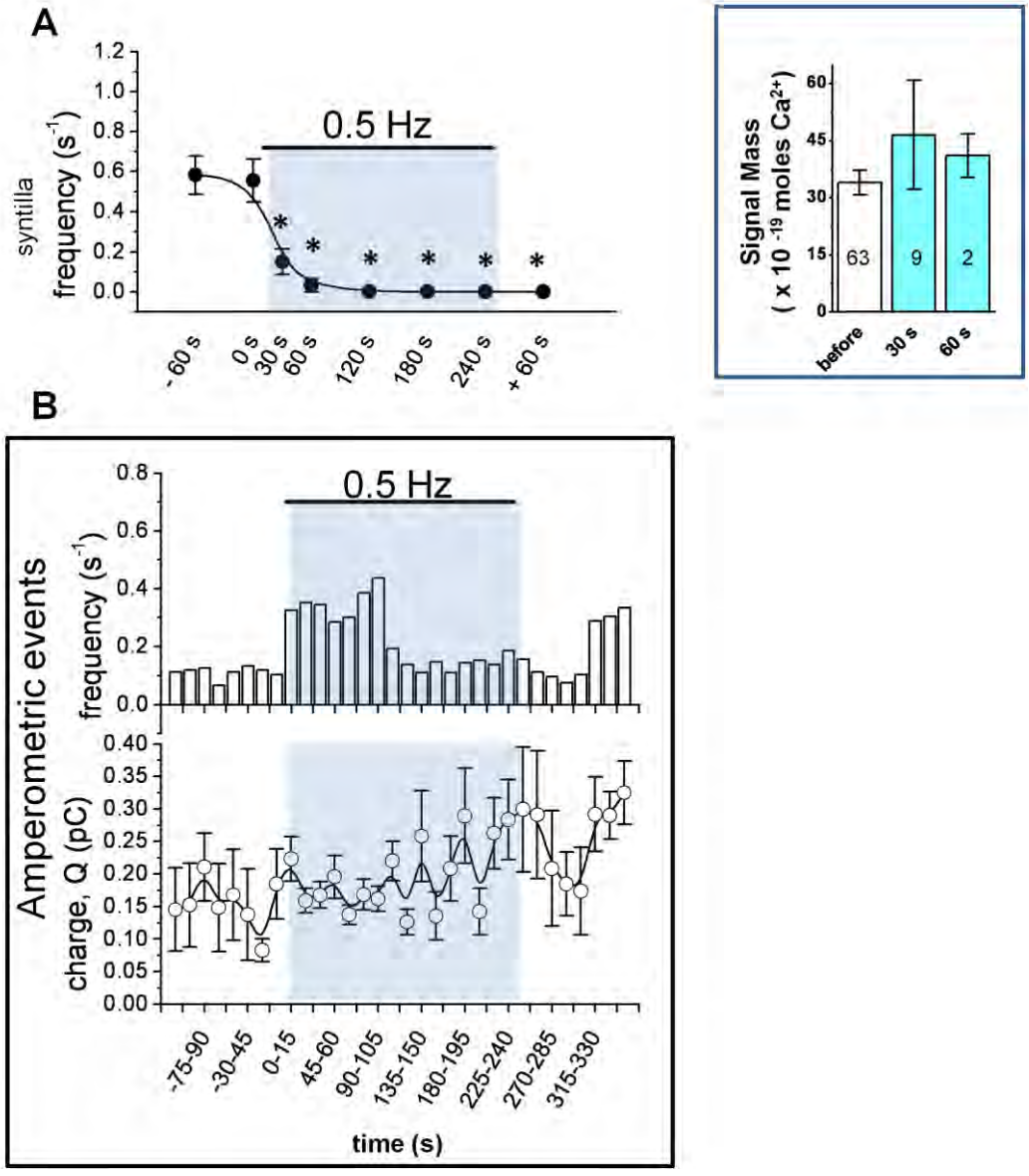
A
0.5 Hz
syntilla
frequency (s-1)
1.2
1.0
0.8
0.6
0.4
0.2
0.0
- 60 s
0 s
30 s
60 s
120 s
180 s
240 s
+ 60 s
Signal Mass
(x 10 -19 moles Ca2+)
60
45
30
15
0
63
9
2
before
30 s
60 s
B
0.5 Hz
Amperometric events
frequency (s-1)
charge, Q (pC)
0.40
0.35
0.30
0.25
0.20
0.15
0.10
0.05
0.00
-75-90
-30-45
0-15
45-60
90-105
135-150
180-195
225-240
270-285
315-330
time (s)

Figure 6.3 **Effects of basal stimulation (0.5 Hz) on Ca^{2+} syntillas and exocytosis.** **A.** 0.5 Hz stimulation completely suppresses syntillas. **(Left)** sAPs were applied to the ACC at a frequency of 0.5 Hz for 4 minutes and syntilla recordings were made before, during and after stimulation. The frequency of syntillas is completely suppressed after 2 minutes of stimulation and remains suppressed after stimulation stops (N=15cells, 114 records). **(Right)** The mean signal mass of individual syntillas is not significantly altered during the 2 minutes of stimulation while syntillas are being suppressed. Blue bars indicate stimulation and numbers inside bars indicate number of records. Asterisks represent statistical significance at the $P<0.05$ level compared to -60 s (or pre-stimulus) using a one ANOVA and Fisher's LSD test for pair-wise multiple means comparisons. **B.** Effect of 0.5 Hz stimulation on exocytosis at 15 s intervals over time. **(Top)** The frequency of amperometric events increases moderately upon stimulation then returns to basal levels after 2 minutes. Note that amperometric frequency increases again about 2 minutes after stimulation has ended. **(Bottom)** Amperometric charge shows a gradually increasing trend over time and continues to increase even after stimulation ceases. (N = 9 cells, 120 events before; 18 cells, 944 events during and; 9 cells, 198 events after stimulus).

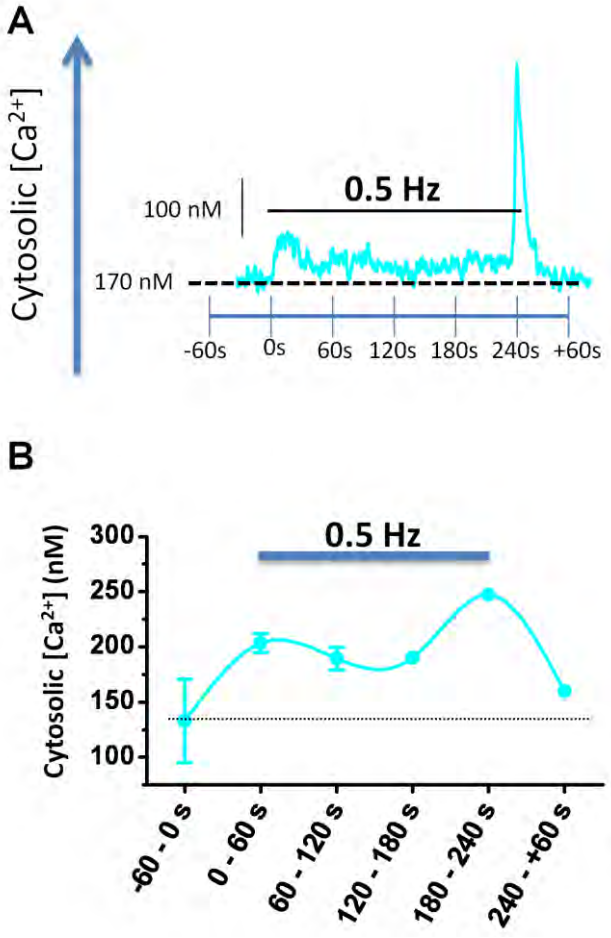

Figure 6.4 Global $[Ca^{2+}]_i$ during 0.5 Hz stimulation. Changes in global $[Ca^{2+}]_i$ were measured using the Ca^{2+} indicator dye Fura-2 before, during and after sAP stimulation at 0.5 Hz. **A.** Representative recording from an individual ACC stimulated at 0.5 Hz. **B.** Mean $[Ca^{2+}]_i$ for each 60 s interval is shown before, during and after stimulation. (N= 2 cells).

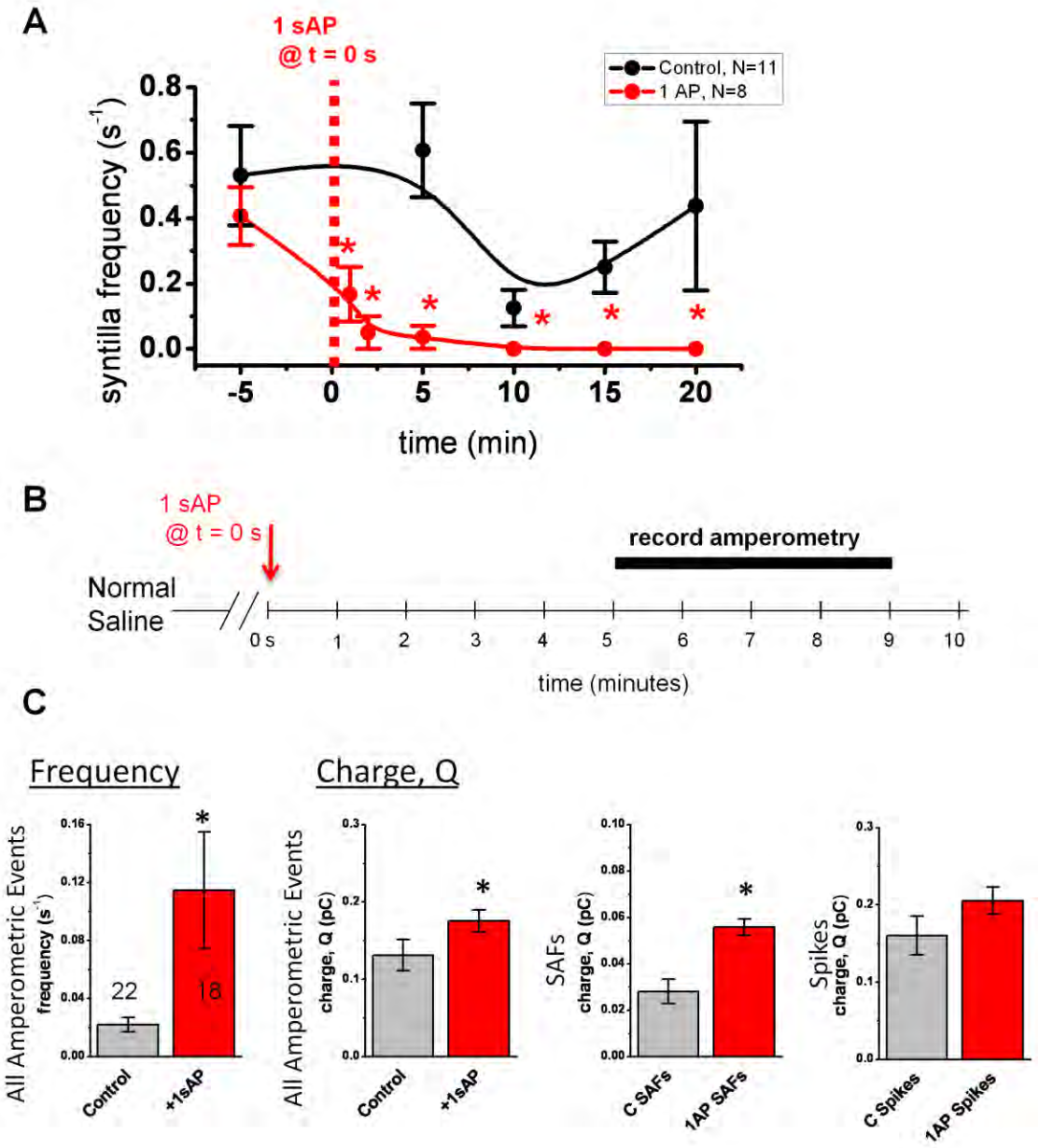
A
1 sAP
@ t = 0 s
Control, N=11
1 AP, N=8
syntilla frequency (s-1)
0.8
0.6
0.4
0.2
0.0
-5
0
5
10
15
20
time (min)
B
1 sAP
@ t = 0 s
record amperometry
Normal
Saline
0 s
1
2
3
4
5
6
7
8
9
10
time (minutes)
C
Frequency
Charge, Q
All Amperometric Events
frequency (s-1)
22
18
Control
+1sAP
All Amperometric Events
charge, Q (pC)
Control
+1sAP
SAFs
charge, Q (pC)
C SAFs
1AP SAFs
Spikes
charge, Q (pC)
C Spikes
1AP Spikes

Figure 6.5 Effects of a single action potential on Ca^{2+} syntillas and exocytosis. A. Stimulation with a single sAP completely suppresses syntillas. A single sAP was applied to the ACC at t = 0 s and syntilla frequency was recorded at 5 minute intervals before and after stimulation. Control cells (black) did not receive any stimulation and syntillas could be detected at the normal frequency up to 30 minutes after cell loading with fluo-3 (N = 11). In ACCs receiving a single sAP the syntilla frequency was completely suppressed between 5 and 10 minutes post stimulus (N = 8). Asterisks represent statistical significance at the $P<0.05$ level compared to -60 s (or pre-stimulus) using a one way ANOVA and Fisher's LSD test for pair-wise multiple means comparisons. **B.** Diagram of the protocol for recording amperometric events after stimulation with 1 sAP. Amperometry was recorded for 4 minutes after a 5 minute rest once the ACC received a single sAP. **C.** Mean changes in frequency and charge of amperometric events after 1 sAP compared to control. The frequency of all amperometric events is significantly increased from 0.022 ± 0.005 Hz (N = 22) to 0.115 ± 0.04 Hz (N = 18) between 5 – 9 minutes after a single sAP. After simulataion with 1 sAP the mean charge of all amperometric events and stand alone feet events (SAFs) are significantly increased from 0.12 ± 0.019 pC to 0.16 ± 0.04 pC and from 0.028 ± 0.005 pC to 0.05 ± 0.003 pC, respectively. Asterisks indicate significance at $P<0.05$ by a log transformed student's t-test. The mean charge of spike events is not significantly altered.

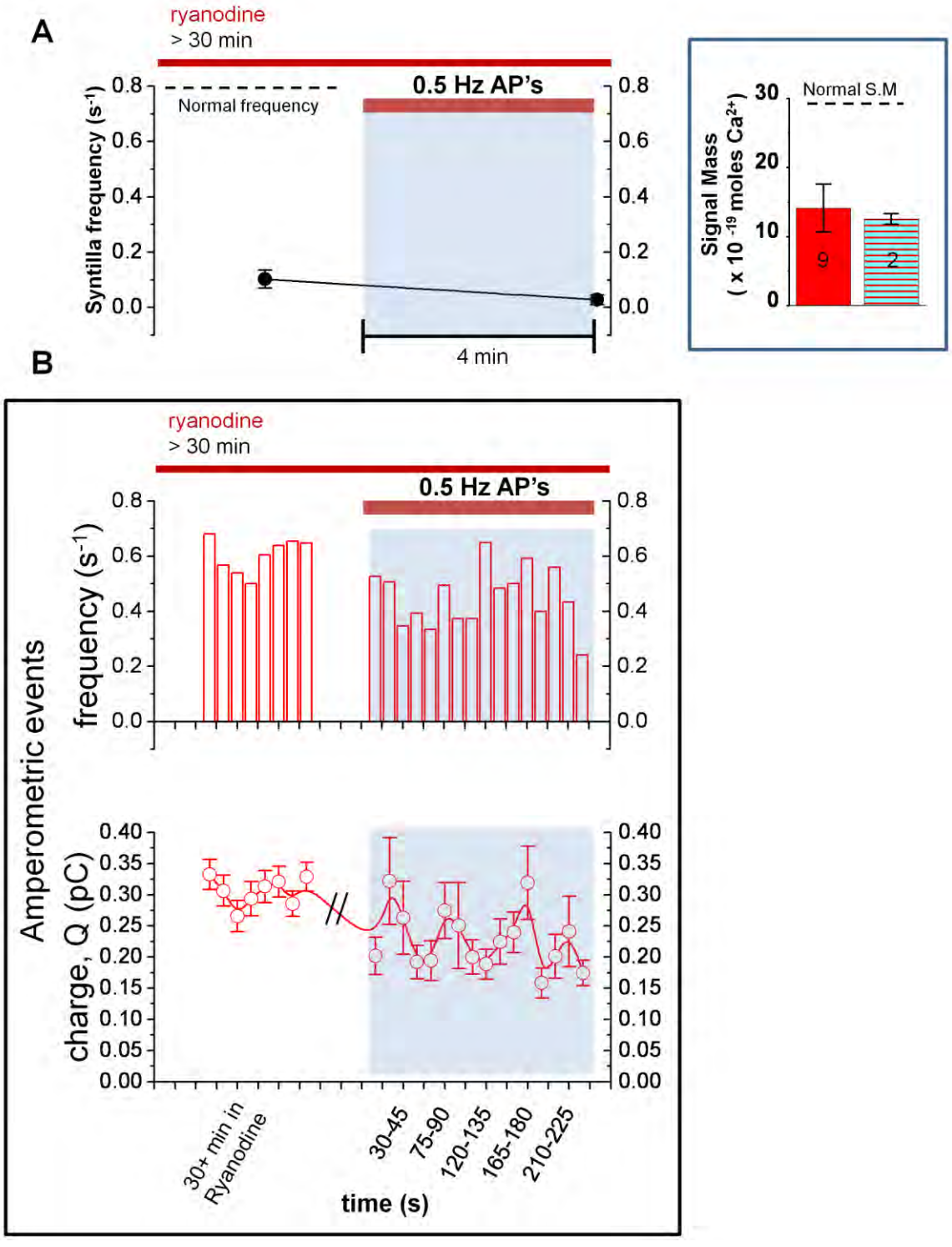
A
ryanodine
> 30 min
0.5 Hz AP's
Normal frequency
Syntilla frequency (s-1)
4 min
Signal Mass
(x 10 -19 moles Ca2+)
Normal S.M
9
2
B
ryanodine
> 30 min
0.5 Hz AP's
Amperometric events
frequency (s-1)
charge, Q (pC)
30+ min in Ryanodine
30-45
75-90
120-135
165-180
210-225
time (s)

Figure 6.6 **Effects of basal stimulation (0.5 Hz) after syntillas have been blocked with ryanodine for over 30 minutes.** **A. (Left)** Syntillas are suppressed to 0.10 ± 0.033 Hz (n = 11) after exposure to 100 μM ryanodine for over 30 minutes. Immediately after 4 minutes of 0.5 Hz sAP stimulation, syntillas are almost completely blocked, 0.028 ± 0.018 Hz (n = 9). Compare to normal syntilla frequencies near 0.8 Hz, dashed line. **(Right)** The mean signal mass of individual syntillas in ACCs exposed to ryanodine (red bar) and ryanodine + 0.5 Hz stimulation (red and blue striped bar) is decreased compared to normal (dashed line). Numbers inside bars indicate number of records. **B.** Effect of exposure to 100 μM ryanodine for over 30 minutes and 0.5 Hz sAP stimulation after ryanodine exposure on exocytosis at 15 s intervals over time. **(Top)** The frequency of amperometric events is high when syntillas are blocked by ryanodine alone. During 0.5 Hz stimulation after syntillas have been blocked for 30+ minutes with ryanodine, the frequency of events is still high but shows a decreasing trend. **(Bottom)** Amperometric charge shows a gradually decreasing trend over time during 0.5 Hz stimulation in ryanodine compared to ryanodine alone. (N = 13 cells, ryanodine alone; N = 10 cells, ryanodine + 0.5 Hz.).

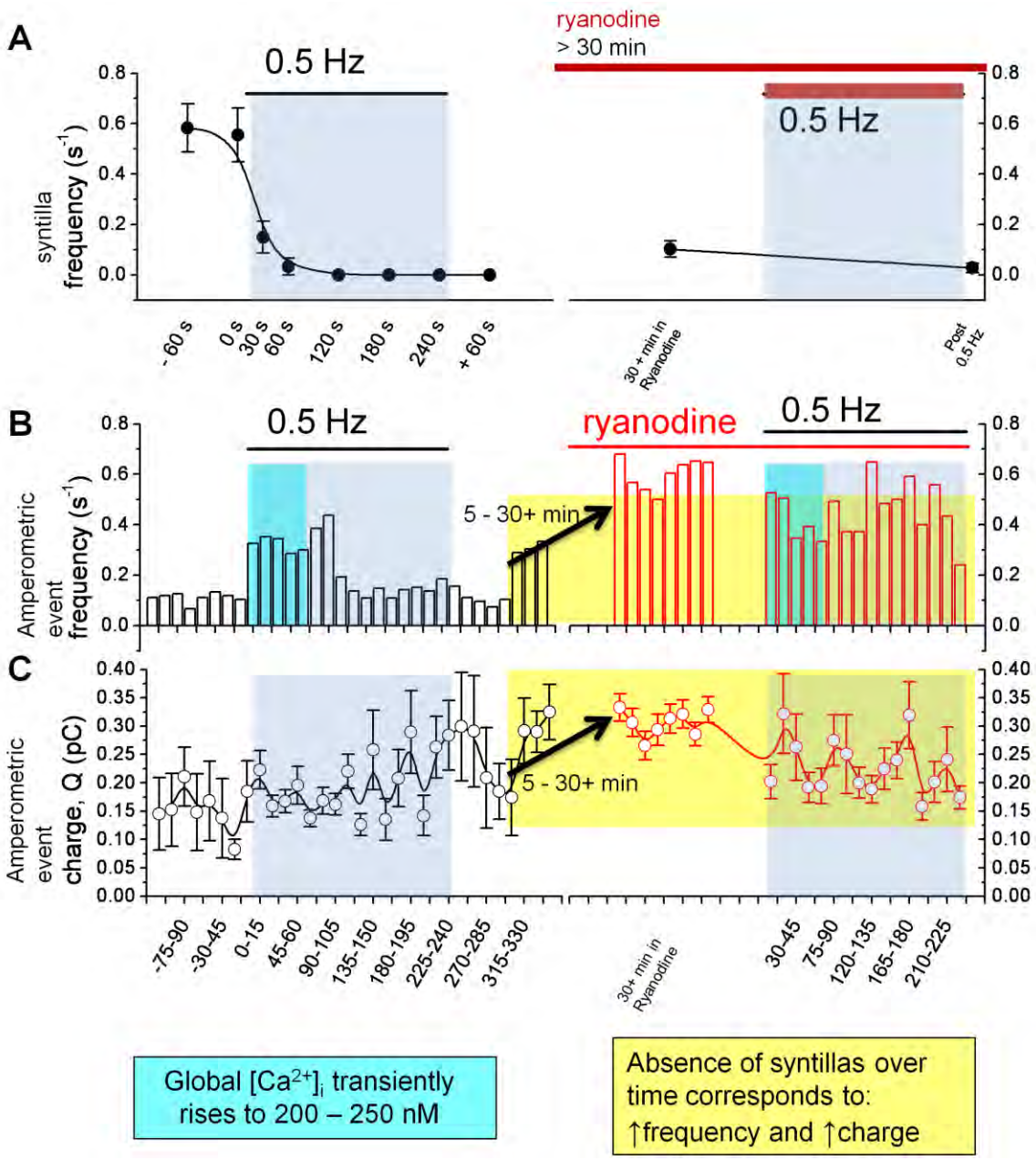

Figure 6.7 **0.5 Hz stimulation compared with 0.5 Hz stimulation after syntillas have been blocked for over 30 minutes.** See text for details.

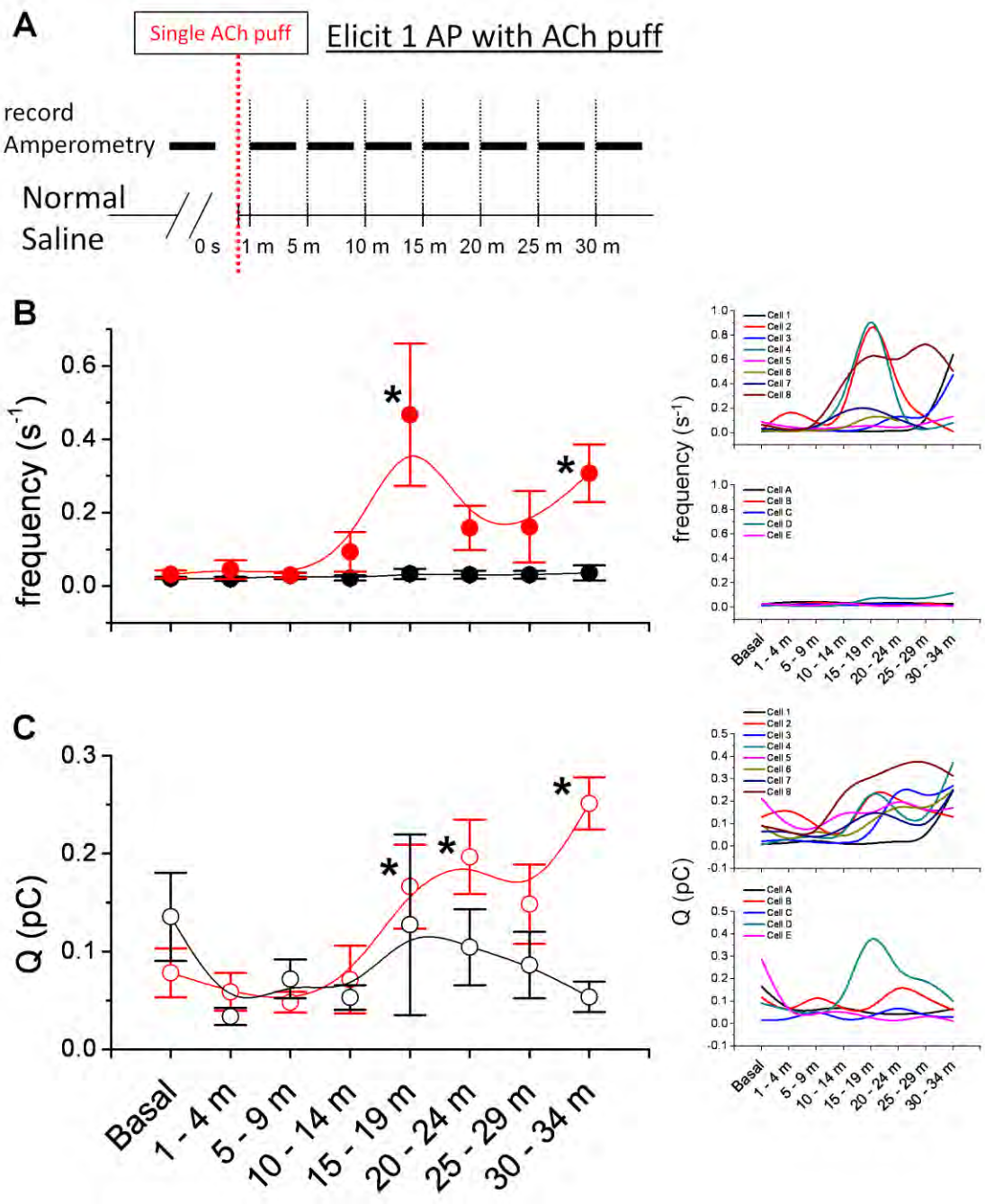
A
Single ACh puff
Elicit 1 AP with ACh puff
record
Amperometry
Normal
Saline
0 s
1 m
5 m
10 m
15 m
20 m
25 m
30 m
B
frequency (s-1)
0.6
0.4
0.2
0.0
*
*
Cell 1
Cell 2
Cell 3
Cell 4
Cell 5
Cell 6
Cell 7
Cell 8
Cell A
Cell B
Cell C
Cell D
Cell E
Basal
1 - 4 m
5 - 9 m
10 - 14 m
15 - 19 m
20 - 24 m
25 - 29 m
30 - 34 m
C
Q (pC)
0.3
0.2
0.1
0.0
*
*
*

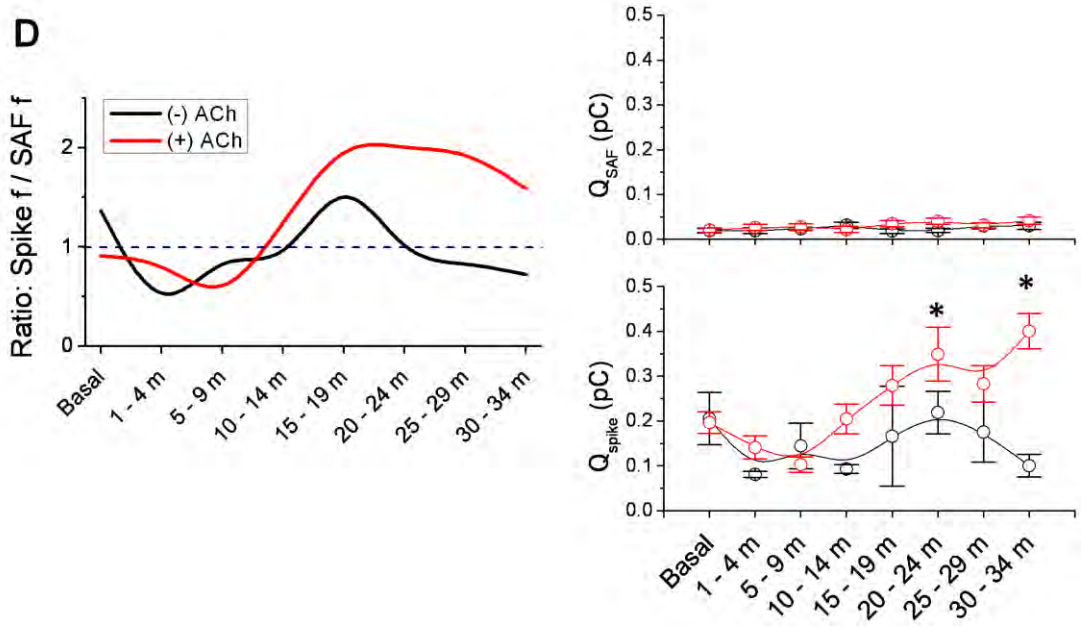
D
Ratio: Spike f / SAF f
(-) ACh
(+) ACh
0
1
2
Basal
1 - 4 m
5 - 9 m
10 - 14 m
15 - 19 m
20 - 24 m
25 - 29 m
30 - 34 m
Q_{SAF} (pC)
Q_{spike} (pC)
0.0
0.1
0.2
0.3
0.4
0.5
*
*

Figure 6.8 Time is necessary for syntilla suppression to exert its effect on exocytosis. Long term effects on amperometry in unpatched ACCs after a brief puff of acetylcholine (ACh) is used to induce a single action potential. **A.** Diagram showing amperometry recording paradigm. 4 minute recordings are made every 5 minutes before and then after a brief, 25 ms puff of 30 μM ACh is applied to the ACC. **B.** ACCs that did not receive an ACh puff showed no signs of increased amperometric frequency over time (black line). The lower right chart shows individual cell recordings (N = 5). Amperometric frequency increases begin to show up between 15 – 20 minutes after receiving an ACh puff (red line). The upper right chart shows individual cell recordings (N = 8). Note that the amount of time necessary for an amperometric frequency increase to develop after the ACh puff differs from cell to cell. Asterisks indicate significance at the $P<0.05$ level compared to pre-stimulus levels (basal or first data point) using a one way ANOVA for repeated measures and Fisher's LSD test for pair-wise multiple means comparisons (e.g., comparisons are made within groups over time and not between groups). **C.** ACCs that did not receive an ACh puff also showed no significant signs of increased amperometric charge over time (black line). The lower right chart shows individual cell recordings (N = 5). Charge increases begin to show up between 15 – 20 minutes after receiving an ACh puff (red line). The upper right chart shows individual cell recordings (N = 8). Again, the amount of time necessary for an amperometric charge increase to develop after the ACh puff also differs from cell to cell. Asterisks indicate significance at the $P<0.05$ level compared to pre-stimulus levels (basal or first data point) using a one way ANOVA for repeated measures and Fisher's LSD test for pair-wise multiple means comparisons (e.g., comparisons are made within groups over time and not between groups). **D.** Analysis of spike and SAF events over time after an ACh puff. **(Left)** The ratio of the mean frequency of spike events to SAF

events at each time interval is plotted for ACCs that did not receive an ACh puff (black line) and those ACCs that did (red line). A ratio above 1.0 indicates preference for the full fusion mode of release over the kiss and run mode. (**Right, upper)** The mean charge of SAF events over time is not increased by an ACh puff. **(Right, lower)** Instead, it is the mean charge of spike events that increases over time Asterisks indicate significance at the $P<0.05$ level compared to pre-stimulus levels (basal or first data point) using a one way ANOVA for repeated measures and Fisher's LSD test for pair-wise multiple means comparisons.

Chapter 7

Conclusions, speculation and the road ahead

Spontaneous release

This dissertation describes in detail a novel and unexpected function for Ca^{2+} in the process of exocytosis. Ca^{2+} syntillas, brief, focal cytosolic Ca^{2+} transients arising from Ca^{2+} stores and mediated by RYRs function to *inhibit* spontaneous exocytosis in mouse chromaffin cells.

Ca^{2+} syntilla ⊣ Exocytosis

This conclusion is based on the core findings presented in Chapter 5 which show that decreasing the frequency of syntillas leads to an increase in the frequency and magnitude (quantal charge measured amperometrically) of exocytosis. There can be little doubt about this finding since it was based on concurring results of two independent and separate lines of experimentation, each employing a quite different strategy to suppress syntillas. That is, we found

exocytosis to be increased both when syntillas were suppressed by: 1.) blocking the actual RYRs through which Ca^{2+} syntillas are released; and, 2.) decreasing the amount of Ca^{2+} in the stores by blocking the Ca^{2+} ATPase pump to prevent refilling and then activating RYRs to promote emptying of the stores.

Elicited release

By shifting from spontaneous release to studying Ca^{2+} syntillas in elicited release, this dissertation further provides detailed insight for the first time into the physiologic relevance of syntilla mediated exocytic inhibition. Chapter 6 demonstrated unexpectedly, that physiologically relevant levels of stimulation using simulated action potentials delivered at 15 Hz or 0.5 Hz completely abolished Ca^{2+} syntillas within a timeframe of two minutes.

Action potential ⊣ Ca^{2+} syntilla

It was found that the different levels of stimulation could differentially regulate Ca^{2+} syntillas. During stimulation at 15 Hz, associated with the sympathetic stress response, the syntillas are only temporarily suppressed, where they come back halfway through stimulation. Stimulation at 0.5 Hz, set by the basal sympathetic tone, completely suppressed syntillas. While the direct triggering of exocytosis by Ca^{2+} influx was found to be the major driving force behind large increases in elicited exocytosis under stressful conditions, this mechanism could not account for increases in elicited exocytosis beyond two minutes under basal conditions. Instead, a prolonged suppression of Ca^{2+} syntillas during 0.5 Hz

stimulation, and not Ca^{2+} influx, correlated with smaller increases in exocytosis over the long term. These findings suggest that internal Ca^{2+} stores not only serve as an important mediator of the exocytotic output based on physiologic input, but that syntilla suppression may account for basal levels of catecholamine output into the circulation during resting conditions in an organism.

Ca^{2+} syntilla model for neurotransmission

Overall, the findings presented here suggest that internal Ca^{2+} stores serve as an important mediator of the exocytotic output based on physiologic input. That is, the Ca^{2+} syntilla lies at the center of cell to cell communication in excitable cells and neurotransmission.

Action potential ⊣ Ca^{2+} syntilla ⊣ Exocytosis

As detailed in Chapter 6, the Ca^{2+} syntilla can be seen as a brake on exocytosis. Physiologic input in the form of an action potential relieves the brake by inactivating RYRs and therefore Ca^{2+} release from stores. Thus, under resting conditions, Ca^{2+} generated from channel influx must intermittently enter the syntilla microdomain to ensure steady and slow release. *In vivo* syntillas are suppressed most of the time, while the animal is in the resting state. Ca^{2+} syntillas appear only after intense stimulation, when the stress response is initiated and serve to quickly punctuate massive exocytic release.

Ca^{2+} syntillas in physiology and neuroscience

The general physiological and philosophical implications of this work are quite substantial. Since the experiments were done in the adrenal chromaffin cell, it directly implies that syntillas can serve as a potent regulator of catecholamine release into the circulation. At rest, low levels of catecholamine are constantly released into the blood, sub-serving multiple tasks such as regulating basal enteric activity, insulin secretion and maintaining a normal blood pressure. As pointed out in Chapter 6, catecholamine release elicited by 0.5 Hz stimulation associated with the basal sympathetic tone can only produce increases in exocytosis for up to 2 minutes. Therefore any release beyond the first 2 minutes of stimulation is actually due to spontaneous release. Thus, *in vivo*, during resting conditions where the ACC receives constant input at low frequency, all exocytic output is likely in the form of spontaneous release, regulated by the presence or absence of Ca^{2+} within the syntilla microdomain.

As discussed at length in the introductory Chapter 2, the ACC has long been used as a model for neurotransmission in neurons since ACCs are unique in that they share the same properties of neurons (Winkler and Fischer-Colbrie, 1998; Garcia et al., 2006). Therefore the conclusions in this work are likely to carry over to the process of neurotransmission. This is supported by the existence of Ca^{2+} syntillas in hypothalamic nerve terminals (De Crescenzo et al.,

2004; McNally et al., 2009) as well as the existence of spontaneous elementary Ca^{2+} release events, that seem to resemble syntillas, in pyramidal neurons (Manita and Ross, 2009). Furthermore, RYRs are widely expressed in the mammalian brain (Giannini et al., 1995; Galeotti et al., 2008), where they play a central role in the regulation of intracellular Ca^{2+} homeostasis (Simpson et al., 1995) and regulate vital brain functions, including protein synthesis (Paschen et al., 1996) and neurotransmitter release (Mothet et al., 1998; He et al., 2000). While all three isoforms of the receptor (RYR1, RYR2, and RYR3) are present in brain, the RYR2 is predominant (Zalk et al., 2007). Thus the work presented herein is especially relevant to secretion in neurons since the Ca^{2+} syntillas that regulate exocytosis in ACCs are thought to be mediated by RYR2.

It is tempting to speculate that the syntilla suppression described here could also serve as a mechanism to control release rates of what is termed "spontaneous" or "unsynchronized" release in neurotransmission. Neurons constantly receive basal input even if at very low frequency. Unsynchronized release events that occur in between or in the absence of action potentials cannot proceed by a direct Ca^{2+} influx triggering mechanism. Thus, fluctuations in the rates of basal release could be altered by controlling release from internal stores based on prior action potential input. Therefore the regulation of Ca^{2+} release from internal stores via syntillas may constitute another basis of

potentiation in synaptic plasticity (e.g., by increasing the size of the RRP). Furthermore, spontaneous exocytosis has specific functions in a range of neurons including synapse stabilization and maintenance, regulation of post synaptic protein synthesis, and regulation of excitability in postsynaptic neurons. Therefore syntillas could serve as an upstream regulator of these important functions as well.

Molecular mechanisms

The biggest questions to arise from this work revolve around the molecular components involved in the pathway from physiologic input to exocytic output through the release of Ca^{2+} from internal stores in the form of the Ca^{2+} syntilla. That is, first, how can an action potential inactivate Ca^{2+} syntillas? And second, how does the Ca^{2+} entry into the syntilla microdomain exert an inhibitory effect on exocytosis?

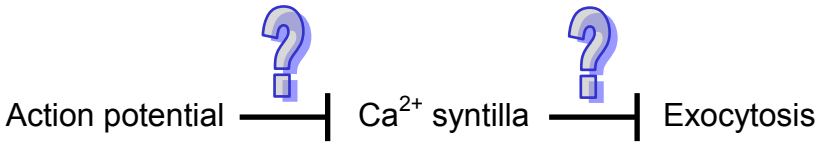

As a final part to this dissertation, speculation into the molecular mechanisms involved and future lines of experimentation are offered.

Regulation of exocytosis by Ca^{2+} syntillas:

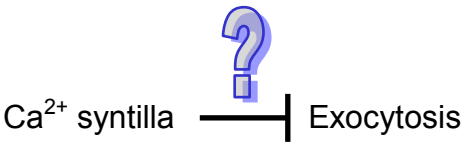

The molecular components of the inhibitory effect of Ca^{2+} syntillas on spontaneous exocytosis are only partially known at this point. Clearly, RYRs mediate the effect, more specifically type 2 RYRs, the "cardiac" type. The evidence for this comes from a previous study in which we detected high levels of RYR2 by RT-PCR, but only low levels of RYR3 and virtually no trace of RYR1 (ZhuGe et al., 2006). By immunocytochemistry, there was no trace of RYR1, and RYR3 was found only in an isolated clump in the cell center. RYR2 by contrast was found in a subplasmalemmal distribution throughout the cell (ZhuGe et al., 2006), which seems to be consistent with the localization of syntillas by imaging. In addition the ability of Tg to affect the syntillas indicates that the SERCA pump is also involved in replenishing the Ca^{2+} that appears in the form of syntillas.

Ultimately the syntillas must affect either the granules or the plasmalemmal sites of spontaneous fusion. One simple mechanism that could account for the decrease in frequency is that the LDCGs carry with them a Ca^{2+} sensor which detects the syntilla and inhibits or limits the LDCG's ability to

complex with the exocytotic machinery. It is tempting to postulate that this sensor is synaptotagmin. In the absence of the T-SNARE complex at the plasma membrane synaptotagmin will undergo a cis interaction with the vesicle membrane in the presence of elevated [Ca^{2+}] (Hui et al., 2005; Stein et al., 2007). Such an interaction renders the synaptotagmin incapable of complexing with the T-SNARE complex at the plasma membrane. The source of Ca^{2+} to disable the synaptotagmin might be provided by the Ca^{2+} syntilla before the LDCG reaches the plasma membrane. If the effect of Ca^{2+} syntillas were targeted to only a population of large granules, then this hypothesis could explain both the increase in frequency and magnitude. Alternatively, the Ca^{2+} sensor might have more than one effect; for example, the vesicles that are not completely inhibited might be rendered less competent to undergo complete emptying, resulting in smaller magnitude of the fusion events.

Another attractive hypothesis involves the subplasmalemmal filamentous actin (F-actin) mesh. It is well documented in chromaffin cells that dissolution of the dense actin cortex is necessary to sustain recruitment of LDCGs to the membrane during stimulation (Nakata and Hirokawa, 1992; Vitale et al., 1995; Tchakarov et al., 1998; Giner et al., 2007). Therefore syntillas could play a role in maintaining the actin mesh under spontaneous conditions. If the actin network breaks down in the absence of syntillas this could explain the increase in

frequency of amperometric events observed in the presence of ryanodine. But it could also explain the increase in quantal size of events. A period of time would be required for the actin network to break down, which would be consistent with the findings in Chapter 6 that show a period of time between 5 and 30 minutes necessary before syntilla suppression correlates with increases in exocytosis. It has been shown that disruption of F-actin favors the full fusion mode of exocytosis over kiss and run (Doreian et al., 2008; Doreian et al., 2009). That is, one role of the intact dense F-actin mesh in mouse chromaffin cells is to stabilize the fusion pore during exocytosis and keep it from expanding to full fusion. If syntillas help stabilize the F-actin mesh, then their absence would actually have two effects; 1. More LDCGs recruited to the membrane (actin mesh as the barrier). 2. LDCGs at the membrane would primarily undergo full fusion exocytosis. In support of this idea, it is interesting that Doreian et al. (2009) find a mean amplitude and charge of 4.0 ± 0.43 pA and 0.08 ± 0.01pC for events that undergo kiss and run exocytosis that is similar to the mean amplitude and charge of amperometric events we record under spontaneous control conditions 5.4 ± 1. 3 pA and 0.08 ± 0.01pC, respectively. Moreover, the same study finds a mean amplitude and charge of 16.3 pA and 0.31 pC for full fusion events, when the actin network is broken down during high frequency stimulation, which compares well with our mean amplitude and charge of events recorded in ryanodine 14.5 pA, 0.28 pC.

A line of investigation is currently being pursued in our laboratory examining the hypothesis that syntillas exert their mechanism of action by maintaining the F-actin mesh barrier. Preliminary results show that in ACCs, blockade of syntillas for more than 1 hour with 100 μM ryanodine leads to lower density of polymerized actin, as visualized with phalloidin, in the region 1 μm below the ACC periphery compared to control. Thus, future investigation into the effects of Ca^{2+} syntillas on F-actin will continue.

Regulation of Ca^{2+} syntillas by physiologic stimulation

Action potential ⊣ Ca^{2+} syntilla

We believe that physiologic stimulation in the form of an action potential leads to a direct or indirect interaction with RYR2, since these are the channels most likely to mediate Ca^{2+} syntillas in mouse ACCs (ZhuGe, 2006). It may be less likely to involve a direct interaction since syntilla suppression is not immediate. The time frame in which multiple sAPs are able to completely abolish syntillas (about 2 minutes) versus the time frame required for a single sAP to accomplish complete suppression (about 5 minutes) suggests that the pathway can be amplified. Taken together, this argues against a quick acting all or none response that might be expected for a direct protein – protein interaction, such as the DHPR voltage-gated Ca^{2+} channel with the RYR (Li and Bers, 2001), though experimentation to rule this out is already underway in our laboratory by checking syntilla suppression after sAP stimulation in the presence of different Ca^{2+} channel type blockers. Instead, the activation of a 2^{nd} messenger pathway that targets RYR2 or leads to store emptying offers a more attractive hypothesis. Moreover, the mechanism must be regulated by $[Ca^{2+}]_i$, since the levels of global

$[Ca^{2+}]_i$ were the main difference in the experiments with 0.5 Hz versus 15 Hz stimulation.

The RYR2 could be targeted either on the cytosolic or the luminal side. For example, calmodulin is known to be bound to RYRs on it cytosolic face (Yamaguchi et al., 2003). In bilayer experiments, free calmodulin has been demonstrated to activate RYRs, while Ca^{2+}-calmodulin inactivates them (Fruen et al., 2000; Balshaw et al., 2001; Balshaw et al., 2002; Fruen et al., 2003; Meissner et al., 2009). Therefore the possibility that calmodulin serves as a sensor to modulate syntilla suppression is an attractive one that will be followed up on in the future. It is also interesting that the cytosolic form of Ca^{2+}-calmodulin kinase IIδ_C (CAMKIIδ_C) is able to increase spark frequency in rabbit ventricular myocytes (Kohlhaas et al., 2006). Future lines of experimentation in our laboratory will consider ablating or knocking down the CAM-binding domain or expressing RYR2s without the CAM-binding domain in cultured ACCs. Another potential 2nd messenger target is the 22 kDa Ca^{2+}-binding protein, sorcin. Sorcin has been shown to inhibit Ca^{2+} sparks, the homologues of Ca^{2+} syntillas, in cardiac muscle and is capable of rapid, reversible inhibition of RYR2 in bilayer experiments (Lokuta et al., 1997; Farrell et al., 2003; Seidler et al., 2003).

Syntilla suppression could also be mediated by a target on the luminal side of the RYR2. For example, in cardiac muscle the termination of Ca^{2+} sparks

largely depends on a signal that depends on Ca^{2+} depletion in the sacroplasmic reticulum (SR), conveyed through ancillary proteins such as calsequestrin and triadin (Gyorke et al., 2002; Stern and Cheng, 2004). It will indeed be interesting in the future to see if the Ca^{2+} stores in these ACCs can be depleted by a sAP and if the time frame of depletion matches syntilla suppression.

Final remark

Ca^{2+} released from internal stores, in the form of the Ca^{2+} syntilla, lies at the center of cell to cell communication in excitable cells and neurotransmission. By describing a new mechanistic regulation of exocytosis, the Ca^{2+} syntilla clearly increases the complexity as well as the sites of action for the Ca^{2+} ion in neurosecretion. The work described here reinforces the importance of thinking in terms of multiple Ca^{2+} microdomains in excitable secretory cells.

References

Balshaw DM, Yamaguchi N, Meissner G (2002) Modulation of intracellular calcium-release channels by calmodulin. J Membr Biol 185:1-8.

Balshaw DM, Xu L, Yamaguchi N, Pasek DA, Meissner G (2001) Calmodulin binding and inhibition of cardiac muscle calcium release channel (ryanodine receptor). J Biol Chem 276:20144-20153.

De Crescenzo V, ZhuGe R, Velazquez-Marrero C, Lifshitz LM, Custer E, Carmichael J, Lai FA, Tuft RA, Fogarty KE, Lemos JR, Walsh JV, Jr. (2004) Ca2+ syntillas, miniature Ca2+ release events in terminals of hypothalamic neurons, are increased in frequency by depolarization in the absence of Ca2+ influx. J Neurosci 24:1226-1235.

Doreian BW, Fulop TG, Smith CB (2008) Myosin II activation and actin reorganization regulate the mode of quantal exocytosis in mouse adrenal chromaffin cells. J Neurosci 28:4470-4478.

Doreian BW, Fulop TG, Meklemburg RL, Smith CB (2009) Cortical F-Actin, the Exocytic Mode and Neuropeptide Release in Mouse Chromaffin Cells Is Regulated by MARCKS and Myosin II. Mol Biol Cell.

Farrell EF, Antaramian A, Rueda A, Gomez AM, Valdivia HH (2003) Sorcin inhibits calcium release and modulates excitation-contraction coupling in the heart. J Biol Chem 278:34660-34666.

Fruen BR, Bardy JM, Byrem TM, Strasburg GM, Louis CF (2000) Differential Ca(2+) sensitivity of skeletal and cardiac muscle ryanodine receptors in the presence of calmodulin. Am J Physiol Cell Physiol 279:C724-733.

Fruen BR, Black DJ, Bloomquist RA, Bardy JM, Johnson JD, Louis CF, Balog EM (2003) Regulation of the RYR1 and RYR2 Ca2+ release channel isoforms by Ca2+-insensitive mutants of calmodulin. Biochemistry 42:2740-2747.

Galeotti N, Quattrone A, Vivoli E, Norcini M, Bartolini A, Ghelardini C (2008) Different involvement of type 1, 2, and 3 ryanodine receptors in memory processes. Learn Mem 15:315-323.

Garcia AG, Garcia-De-Diego AM, Gandia L, Borges R, Garcia-Sancho J (2006) Calcium signaling and exocytosis in adrenal chromaffin cells. Physiol Rev 86:1093-1131.

Giannini G, Conti A, Mammarella S, Scrobogna M, Sorrentino V (1995) The ryanodine receptor/calcium channel genes are widely and differentially expressed in murine brain and peripheral tissues. J Cell Biol 128:893-904.

Giner D, Lopez I, Villanueva J, Torres V, Viniegra S, Gutierrez LM (2007) Vesicle movements are governed by the size and dynamics of F-actin cytoskeletal structures in bovine chromaffin cells. Neuroscience 146:659-669.

Gyorke S, Gyorke I, Lukyanenko V, Terentyev D, Viatchenko-Karpinski S, Wiesner TF (2002) Regulation of sarcoplasmic reticulum calcium release by luminal calcium in cardiac muscle. Front Biosci 7:d1454-1463.

He X, Yang F, Xie Z, Lu B (2000) Intracellular Ca(2+) and Ca(2+)/calmodulin-dependent kinase II mediate acute potentiation of neurotransmitter release by neurotrophin-3. J Cell Biol 149:783-792.

Hui E, Bai J, Wang P, Sugimori M, Llinas RR, Chapman ER (2005) Three distinct kinetic groupings of the synaptotagmin family: candidate sensors for rapid and delayed exocytosis. Proc Natl Acad Sci U S A 102:5210-5214.

Kohlhaas M, Zhang T, Seidler T, Zibrova D, Dybkova N, Steen A, Wagner S, Chen L, Brown JH, Bers DM, Maier LS (2006) Increased sarcoplasmic reticulum calcium leak but unaltered contractility by acute CaMKII overexpression in isolated rabbit cardiac myocytes. Circ Res 98:235-244.

Li Y, Bers DM (2001) A cardiac dihydropyridine receptor II-III loop peptide inhibits resting Ca(2+) sparks in ferret ventricular myocytes. J Physiol 537:17-26.

Lokuta AJ, Meyers MB, Sander PR, Fishman GI, Valdivia HH (1997) Modulation of cardiac ryanodine receptors by sorcin. J Biol Chem 272:25333-25338.

Manita S, Ross WN (2009) Synaptic activation and membrane potential changes modulate the frequency of spontaneous elementary Ca2+ release events in the dendrites of pyramidal neurons. J Neurosci 29:7833-7845.

McNally JM, De Crescenzo V, Fogarty KE, Walsh JV, Lemos JR (2009) Individual calcium syntillas do not trigger spontaneous exocytosis from nerve terminals of the neurohypophysis. J Neurosci 29:14120-14126.

Meissner G, Pasek DA, Yamaguchi N, Ramachandran S, Dokholyan NV, Tripathy A (2009) Thermodynamics of calmodulin binding to cardiac and skeletal muscle ryanodine receptor ion channels. Proteins 74:207-211.

Mothet JP, Fossier P, Meunier FM, Stinnakre J, Tauc L, Baux G (1998) Cyclic ADP-ribose and calcium-induced calcium release regulate neurotransmitter release at a cholinergic synapse of Aplysia. J Physiol 507 (Pt 2):405-414.

Nakata T, Hirokawa N (1992) Organization of cortical cytoskeleton of cultured chromaffin cells and involvement in secretion as revealed by quick-freeze, deep-etching, and double-label immunoelectron microscopy. J Neurosci 12:2186-2197.

Paschen W, Doutheil J, Gissel C, Treiman M (1996) Depletion of neuronal endoplasmic reticulum calcium stores by thapsigargin: effect on protein synthesis. J Neurochem 67:1735-1743.

Seidler T, Miller SL, Loughrey CM, Kania A, Burow A, Kettlewell S, Teucher N, Wagner S, Kogler H, Meyers MB, Hasenfuss G, Smith GL (2003) Effects of adenovirus-mediated sorcin overexpression on excitation-contraction coupling in isolated rabbit cardiomyocytes. Circ Res 93:132-139.

Simpson PB, Challiss RA, Nahorski SR (1995) Neuronal Ca2+ stores: activation and function. Trends Neurosci 18:299-306.

Stein A, Radhakrishnan A, Riedel D, Fasshauer D, Jahn R (2007) Synaptotagmin activates membrane fusion through a Ca2+-dependent trans interaction with phospholipids. Nat Struct Mol Biol 14:904-911.

Stern MD, Cheng H (2004) Putting out the fire: what terminates calcium-induced calcium release in cardiac muscle? Cell Calcium 35:591-601.

Tchakarov LE, Zhang L, Rose SD, Tang R, Trifaro JM (1998) Light and electron microscopic study of changes in the organization of the cortical actin cytoskeleton during chromaffin cell secretion. J Histochem Cytochem 46:193-203.

Vitale ML, Seward EP, Trifaro JM (1995) Chromaffin cell cortical actin network dynamics control the size of the release-ready vesicle pool and the initial rate of exocytosis. Neuron 14:353-363.

Winkler H, Fischer-Colbrie R (1998) Regulation of the biosynthesis of large dense-core vesicles in chromaffin cells and neurons. Cell Mol Neurobiol 18:193-209.

Yamaguchi N, Xu L, Pasek DA, Evans KE, Meissner G (2003) Molecular basis of calmodulin binding to cardiac muscle Ca(2+) release channel (ryanodine receptor). J Biol Chem 278:23480-23486.

Zalk R, Lehnart SE, Marks AR (2007) Modulation of the ryanodine receptor and intracellular calcium. Annu Rev Biochem 76:367-385.

ZhuGe R, DeCrescenzo V, Sorrentino V, Lai FA, Tuft RA, Lifshitz LM, Lemos JR, Smith C, Fogarty KE, Walsh JV, Jr. (2006) Syntillas release Ca2+ at a site different from the microdomain where exocytosis occurs in mouse chromaffin cells. Biophys J 90:2027-2037.

Appendix A. Comparison of our amperometry values with the literature

Table A1. Comparative spike amplitude and charge, Q parameter values from studies on mouse adrenal chromaffin cells.

Laboratory	Study	Cell preparation	Criteria for analysis	Stimulation	I_{Amp}(pA)	Q (pC)
Our laboratory	(Lefkowitz et al., 2009)	Freshly isolated	Threshold =0.5 pA	None +ryanodine	5.4 ± 1. 3 14.5 ± 1. 4	0.08 ± 0.01 0.28 ± 0.03
	(ZhuGe et al., 2006)	Freshly isolated *Calcium-free bath*	Threshold =2.5 times baseline rms	None	7.0 ± 0.6	0.11 ± 0.01
Corey Smith	(Doreian et al., 2009)	Cultured 1-2 days	Baseline noise <10 pA	0.5 Hz APs 15 HZ APs	4.0 ± 0.43 16.3 ± 1.2	0.08 ± 0.01 0.31 ± 0.02
	(Doreian et al., 2008)	Cultured 1-2 days	Baseline noise < 10pA	0.5 Hz APs 15 HZ APs	5.2 ± 0.82 19.1 ± 1.4	0.12 ± 0.01 0.36 ± 0.02
Aaron Fox	(Grabner et al., 2005)	Cultured 2-3 days Digitonin-permeabilized	Baseline noise <2pA	High Ca^{2+} in bath post permeabil-ization	na	0.064 for small events 0.329 for large events
	(Grabner et al., 2006)	Cultured 2-3 days Digitonin-permeabilized	Baseline noise <2pA	High Ca^{2+} in bath post permeabil-ization	na	0.28 ± 0.03 All events
Erwin Neher	(Sorensen et al., 2003)	Cultured 1-3days	Threshold=10pA	1 μM Ca^{2+} in patch pipette	~ 58pA Median	~ 0.42 ($Q^{1/3}$ ~ 0.75 $pC^{1/3}$)
	(Moser and Neher, 1997)	Used day of culture – 48Hrs	Threshold=4pA AND 30/90% risetime <1.5 ms	10 μM Ca^{2+} in patch pipette	27.0 ± 2.2	~ 0.16 ($Q^{1/3}$ = 0.542 $pC^{1/3}$)

There is to date, relatively little information about spontaneous exocytosis in adrenal chromaffin cells in the literature.

However as we show in detail in the table above, when comparisons are made with mouse data and the threshold of detection is low, our data matches that of others. In our study, we report a mean Q value of 0.08 ± 0.01 pC for all amperometric events and 0.14 ± 0.03 for spikes alone and 0.02 ± 0.00 for SAFs under control conditions in normal saline. (To select a spike for analysis, the peak amplitude must be ≥0.5 pA and our baseline root mean square (rms) noise is typically < 0.2 pA.)

As evidenced in Table A1, the most meaningful comparisons in the literature are found in the recent studies from the Smith laboratory (Doreian et al., 2008; Doreian et al., 2009). In these studies two forms of stimulation were applied to mouse chromaffin cells cultured for 1 to 2 days. In the first, light electrical stimulation in the form of simulated action potentials (sAPs) was administered at 0.5Hz, a stimulus thought to mimic input under basal sympathetic tone. In the second, sAPs were administered at 15 Hz, and thought to mimic input under an acute stress response.

The literature shows that when minimal forms of stimulation are used, or when the small events are separated from large events during intense stimulation, the spike parameters closely resemble those measured under our spontaneous conditions. In fact, a major source of discrepancy across the studies has mostly to do with how spikes are chosen for analysis. For example,

where Sorensen *et al*. (2003) choose to only analyze events greater than 10 pA, the average spike amplitude and charge is going to be much greater than when Grabner *et al*. (2005) choose to analyze events above 2 pA, regardless of the stimulation intensity. In our study, since we examine stand alone feet as well as spikes it is necessary to use a very low baseline cut off, requiring that events be greater than 0.5 pA. To discard the data between 0.5 pA and some arbitrary cut off value up to 10 pA is to throw out valuable information at least for the purposes of our studies.

References:

Doreian BW, Fulop TG, Smith CB (2008) Myosin II activation and actin reorganization regulate the mode of quantal exocytosis in mouse adrenal chromaffin cells. J Neurosci 28:4470-4478.

Doreian BW, Fulop TG, Meklemburg RL, Smith CB (2009) Cortical F-Actin, the Exocytic Mode and Neuropeptide Release in Mouse Chromaffin Cells Is Regulated by MARCKS and Myosin II. Mol Biol Cell.

Grabner CP, Price SD, Lysakowski A, Fox AP (2005) Mouse chromaffin cells have two populations of dense core vesicles. J Neurophysiol 94:2093-2104.

Grabner CP, Price SD, Lysakowski A, Cahill AL, Fox AP (2006) Regulation of large dense-core vesicle volume and neurotransmitter content mediated by adaptor protein 3. Proc Natl Acad Sci U S A 103:10035-10040.

Lefkowitz JJ, Fogarty KE, Lifshitz LM, Bellve KD, Tuft RA, ZhuGe R, Walsh JV, Jr., De Crescenzo V (2009) Suppression of Ca2+ syntillas increases spontaneous exocytosis in mouse adrenal chromaffin cells. J Gen Physiol 134:267-280.

Moser T, Neher E (1997) Estimation of mean exocytic vesicle capacitance in mouse adrenal chromaffin cells. Proc Natl Acad Sci U S A 94:6735-6740.

Sorensen JB, Fernandez-Chacon R, Sudhof TC, Neher E (2003) Examining synaptotagmin 1 function in dense core vesicle exocytosis under direct control of Ca2+. J Gen Physiol 122:265-276.

ZhuGe R, DeCrescenzo V, Sorrentino V, Lai FA, Tuft RA, Lifshitz LM, Lemos JR, Smith C, Fogarty KE, Walsh JV, Jr. (2006) Syntillas release Ca2+ at a site different from the microdomain where exocytosis occurs in mouse chromaffin cells. Biophys J 90:2027-2037.